Science
with an
Energy Recovery Linac

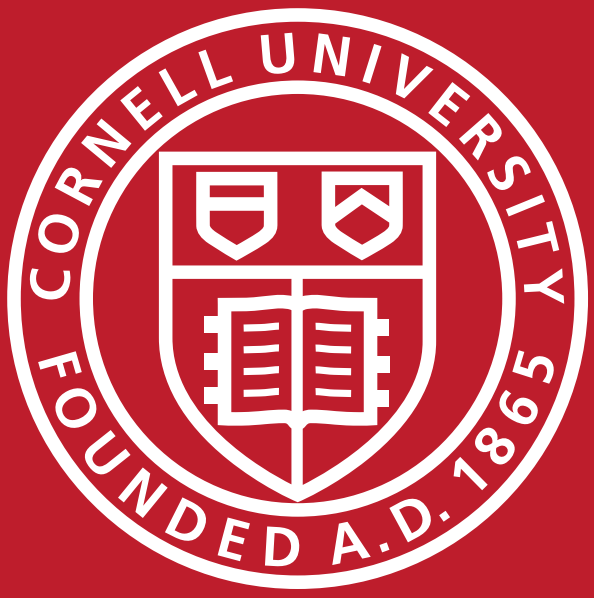

June 2013

Science with an Energy Recovery Linac (ERL)

Editors: D.H. Bilderback, J.D. Brock, E. Fontes, G.H. Hoffstaetter

Contributors from Cornell University:
H. Abruña, N. Ashcroft, W. Bassett, I. Bazarov, D. Bilderback, J.D. Brock, B. Crane, D. Dale, K. Finkelstein, E. Fontes, R. E. Gillilan, S.M. Gruner, R. Hoffmann, G.H. Hoffstaetter, C.U. Kim, K. Lancaster, D. Muller, J.R. Patterson, M. Pfeifer, L. Pollack, J. Ruff, M. Tigner, D. Schuller, D.M. Smilgies, Z. Wang, A. Woll

Contributors outside Cornell University:
S. Adachi (KEK), H. Ade (North Carolina State University), M. Agbandje-McKenna (University of Florida), P. Anfinrud (NIH), S. Billinge (Columbia University). R. Boehler (CIW), S. Bonev (LLNL), C. Bressler (European X-FEL), W. Burghardt (Northwestern University), M. Caffrey (Trinity College, Ireland), E. Castner (Rutgers University), L. Chen (Northwestern University), E. Dufresne (APS), D. Eisenberg (UCLA), P.G. Evans (University of Wisconsin, Madison), K. Evans-Lutterodt (BNL), J. Fienup (University of Rochester), R. Fischetti (ANL), S. Fraden (Brandeis University), A. Fluerasu (BNL), A. Goncharov (CIW), Y. Gupta (Washington State University), R. Harder (ANL), R. Hemley (CIW), J. Holton, (LBNL), G. Ice (ORNL), J. Jackson (Caltech), C. Jacobsen (Northwestern University), C.-C. Kao (SLAC), J. Kirz (LBNL), E. Lattman (HWI), A.M. Lindenberg (Stanford University), K. Ludwig (Boston University), L. Lurio (Northern Illinois University), M. McMahon (University of Edinburgh), W. Mao (Stanford University), L. Makowski (Northeastern University), A.M. March (APS), S. Marchesini (LBNL), J. Maser (APS), J. Mass (University of Delaware and Winterthur Museum), I. McNulty (APS), A. McPhereson (University of California at Irvine), J. Miao (UCLA), S. Mochrie (Yale University), K. Moffat (University of Chicago). Y. Nishino (Hokkaido University), J. Parise (SUNY-Stony Brook), G. Phillips (University of Wisconsin at Madison), M. Pierce, (Rochester Institute of Technology), V. Prakapenka (University of Chicago), D.A. Reis (Stanford University), D. Rees (Caltech), H. Reichert (ESRF), M. Rheinstadter, (McMaster University), C. Riekel (ESRF), S.V. Roth (DESY), R. Schoenlein (LBNL), C. Schroer (Technical University Dresden), B. Sepiol (University of Vienna), R. Sension (University of Michigan), D. Shapiro (NSLS-II), Q. Shen (NSLS-II), Y. Shinohara (University of Tokyo), O. Shpyrko (University of California at San Diego), I. Schlichting (Max Planck Institute for Medical Research), I. Silvera (Harvard University), J. Spence (Arizona State University), B. Stephenson (ANL), R. Sunahara (University of Michigan), M. Sutton (McGill University), D. Svergun (EMBL), S. Techert (Max Planck Institute for Biophysical Chemistry), P. Thibault (Technical University of Munich), C. Thompson (Northern Illinois University), I. Vartaniants (DESY), L. Vincze (Ghent University), S. Vogt (APS), G. Williams (LCLS), W. Yang (CIW), C.-S. Yoo (Washington State University), D. Zhang (Caltech), Y. Zhao (University of Nevada at Las Vegas)

Note: This document is a compilation of ideas presented and discussed by nearly 500 participants who attended a series of six international workshops held at Cornell University in 2011 on "X-rays at the Diffraction Limit" (XDL2011) [1,2]. Above we list those who helped organize workshop sessions, gave presentations, and contributed summary statements in their fields of expertise. Errors in interpreting or communicating those ideas are solely the responsibility of the editors.

Commonly used abbreviations

APS	Advance Photon Source
ANL	Argonne National Laboratory
BNL	Brookhaven National Laboratory
CIW	Carnegie Institute of Washington
DESY	Deutsches Elektronen-Synchrotron
DOE	Department of Energy
EMBL	European Molecular Biology Laboratory'
ERL	Energy Recovery Linac
ESRF	European Synchrotron Radiation Facility
HWI	Hauptmann-Woodward Medical Research Institute
KEK	High Energy Accelerator Research Organization (Japan)
LBNL	Lawrence Berkeley National Laboratory
LCLS	Linac Coherent Light Source
LINAC	Linear Accelerator
LLNL	Lawrence Livermore National Laboratory
NIH	National Institutes of Health
NSF	National Science Foundation
NSLS-II	National Synchrotron Light Source II (BNL)
ORNL	Oak Ridge National Laboratory
PF/KEK	Photon Factory at KEK, Tsukuba, Japan
SLAC	SLAC National Accelerator Laboratory
SSRL	Stanford Synchrotron Radiation Laboratory
SUNY	State University of New York
XDL2011	"X-rays at the Diffraction Limit" 2011 Workshop
X-FEL	X-ray Free Electron Laser

Editorial note: this document is a companion to

"**Cornell Energy Recovery Linac Project Definition Design Report" (PDDR)**

Bazarov *et al.*, (2012),
http://erl.chess.cornell.edu/PDDR/PDDR.pdf


Cornell Energy Recovery Linac

Project Definition Design Report

Editors: Georg Hoffstaetter, Sol Gruner, Maury Tigner

Contributors: I. V. Bazarov, S. A. Belomestnykh, D. H. Bilderback, M. G. Billing, J. D. Brock, R. W. Buckley, S. S. Chapman, E. P. Chojnacki, Z. A. Conway, J. A. Crittenden, D. Dale, J. A. Dobbins, B. M. Dunham, R. D. Ehrlich, M. P. Ehrlichman, K. D. Finkelstein, E. Fontes, M. J. Forster, S. W. Gray, S. Greenwald, S. M. Gruner, C. Gulliford, D. L. Hartill, R. G. Helmke, G. H. Hoffstaetter, A. Kazimirov, R. P. Kaplan, S. S. Karkare, V. O. Kostroun, F. A. Laham, Y. H. Lau, Y. Li, X. Liu, M. U. Liepe, F. Loehl, L. Cultrera, T. Miyajima, C. E. Mayes, J. M. Maxson, A. Mesek, A. A. Mikhailichenko, D. Ouzounov, H. S. Padamsee, S. B. Peck, M. A. Pfeifer, S. E. Posen, P. G. Quigley, P. Revesz, D. H. Rice, U. Sae-Ueng, D. C. Sagan, J. O. Sears, V. D. Shemelin, C. K. Sinclair, D. M. Smilgies, E. N. Smith, K. W. Smolenski, Ch. Spethmann, C. Song, T. Tanabe, A. B. Temnykh, M. Tigner, N. R. A. Vallis, V. G. Vaslchenvich, Z. Wang, A. R. Woll, Y. Xie, Z. Zhao

Special Thanks: Chris Mayes is acknowledged for tireless editorial help and layout organization, and Sherrie Negrea for language editing.

September 12, 2012

Contents

Executive Summary

Linear accelerator based synchrotron light sources have the potential to produce hard x-ray beams limited only by the fundamental wave nature of light. These intense beams can focus to (sub)-nanometer beam waists while maintaining precise collimation, photon energy, and polarization. Such beams will enable three-dimensional, real-time characterization of atomic structure, electronic structure, and chemical composition, even in macroscopic, non-periodic, heterogeneous systems and imperfect samples. Since x-ray measurements are responsible for most of what we know about the fundamental atomic-scale structure of materials, the obvious question arises, "Are there new x-ray opportunities that would lead to novel and transformative science?" There are at least five resoundingly positive answers to this question.

"Linear accelerator technology produces superlative x-ray sources." Consider first the enormous technological change introduced since simple x-ray tube sources caused a barely visible glow for Roentgen, or helped the Braggs determine the crystal structure of rock salt, or produced "photo 51" that led to the famous model of DNA by Watson and Crick. In the intervening decades, extraordinary advances in relativity, electrodynamics, superconductivity, and myriad generations of x-ray detectors have driven scientists to build storage rings with exquisite control over the size, shape and trajectories of the relativistic charged particle beams – the modern sources of the most brilliant x-ray beams. Now, going beyond storage rings, a completely new generation of coherent x-ray sources based on linear accelerators (Linacs) has been invented; these machines have the potential to be "diffraction-limited" X-ray sources, limited only by the fundamental wave nature of light.

The quality of radiation from a charged particle beam is determined by the radiative properties of a single point particle [3] and by the six-dimensional phase space distribution of a macroscopic bunch of such particles [4,5]. The phase space volume occupied by a particle beam is a key measure of accelerator performance. Smaller is better, yielding smaller x-ray beams and producing higher spectral brightness (flux in an energy band divided by source size and angular divergence). In a storage ring, the phase space volume grows due to repeated emission of synchrotron radiation as the particle bunches circulate. Because Linac-based sources use each electron bunch only once, phase space growth does not occur; the exquisite quality of the electron beam in the linear accelerator transfers directly to the x-ray beam.

Linac-based light sources can provide either low duty-cycle pulsed beams with enormous peak power – X-ray Free Electron Lasers (X-FELs) such as the LCLS – or quasi-continuous beams with exquisite stability and control – the Energy Recovery Linacs (ERLs). The radiation from X-FEL and ERL sources is unique in many ways, both enabling and challenging scientists of all types to invent new tools, techniques and methods to harness the potential of these transformative new sources.

"**Many tools are still missing from the tool chest**." New tools are needed to characterize atomic-scale structure, function and dynamics of time-varying and non-equilibrium systems. The earliest synchrotron radiation (SR) sources utilized storage rings designed, built, and operated primarily for high-energy physics experiments. Nevertheless, the extraordinary flux and continuous spectrum from parasitic sources transformed x-ray science. More recently, 3rd generation storage rings were built to utilize the spectral brightness of undulator sources. Currently, many storage ring sources are working to optimize transverse coherence, the ability of a photon beam to create interference patterns. An x-ray beam has optimal transverse coherence when it emerges from a point source. A Linac-based ERL source approaches this ideal, producing quasi-continuous, high-energy x-ray beams with full transverse coherence.

The ERL design described in detail in the Preliminary Design Definition Report (PDDR) produces 50 femtosecond to 2 picosecond pulses continuously at a rate of 1.3 GHz, enabling new classes of continuous-duty x-ray experiments complementary to those served by low pulse-rate X-FEL sources. With ERLs, scientists will be able to focus down to nanometers, pre-

cisely control photon energy and polarization, and benefit from full coherence. These beams will allow current probes to be extended and novel approaches to be developed, and will enable three-dimensional, real-time characterization of structure (atomic, nanoscale and mesoscale) and chemical composition in realistic environments. This compelling vision is responsible for the current decades-long and worldwide race to build coherent SR facilities.

"**Answers beget questions that demand novel approaches**." The utilization of SR is following a strong growth curve, and the number of novel applications (and needs) of SR is growing without bounds. With almost one hundred facilities worldwide, SR is a key multi-disciplinary tool enabling major discoveries in diverse fields across the physical, chemical, environmental, engineering, geological and planetary science, medical and biological disciplines, and archaeology and art history. Will existing and novel applications prove transformational? We think so. For example, nothing has impacted bioscience more than the revolutionary advances in protein crystallography. As just one example, SR based crystallography solved the atomic structure of three key HIV reverse transcriptase complexes [6] that bear directly on the design of new AIDS treatments. These new drugs will save lives. At the same time, these advances have generated new challenges; questions are now shifting from determining static structures to understanding flexibility, fluctuations and function, with focus shifting from measuring static protein crystals to protein complexes that do not form high quality crystals. Better sources like the ERL, with new methods to capture and interpret data, are needed to meet these emerging challenges.

"**Users vote with their feet**." A fourth way to answer the question whether future x-ray sources will lead to novel and transformative science is to note the phenomenal growth in size and breadth of user communities at SR sources. Remarkably, over 50% of all SR facility visitors are students or early career scientists at the post-doctoral and junior faculty levels and they see SR x-ray techniques as their best route to the future.

"There is a world-wide drive for increased coherence" A fifth answer recognizes the enthusiasm the scientific community expresses each time there is the prospect of a new, powerful x-ray tool. The newest storage ring sources under construction or upgrade (e.g., Petra-III, APS-U, MAX-4, and NSLS-II) will improve transverse coherence, increase intensity and reduce source dimensions to achieve nanometer spatial resolution [7-9]. However, storage ring tech-

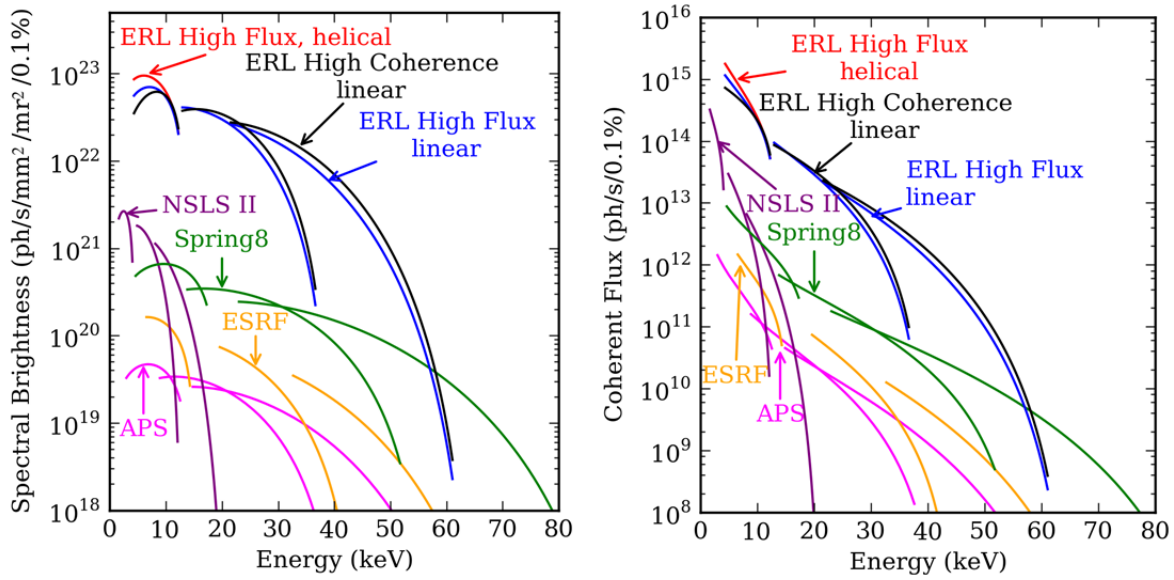

Figure 1: Nominal spectral brightness and coherent flux for various sources, as calculated with SPECTRA using the parameters of Table 1 (see end of document).

nology limits the coherence of these machines. Because of the interest in fully coherent, high repetition-rate, hard x-ray sources, two series of international workshops were held at Cornell, during 2006 and 2011, covering opportunities and challenges of ERLs [1,2,10]. In 2011 CHESS, SSRL, DESY, and PF/KEK joined forces to host six workshops on "Science at the Hard X-ray Diffraction Limit" (XDL-2011). With NSF and DOE support, almost 500 participants gathered to brainstorm and discuss experiments that cannot be done with existing sources. Speakers presented innovative ideas, new approaches, and out-of-the-box thinking. The talks highlighted challenges facing society, gaps in scientific understanding or experimental capabilities, and recent landmarks in scientific inquiry and technique development. Below we give examples of the results of brainstorming from each of the six workshops, highlighting the novel and potentially transformational nature of ERL technology.

What are the outstanding and unique features of new ERL light sources? An ideal x-ray source would provide complete control over the space/time structure of radiation pulses. Linac-based sources achieve that by exercising exquisite control over the electron source bunch structure and 6-dimensional phase space. An ERL source has a flexible, quasi-continuous bunch structure, intrinsically small round beams, short but variable native pulse lengths, and very high transverse coherence. With this outstanding flexibility, we envision that ERL facilities will alternate, as needed by scientific applications, between different operating modes: (A) high-flux mode, (B) high-coherence mode (C) a short-pulse, low-charge mode, and (D) a short-pulse, high-charge mode. Figure 1 shows spectral curves and Table 1 (see end of document) shows design parameters for several modes of operation as well as light source comparisons [11,12].

One of the unique features of ERL (and X-FEL) sources is the ability to operate a new type of insertion device – called a "delta undulator" - that provides unprecedented tunability of x-ray fundamental energy, harmonic suppression, and polarization (helical or planar) (Fig. 2) [13-15]. When run in helical mode, the delta undulator suppresses on-axis intensity of unwanted higher harmonics (and heat). Combining delta undulators, micron-sized round, coherent beams and zone-plate focusing, the ERL will power the most intense and flexible continuous hard x-ray nanobeam probes in the world [16]. In addition, ERLs can utilize very long undulators to produce x-ray beams with very narrow energy bandwidths; these will power beamlines for high-resolution spectroscopies or beamlines that avoid x-ray optics altogether [17].

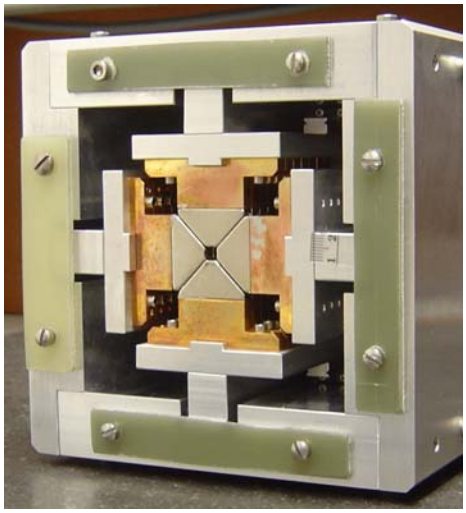

Figure 2: First working prototype of delta undulator. The four "delta-shaped" permanent magnets surround a 5 millimeter gap suitable for an ERL or X-FEL electron beam. The four arrays of magnets can translate independently, maintaining a 5 mm gap but varying the phase of the transverse magnetic fields; this type of tuning allows separate control of the energy and polarization of the X-ray radiation. The polarization of the beam can be planar – from horizontal to vertical and anywhere in between – or helical.

"Is ERL technology ready?" Yes. The guiding concept for an ERL source was originated at Cornell by Tigner in 1965 [18]. For many years, the DOE has supported a low-energy ERL at Jefferson Laboratory to drive the world's highest-power tunable infrared and VUV laser. KEK in Japan is building a low-energy compact ERL, and is planning to build a full-scale high-energy ERL x-ray source. NSF has supported a decade-long ERL R&D project at Cornell; this project has succeeded in designing and fabricating technologies needed to create a prototype minimum phase space injector – the heart of the ERL light source. **At this time all the necessary technology milestones have been realized or proven through validated models [19,20].** An engineering study was funded by New York State and the ac-

companying “Project Definition Design Report” (PDDR) outlines an ERL upgrade to the Cornell synchrotron site [21]

This document and the accompanying PDDR demonstrate that the ERL has the potential to be a superb coherent hard x-ray source. The science experiments outlined in this document use a model 5 GeV ERL light source with the parameter tables given in the Cornell ERL Project Definition Design Report [21]. The PDDR, which describes an upgrade to the storage ring that currently powers CHESS, is augmented by engineering studies of accelerator components, tunnels, x-ray user-halls, cryogenic buildings, and an environmental impact study that can be obtained by request.

The many advantages of ERL beams for coherent x-ray experiments have been analyzed for a variety of classes of ERL experiments [12]. As shown in the science examples below, ERLs are complementary to X-FEL sources. ERL strengths include very high coherent flux, inherently round beams, flexibility and quasi-continuous time structure, and high energy resolution. ERLs will be especially advantageous where coherence and nanobeams are needed to repetitively probe unique specimens, where the requisite scattering information cannot be obtained with a single X-FEL pulse, or where high coherent flux and quasi-continuous time structure are required to study how samples change in time. It is also important to realize that designs for ERL sources are only a decade old; prior generations of x-ray sources matured and improved in performance continually – we expect the ERL will improve dramatically with ingenuity and need. For instance, it was realized early on that an ERL source would be an ideal host for an X-FELO (an X-FEL oscillator), an x-ray resonant cavity that will produce transform-limited x-ray beams with a coherent intensity boosted more than 3 orders of magnitude to over 10^9 x-rays/second per pulse with MHz repetition rates and extremely high energy resolution [22].

The structure of the document follows the topics of the XDL2011 workshop, giving examples of how ERL sources can address ”grand challenge” of science in the following areas: 1) Diffraction Microscopy, Holography and Ptychography using Coherent Beams; 2) Biomolecular Structure from Nanocrystals and Diffuse Scattering; 3) Ultrafast Science with ”Tickle and Probe”; 4) High Pressure Science at the Edge of Feasibility; 5) Materials Science with Coherent Nanobeams at the Edge of Feasibility; and 6) X-ray Photon Correlation Spectroscopy (XPCS) using Continuous Beams.

Workshop 1: Diffraction Microscopy, Holography, and Ptychography using Coherent Beams

1.1 Introduction

Since the discovery of x-rays and Laue diffraction over one hundred years ago, x-ray diffraction has been a phenomenally successful and critical tool for solving the periodic structure of crystalline materials. However, the structures of many important materials such as glasses and polymers are not periodic. Even in crystalline materials, some of the most important and useful properties are strongly influenced by deviations from long-range periodic order: the influence of surfaces, grain boundaries, and local structure deriving from impurities or dislocations. Adding even greater complexity, these structures are not static. They evolve as materials process or function. Many current technologies and applications are constrained by these effects. Consequently, there is a growing emphasis on the challenge to understand non-periodic structures and how they evolve over time.

New methods enabled by the coherent X-ray beams produced by ultra-low emittance synchrotron radiation offer the potential of meeting this challenge [12]. Already, the limited coherence available at 3rd generation storage rings has enabled pioneering techniques such as X-ray holography [23-25] and coherent diffraction imaging (CDI) [26-29]. These take advantage of ideas originating from information theory (oversampling) [30] and of computational techniques (phase retrieval) [31-33], allowing for the structural solution to non-periodic systems (see figure 1.1.1) [28,34,35]. Furthermore, due to the nature of their interaction with matter, X-rays are uniquely suited for studies of thicker samples and samples in particular environments or conditions, or operating in real devices. Multiple scattering is generally not an important consideration with X-rays, allowing for direct and quantitative analysis. These new coherent imaging techniques can be combined with other techniques based upon rich spectroscopies that are possible with X-rays, allowing elemental sensitivity via resonant scattering, trace element sensitivity via X-ray fluorescence, and imaging the distribution of chemical states via X-ray absorption near-edge spectroscopy.

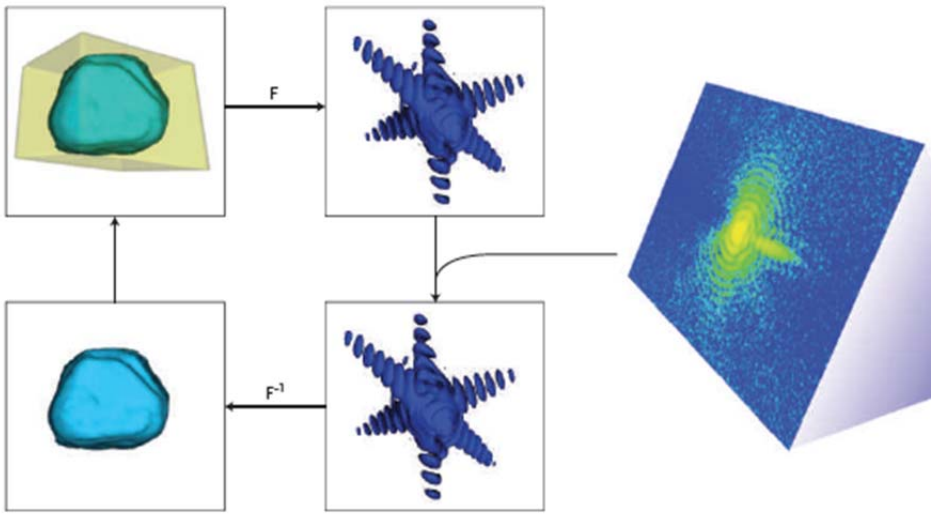

Figure 1.1.1: Top: coherent scattering pattern (right) and real-space volumetric iterative reconstruction of a single crystalline grain (left). (From [27])

These techniques are currently limited by the coherent X-ray flux that can be delivered to the sample. The ERL will produce an X-ray source with orders of magnitude higher coherent flux than state-of-the-art storage rings [12], but with a quasi-continuous time structure that provides capabilities unique and complementary to X-FELs. Three-dimensional coherent scattering measurements that currently take hours could be completed in a few seconds. Studies of the

evolution of non-periodic structures operating under conditions of interest for specific applications could revolutionize the way we approach materials design, synthesis, and processing, which in turn would have far-reaching and profoundly positive effects on society.

1.2 Materials Processing and Engineered Materials

Most materials are polycrystalline and the size, structure, and interfaces between crystalline grains often controls material properties. A detailed understanding of polycrystalline materials, and better methods of synthesis, would have far-reaching and profoundly positive effects on society. One of the grand challenges in materials science is to explain properties of polycrystalline substances starting from measured properties of large perfect crystals. For instance crack propagation, fatigue and failure in common metals used for bridges and aircraft parts are of great interest to the engineering and industrial communities [36]. Our understanding and predictive capabilities are limited because we lack tools that provide sufficiently detailed, 3D spatially-resolved measurements of deformation and microstructure on length scales of a typical grain. Submicron spatial resolution of grains and their interfaces is required to provide definitive benchmarks for theory and simulations. Given such information, scientists could link mesoscopic structure with macroscopic properties to explain strength and failure modes of metals and ceramics, ionic diffusion in fuel cell electrodes, dynamical properties of alloys, etc. As grains shrink, the relative contribution of the surface to the overall free energy becomes increasingly important. This is why nanocrystalline materials often have very different properties than materials of the

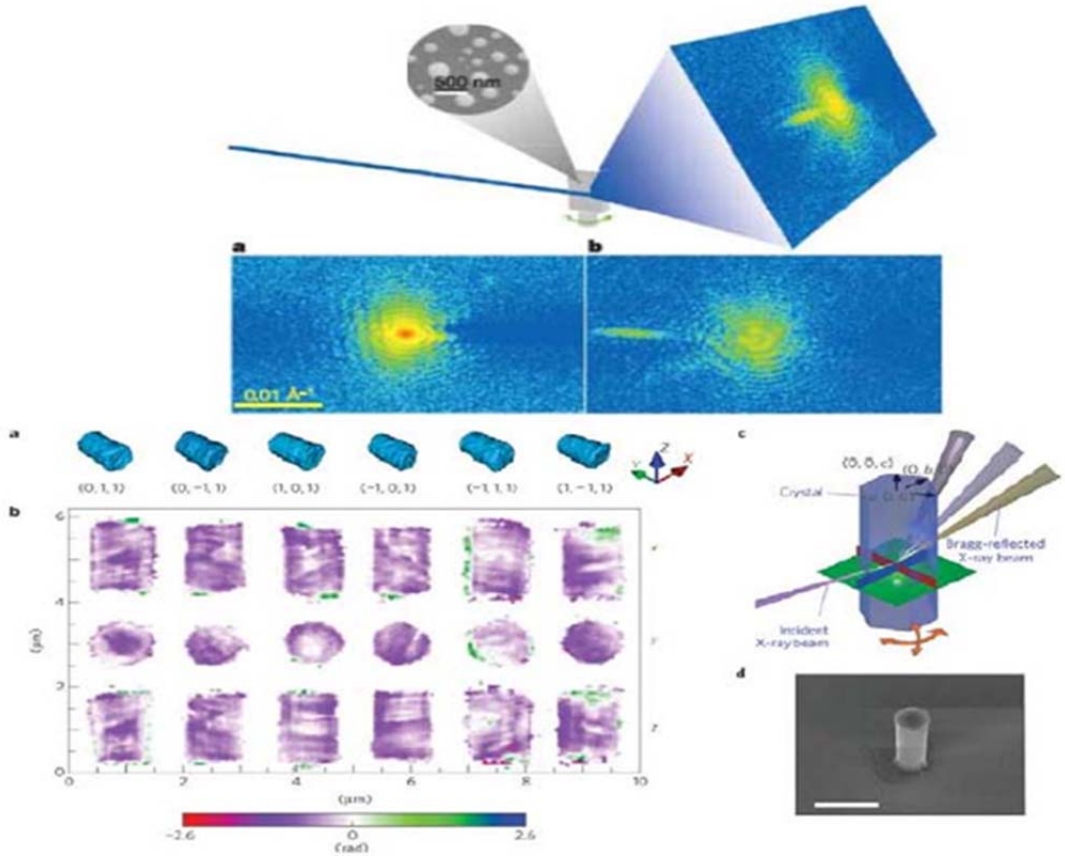

Figure 1.2.1: top: CDI experimental geometry and three examples of the coherent scattering patterns used to reconstruct a real-space density map (top) of the single ZnO nanorod (see [45]) and (bottom) including three-dimensional reconstructions of the three-dimensional strain vector (seen in the projections in bottom, b). (From [43])

same composition with micron-sized grains. Nanocrystalline materials have enormous potential for society, but are even harder to analyze at the single crystal level. Hard X-ray beams are among the few probes that can penetrate and measure polycrystalline grain properties within bulk materials on appropriate length scales. It is necessary to nondestructively study crystal morphology, orientation, strain, texture, and phase with a spatial resolution below the grain size. Better still would be to perform these measurements in a time-resolved manner, to experiment and study how such properties evolve in response to varying processing conditions.

Of particular interest are microstructural studies of crystal grain size and orientation, local elastic strain, and plastic deformation using the differential aperture 3D X-ray microscopy (DAXM) recently developed by the RISØ group at the European Synchrotron Radiation Source (ESRF) [37] and by the ORNL group at the Advanced Photon Source (APS) [38]. In DAXM, an X-ray beam focused to submicron size by a pair of crossed Kirkpatrick-Baez mirrors will produce diffraction from crystal grains along the entire path length in the sample. A series of images collected as a platinum wire edge is scanned across the sample, shadowing the diffraction pattern and thereby allowing identification of a given Bragg reflection from a diffracting grain at a particular depth. Presently at the APS a single depth scan requires about 30 minutes and collecting an array of 80 x 80 x 80 voxels takes about 3 hours. With the ERL and appropriate detectors we estimate that a 1000 x 1000 x 1000 voxel map could be generated in a few seconds, thereby enabling *in-situ* real time experiments such as rapid annealing and plastic and elastic deformation, to name a few [12]. This advance in methodology would have an enormous impact on understanding polycrystalline materials with submicron grains.

There are fundamental materials questions as well. Since the mid-1950s researchers have only been able to speculate on the microscopic mechanisms of the most fundamental aspects of grain nucleation and defect formation. Annealing twins, which play a critical role in the mechanical strength of FCC metals, are seen to emanate from grain boundaries during growth [39]. Yet very little is known about the mechanisms through which they form at specific locations on grain boundaries, even though they play a critical role in the mechanical strength of materials [40-42].

Coherent diffraction imaging (CDI) in the Bragg geometry offers a unique capability to study the mechanisms of grain growth on the nanoscale [27,43]. The sample is coherently illuminated to measure small-angle scattering features about the Bragg peaks in the far-field diffraction pattern (see Fig. 1.2.1). Iterative phase retrieval methods are then used to generate a model-free reconstruction of the complex transmission function of the sample. Each Bragg peak contains a coherent diffraction pattern which can be analyzed to recover a 3D density map of the diffracting crystal, while ignoring neighboring crystals which have different orientations [44]. Unique to Bragg CDI is an ability to study a single crystalline domain, buried in a thick polycrystalline sample, with nanometer spatial resolution.

Bragg CDI is extremely sensitive to strain; hence, a 3D diffraction pattern about a single Bragg peak can be used to recover a 3D map of the strain projected onto that reciprocal lattice vector [45]. Researchers at the APS have demonstrated the collection of CDI patterns around multiple Bragg peaks of the same crystal, permitting the creation of a 3D map of a strain vector. By taking advantage of the strain sensitivity and orientation selection of Bragg CDI, it should be possible to map in 3D strain due to finite size and boundary effects in an individual grain in a polycrystalline sample with nanometers resolution. The application of CDI is limited by the coherent flux that can be delivered to the sample. A 3D CDI pattern with $\approx$20 nm resolution currently takes hours to record at the APS. Given the inverse fourth power relationship between resolution and flux, at the proposed ERL a 3D CDI pattern at $\approx$2 nm from a radiation hard material could be recorded in a few hours, or a 20 nm resolution pattern recorded in a few seconds. Also, CDI could be performed at considerably higher X-ray energies, where current beamlines suffer from very short coherence lengths, allowing access to higher order Bragg peaks and interrogation of thicker and denser materials, and permitting the design of experiments using diamond anvil cells.

1.3 Nanoscale Phase Separation in Correlated Oxides

Strongly correlated systems often feature competition between spin, charge, orbital and lattice degrees of freedom, which can result in spontaneous emergence of nanoscale inhomogeneities (Fig. 1.3.1) [46-51]. Evocative examples include stripe phases and phase coexistence observed in spin-and charge-density wave materials, underdoped high-Tc superconductors and colossal magnetoresistive (CMR) manganese oxides. Similar effects are implicated in the emergence of metallic domains during Metal-Insulator transitions. Studies of these phenomena typically require coupling to charge, spin, orbital or lattice order parameters with spatial resolution ranging from nanometers to microns. While scanning probe microscopy techniques can provide resolution down to Angstrom scale, and have proven useful in the study of nanoscale structure, these local probes are typically limited to properties of the top-most surface monolayer of the studied material. In addition, while bulk probes such as magnetic susceptibility or electrical transport measurements can couple to various order parameters, these techniques cannot provide information about spatially inhomogeneous nature of the sample, due to averaging over the macroscopic dimensions.

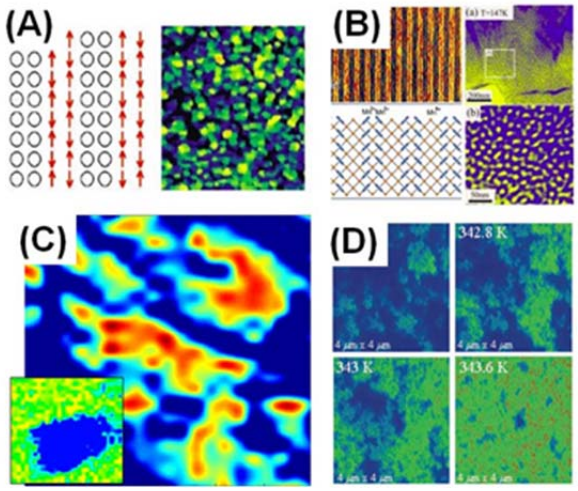

Figure 1.3.1: Examples of nanoscale inhomogeneities in a variety of strongly correlated systems: (A) Scanning Tunneling Spectroscopy of the inhomogeneous superconducting gap distribution as well as stripe (or checkerboard) patterns in under-doped high-Tc superconductors; (B) Phase separation in Colossal Magnetoresistive (CMR) Manganites; (C) Charge-Density Wave and Spin-Density Wave (inset) domains in Chromium; (D) Coexistence of Conducting and Insulating domains in VO2 at the onset of the Metal-Insulator Transition. (From [138])

Inhomogeneous domains in correlated oxides (such as doped Mott insulators and CMR manganites) are typically thought to occur when phase competition is resolved through phase separation. However, it is not yet clear whether the domain formation, for example in CMR manganites, is always entirely due to these intrinsic reasons, or if the crystalline imperfections such as lattice strain, defects or inhomogeneous distribution of dopants strongly influence formation of textured patterns. X-ray micro-

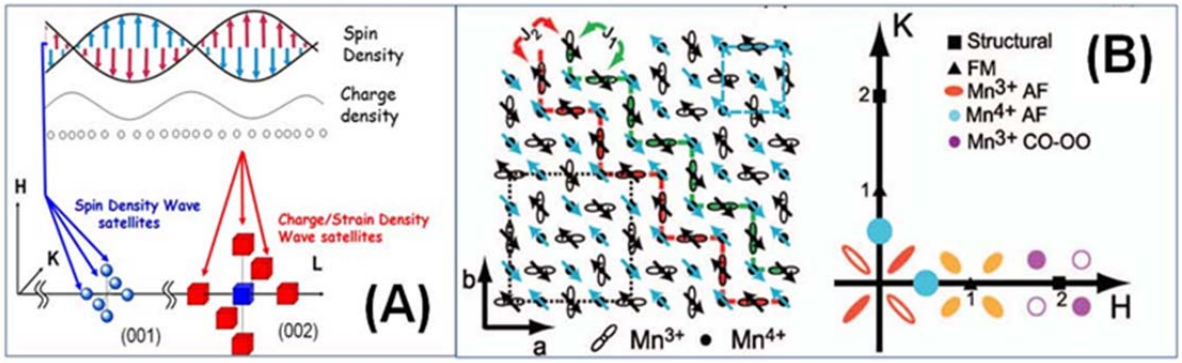

Figure 1.3.2: Representation of Charge-, Spin-and Orbital-order parameters as satellites in reciprocal space: (A) Charge Density Wave and Spin Density Wave in Chromium. Adopted from [9]; (B) Ferromagnetic (FM), Antiferromagnetic (AFM), Charge-Ordered (CO) and Orbital-Ordered (OO) phases in the nearly half-doped perovskite manganites in the cubic setting. (From [53])

diffraction is unique in providing detailed nanoscale distribution of both crystalline imperfections (strain, defects) and the structure of charge-, orbital- or spin-ordered domains. Such studies would provide us with invaluable insight into how competing electronic correlations emerge and what role crystalline disorder plays in their formation.

The ways in which spin-, charge-, orbital- and lattice-order parameters can be accessed with X-ray diffraction are shown in Fig. 1.3.2. By varying scattering geometry, one can tune to various charge density or spin density wave satellites, as well as the Bragg peaks originating from the crystalline lattice, allowing for independent access to relevant lattice, charge and spin order parameters. Examples shown include elemental chromium [52] and a mixed-valence magnetoresistive manganite [53].

The development of lens-less imaging based on phase-retrieval algorithms makes it possible to take advantage of the highly coherent X-ray beams from an ERL facility to probe spin, charge, lattice and orbital degrees of freedom in correlated electron systems with nanometer-scale resolution. These types of microscopy studies will answer many fundamental questions about the interplay between these degrees of freedom resulting in complex competition and often coexistence between various ground states. The high coherent flux produced by an ERL will make it possible to study the dynamics of this competition at timescales 100 to even 10,000 times faster than at current 3rd generation storage ring sources. Imaging structures will be 100 times faster, potentially making nanometer-scale resolution routinely accessible.

1.4 Structures of Biological Cells with <10 nm Resolution in 3D

Of immense value to cellular biology would be the ability to visualize sub-cellular components (e.g. nucleus, chromosomes, Golgi apparatus), in defined functional states, with high, 3D spatial as well as temporal resolution. This information is vital for understanding mechanisms of cellular processes and cellular regulation, and would help develop strategies for treating disease. Because no two biological components are exactly alike, crystallization is impractical in most cases and some form of microscopy is required. However, existing lens-based microscopy techniques have limited ability to image sub-cellular structures. For example, the resolution of optical microscopy is typically poorer than 200 nm (except for new super-resolution imaging techniques that require fluorescent dyes inside the target cells). Electron microscopy provides excellent resolution, but normal TEM is poorly suited for thick cellular samples and requires many sections (thinner than 50 nm) to visualize 3D structures.

Coherent X-ray Diffraction Imaging (CDI) is an emerging microscopic technique that fills the resolution gap between optical microscopy and TEM [54]. CDI is a lens-less or X-ray focusing microscopic technique that uses the high penetrating power of X-rays to image biological cells (up to 10 – 20 μm in size) at high resolution in 3D. CDI has the potential to image whole cancer cells and the structure and connectivity of sub-cellular organelles (Figure 1.4.1) [55]. Recently, a resolution of 10–15 nm has been achieved on biological samples [56]. For biological assemblies, the resolution of CDI is ultimately limited by radiation damage [57]. Using

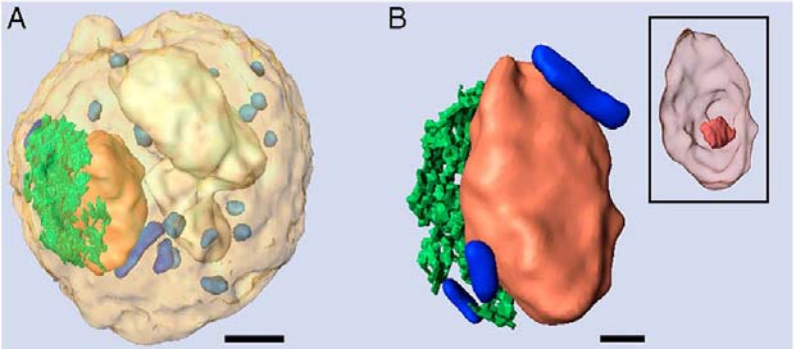

Figure 1.4.1: 3D visualization of the cellular organelles inside a yeast spore cell. (A) 3D rendering of the CDI reconstructed yeast spore. (scale bar: 500 nm) (B) Zoomed view of the nucleus (orange), endoplasmic reticulum (green), and mitochondria (blue) (scale bar: 200 nm). Inset shows the nucleolus, in orange. (From [55])

cryopreservation technologies [58-60], the radiation damage can be mitigated, and a 3D resolution of 5 – 10 nm (or possibly better) might be achieved with the small, bright ERL source. Although CDI has shown potential as a powerful and rapidly developing technique, further development and application has been limited by the availability of intense coherent X-ray sources.

Once routinely available, CDI of biological specimens will have broad impact on medical and biological sciences. For example, CDI in combination with scanning X-ray fluorescence can obtain accurate descriptions of elemental distributions (such as Si, P, Ca, Fe, Cu, Zn) within whole cells [61]. This information can provide clues regarding how trace elements act as carcinogens at the cellular level. The information will also propel our understanding of interactions between cells, such as the competition between hosts and pathogens for critical trace elements. In contrast to electron microscopy and optical fluorescence microscopy, microscopy using highly penetrating X-rays can measure trace elements in whole, unsectioned biological samples, with no need for staining.

1.5 Determine 3D Nanomorphology for Improving Organic Solar Cells

Solution-processed organic solar cells are attractive as low-cost photovoltaic technology [62]. They can be spin-coated or printed like a newspaper, or ink-jet coated onto flexible substrates of plastic or glass. Currently, the most studied solar cell designs are based on bulk heterojunction (BHJ) structures (see Fig. 1.5.1), in which organic electron donor and electron acceptor materials form a complex structure with the goal of optimizing photon absorption, exciton separation and charge transport [63,64].

Commonly discussed is an ideal morphology whereby interconnected, pure phases with domain size of order of the exciton diffusion length (≈ 10 nm) optimize exciton dissociation, and a film thickness of 100 to 200 nm optimizes photon absorption. The complexity of real organic BHJ devices is only partially captured in Fig. 1.5.1. In fact, recent work on miscibility has shown that depicting a BHJ device as a two phase morphology is simplistic [65-67], and a more complex morphology of at least three phases including a mixed phase might have to be considered. Many reports claim control of the nanomorphology [68,69] despite the fact that our ability to characterize film nanomorphology is limited. In order to establish full control over nanomorphology, one needs to not only control the average domain size, but also the domain size distribution, domain purity and domain interface widths. Given the heuristic fashion in which phase separation is manipulated, namely by varying blend ratio [70,71], molecular weight [72], solvent choice [73], solution concentration [74], film drying time [75], co-solvent/processing aids [76,77], or annealing [78], such full control of nanomorphology should not necessarily be expected.

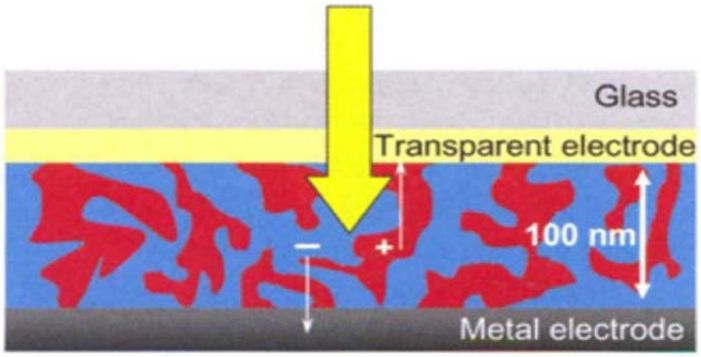

Figure 1.5.1: Visible light enters a solar cell through a transparent upper electrode and is absorbed in the thin organic structure placed between upper and lower (metal) electrodes. The materials and structure of the interdigitated materials determines the efficiency of the solar cell operation. (Courtesy of Harald Ade)

The goal of controlling the nanomorphology of organic photovoltaic blends depends therefore not only on developing new processing approaches, but also upon the ability to characterize structures. Characterization of the three-dimensional structure of organic blends with ≈10 nm resolution thus poses a key technical challenge. Most conventional, high-resolution techniques such as hard X-ray scattering [79] and transmission electron microscopy (TEM) [80] rely on differences in

electron density for contrast in organic materials. This approach has been successful for the study of polymer/fullerene blends, which have sufficient electron density difference. Recent electron tomography measurements have revealed 3D structure in unprecedented detail [81]. However the chemical selectivity of these techniques is limited, and information regarding domain purity cannot be accessed [81]. Furthermore, there is little electron density contrast for polymer/polymer blends, limiting the use of conventional tools for these materials. A new suite of analysis tools such as resonant ptychography or holography with compositional sensitivity are required [24,82,83]. These forms of coherent imaging require bright sources and would be methods ideally matched to ERL.

An ERL source will have great impact on studies of organic materials systems and chemical synthesis and new systems relevant to organic devices under developed by chemists. We are still in the very early stages of the possibilities and opportunities that organic devices offer [84] and a large and growing community is researching these possibilities. For each of these novel materials systems, the miscibility, morphology and domain purity, connectivity of domains, crystallinity, and interface properties need to be measured in order to understand device performance deeply and rationally seek processing and materials improvements. Advanced imaging tools of the future require a high-repetition-rate ultra-high brightness source of coherent soft X-rays that ERLs provide.

Workshop 2: Biomolecular Structure from Nanocrystals and Diffuse Scattering

2.1 Introduction

Open any modern molecular biology textbook and invariably a significant fraction of the figures will have been directly dependent on crystallography. Aside from genetic engineering, nothing has impacted the biosciences more than the ability to obtain structural information on large biomolecules by synchrotron X-ray crystallography. Clearly, the technical challenges of standard protein crystallography have largely been overcome, and the static structures of proteins that yield reasonable sized (~30 μm or larger) crystals and diffract well can usually be solved. Two main challenges in structural biology are looming. First, many important systems in the cell - membrane proteins, large complexes, and labile systems with flexible components – do not readily crystallize. How are structures to be obtained from these species? Second, cellular biomolecular machinery is not static: movement is needed for biomolecules to function. How can we come to understand the structural dynamics of molecular systems as they respond to changes in environmental conditions, binding of substrates, signal transduction across membranes, active site reconfiguration during enzyme catalysis, etc.? Progress on these challenges would have enormous impact on all the biomolecular sciences. It is not an exaggeration to predict that if these two challenges could be solved, the impact on the biomolecular sciences would be every bit as great as the genetic and biostructural revolution of the past 30 years.

The second XDL2011 workshop explored how ultra-bright X-ray sources could help address these two challenges. Note that this workshop was specifically focused on macromolecular structure and dynamics. Biology is a very broad field, and biostructural questions are hardly limited to molecular length scales. For example, much of biology is concerned with the structure, organization and dynamics of cellular organelles, or the hierarchical manner in which biomaterials are organized to make up bone, teeth, shell, skin, etc. These larger scale structural and dynamical questions were addressed in other XDL2011 workshops (see section 1.4).

2.2 Nano-crystallography

Many macromolecular systems that do not readily form large crystals might still yield nanocrystals. Every protein crystallization experiment is actually a nonequilibrium experiment involving two sequential steps: first, homogenous nucleation conditions must be created to induce nanocrystals to form, and then conditions must change to induce a few of the crystals to grow to a size suitable for X-ray analysis [85]. Evidence is accumulating that the first step may be much easier than the second: eight years of experience at the Hauptmann-Woodward high-throughput screening laboratory (HTS) are archived via images of more than 16 million microliter-scale crystallization trials comprising almost 11 thousand proteins. Visual analysis of the archived data show that precipitates obtained in apparently unsuccessful protein crystallization experiments are, more often than not, microcrystalline or contain microcrystalline components. Kim and Gillilan at CHESS have quantified this (through a collaborative effort) analyzing crystal size distributions for images of 68 of these proteins associated with the Northeast Structural Genomics Consortium. They studied 104,448 of the HTS laboratory images (Fig. 2.2.1) and found that tiny visible crystals occurred approximately 50% of the time.

These optical observations have been complemented by X-ray powder diffraction observations by Robert Von Dreele (APS). Protein patterns were recorded from HTS laboratory crystallization precipitates in which it was not possible to distinguish any vertex-edge-face microcrystal morphology by light microscopy. These crystals are in the sub-micron to micron size range, and we refer to them as nanocrystals in the present context. These nanocrystals occur very commonly. Fromme and Spence [86] have argued that even in the case of membrane proteins, for which relatively few crystal structures have been solved, nanocrystals occur relatively commonly in 30% of their trials. It has also been noted that crystalline inclusion bodies form naturally in many cells and can be induced under appropriate conditions [87]. Von Dreele [88] noted that protein powders consisting of very small crystals exhibit Bragg diffraction lines that are instrumentally limited, suggesting that the constituent crystals are nearly perfect. Taken together, these observations suggest that the ability to obtain structure from nanocrystals would in many cases overcome the need for large crystals that presently is the primary bottleneck in the determination many protein structures.

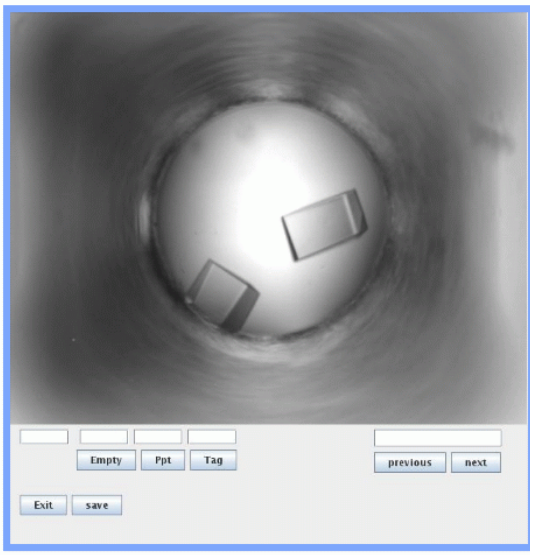

Figure 2.2.1: Well containing small crystals, from the survey of HTS images [S. Kim and R. Gillilan, private communication].

XDL2011 participants generally agreed that it is (or will be) technologically feasible to obtain and handle nanocrystals, and ultimately acquire complete data sets using a large number of nanocrystals. Many questions pertaining to structure from tiny crystals were considered: how difficult is it to grow nanocrystals of membrane proteins and complexes? Are nanocrystals generally more perfect than larger crystals? What are the implications of the larger surface to volume ratio of tiny crystals? How does the time-dependent radiation damage component of room temperature crystals scale with dose rate? What are the best procedures to handle nanocrystals and to acquire and analyze diffraction data? In each of these cases, workshop speakers suggested possible approaches to answer the questions, so as to obtain macromolecular structure from nanocrystals. The single most important X-ray source requirement identified is the need to go beyond storage ring sources to achieve more intense, low-divergence mi-

crobeams for nano-crystallographic experiments. Since the intensity of such beams is directly dependent upon the spectral brightness, it became clear that rapid progress will require sources with greatly enhanced brightness capabilities. It also emerged that while brighter sources are necessary, they are not sufficient: there must also be a large number of technical developments that would enable effective utilization of the microbeams, including: X-ray optics, methods to produce and assay microcrystals, methods to introduce and manipulate microcrystals in the X-ray beam, better detectors, and new methods of data analysis (especially with low count per pixel, Poisson noise limited data).

Protein nano-crystallography with an ERL complements methods being developed at X-FELs, yet differs in distinctive ways. In round numbers, it typically takes on the order of 10^{15} diffracted X-rays to produce a high resolution atomic structure of a typical modest molecular weight protein. Radiation damage limits the number of X-rays that can be tolerated, and hence the structural information that can be obtained from a protein crystal. X-FELs take advantage of the fact that X-rays are diffracted from a nanocrystal before the crystal is destroyed by massive photoelectron ejection and the subsequent Coulomb explosion. However, the number of X-rays per pulse is limited, and most X-rays are not absorbed by the nanocrystal; thus, many pulses, and many nanocrystals are required. For example, Boutet *et al.* [89] used the LCLS to solve the structure of hen egg white lysozyme, a modest-sized protein that crystallizes with a unit cell of 79Å x 79Å x 38Å, to a resolution of 1.9Å. The crystals were typically 3 μm^3 in volume. Over 10^6 images were required. If these were acquired continuously at the maximum 120 Hz repetition rate of the LCLS this would take ~10^4 seconds, or several hours of data collection. This time will certainly decrease as the experiment improves.

The experiment at an ERL would need to be performed by rapidly shuttling crystals into the intense ERL beams for a time (<1 ms) before the room temperature crystals were radiation damaged. However, in principle, many crystals can be examined per second. Depending on the assumptions of how the experiment would be done - which is the subject of current research - one calculates data collection times that range from minutes to a few hours.

The important conclusion was that for both the ERL and X-FEL experiments, data collection times are small relative to the time it would take to prepare samples. Moreover, an ERL can have many ports operating simultaneously. The end result in both cases is that the crystallization bottleneck will move from the preparation of large crystals to the preparation of nanocrystals, assuming the availability of an adequate number of ERL and/or X-FEL experimental stations devoted to this type of experiment.

2.3 New Opportunities in Time-resolved Solution Scattering

The popularity of biological X-ray solution scattering has grown dramatically in recent years due to a confluence of algorithm advances, availability of synchrotron sources, and changing needs of researchers in molecular biology [90]. Continuing advances in computation have pushed solution scattering far beyond the basic structural parameters and model testing once associated with the method. As such, the method now plays an important complementary role in molecular and structural biology [91]. Compared to crystallography, solution scattering is a low-resolution technique, *but advances in algorithms have demonstrated that scattering profiles contain far more detailed information than previously thought.* In addition to answering questions about the basic size, shape, and oligomeric state in solution, the method also yields information about flexibility, unfolding, and interparticle interactions. It can help distinguish between competing structural models. It has been combined with NMR data and atomistic simulations, and used to determine spatial distributions of domains with flexible linkers. Novel uses for the data are appearing regularly in the literature.

Solution scattering data can be collected from a wide range of physiological solution conditions without the need for crystals. In addition to projects such as structural genomics, which

naturally generate large numbers of samples, routine solution scattering requires multiple dilutions of every sample to control for interparticle interference and possible concentration effects. Further, variations in buffer composition, pH, ionic strength, and other additives are of increasing interest as molecular biologists seek to understand the behavior of molecular assemblies in the cellular milieu.

The structural biology community is increasingly shifting emphasis from single proteins towards large multi-component complexes, such as cell surface receptors, molecules with intrinsic disorder, transient conformational intermediates, domains with flexible linkers, and other challenging systems that are often beyond the reach of current crystallographic methods. Solution scattering plays a unique role in biology quite different from that of crystallography. Questions about monodispersity, oligomeric state, and folding are of vital interest during the early stages of sample isolation and purification. Because of its inherently lower information content, solution scattering must be used in conjunction with other complementary biophysical techniques (such as multi-angle or dynamic light scattering, size-exclusion and gel chromatography, sedimentation velocity/equilibrium, circular dichroism, mass spectrometry etc.), but it applies to a very wide range of physiological conditions.

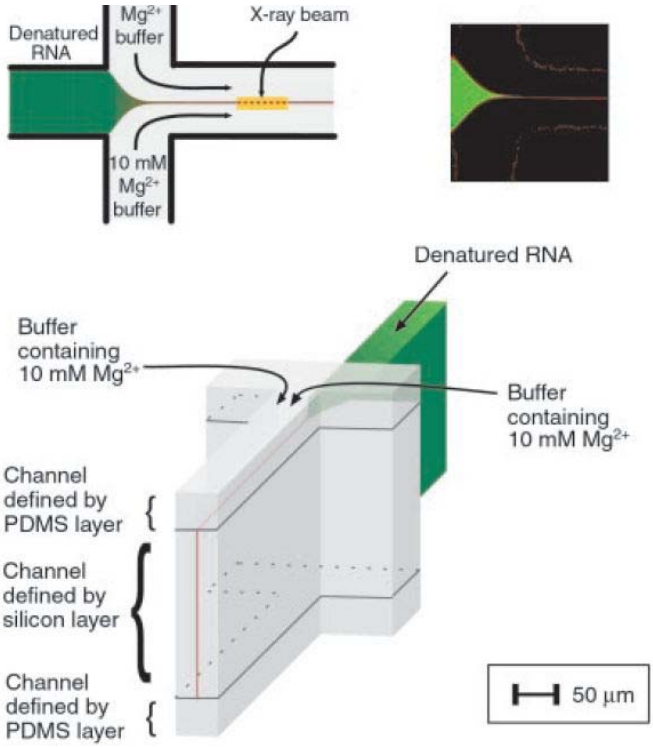

Fig 2.3.1: A lamellar micromixer (top) relies on the rapid diffusional equilibrium between a jet sheet of sample solution, in this cas RNA, and the surrounding buffer solutions. The equilibrium time goes as the square root of the sheet thickness and can be in the microsecond regime for micron widths. The vertical sheet thickness provides substantial length of sample. High X-ray brilliance is required to measure scattering from the micron-wide beams along the vertical sheet thickness. (From [97])

Solution scattering is increasingly yielding information about labile, transient species and time-dependent phenomena. The time resolution of a time resolved solution scattering experiment has both intrinsic and extrinsic components. The intrinsic part is simply the time it takes the macromolecular system to execute a structural change, once excited by some change in an environmental variable, such as solution chemistry, temperature, pressure, or light activation. The extrinsic time resolution is set both by the time it takes to initiate the change for a majority of the specimen and, once initiated, the time needed to acquire the relevant X-ray scattering data. The goal of all time resolved solution scattering experiments is for the time-resolution to be limited by the intrinsic, rather than the extrinsic factors.

Many vitally important processes involve changes of macromolecular structure in solution. Changes in solution pH, solvent or ionic environment cause proteins and nucleic acids to fold and unfold, polymers to collapse or disperse, cell cytoskeletal proteins to assemble or disassemble, multimers to come apart or aggregate, macromolecules to adsorb or desorb from surfaces, motor proteins to change the way they “walk” along tubulin fibers, etc. Understanding these processes experimentally requires a means for rapidly changing solution conditions and a method to probe the subsequent structural alterations. Conventional X-ray methods using

stop-flow mixers are limited to changes on millisecond time scales, and even then are feasible only if adequate quantities of solution are available [92]. These limitations exclude the vast majority of macromolecular systems of interest.

The invention of the lamellar flow X-ray micromixer [93,94] allows solution conditions to be changed on microsecond time scales (Fig. 2.3.1). These mixers take advantage of the fact that diffusional equilibrium occurs on microsecond time-scales for adjacent lamellar flows that are submicron in thickness, and require relatively low-volume, micron-wide streams that conserve scarce chemicals. Lamellar micromixers have been applied to understand protein [94,95] and nucleic acid folding [96,97] using small-angle X-ray scattering (SAXS).

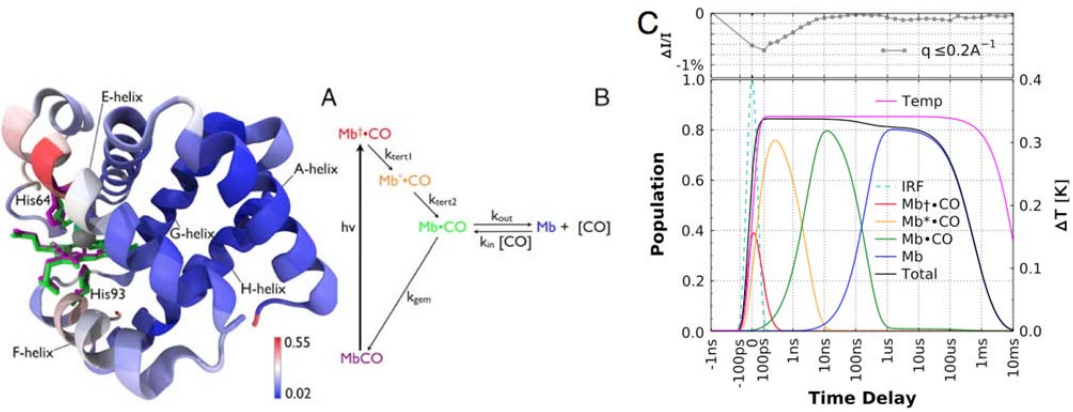

Figure 2.3.2. (A) Time-resolved SAXS/WAXS experiment showing photodissociation of carbon monoxide bound to myoglobin (Mb.CO). A current state-of-the-art 3rd generation synchrotron source (APS) has allowed researchers to follow the evolution of states (B) down to a time resolution of 100 ps. Analysis of the scattering profiles shows the time-evolution of populations of intermediate states and yields valuable structural parameters for putative models (C). (From [98])

Solution SAXS is inherently weak and signal strength is exacerbated by specimen dilution and very small diffracting volumes inside the mixer's central lamellar stream. Experimental signal-to-noise is ultimately set by the strength of scatter from the macromolecule solution relative to that from illuminated side-streams. This necessitates probe beams that are both intense and of submicron size to interrogate the central stream with minimal inclusion of side-streams. Micromixer experiments are presently limited by source brightness to millisecond or greater time resolution at even the most intense X-ray sources. The extremely intense ERL beams will open a new frontier in studies on protein molecule dynamics not presently accessible, enabling micromixer experiments at microsecond timescales, higher spatial resolution, or using more weakly scattering systems, and providing higher spatial resolution.

Time-resolved studies using optical excitation have reached far shorter time resolutions [98] (see Fig. 2.3.2), but the minimum time resolution achievable using X-rays from storage rings is limited by the X-ray pulse width to ≈ 100 ps. ERLs improve the time resolution of SAXS/WAXS to ≈ 100 fs, orders of magnitude better than with present day storage rings.

Solution wide angle X-ray scattering (WAXS) studies can be used to test detailed molecular models of proteins and complexes; to characterize their structural ensembles; to study reaction intermediates; and to locate individual atoms within proteins or complexes. These studies invariably require the measurement of very small difference intensities; comparison of multiple patterns – potentially hundreds – collected sequentially; and multiple exposures of individual samples. These requirements will demand an X-ray source of superb stability and high intensity utilizing X-ray optics that give rise to very low background scattering. Experiments that currently require heroic effort at a storage ring can be made routine once ultra-stable, high brilliance sources are available.

An ERL also has unique advantages for anomalous solution scattering. Anomalous scattering from protein solutions uses the resonant scattering from specific atoms. It can be used to determine the distance an anomalously scattering atom is from the center of mass of a protein; and, in principle, the distance between different anomalously scattering atoms. Use of naturally occurring metals such as sulfur and iron as well as introduced labels such as selenium will make it possible to address numerous biological problems. This type of experiment requires broad energy tunability of the source. Experience has shown that these experiments stretch the capabilities of third generation sources. The experiments are not possible at a X-FEL since precise control of the X-ray energy and intensity is required. An ultra-stable ERL would be an excellent source for these experiments.

Workshop participants discussed other ways in which an ultra-bright source would facilitate study of solutions of biomacromolecules. For example, solution SAXS and WAXS suffer from radiation damage exacerbated by the chemically reactive free radicals induced by the X-rays. This requires the frequent introduction of fresh specimen solution into the beam, thereby limiting experiments in cases where only small amounts of sample material are available. Dmitri Svergun noted that even in the absence of substantial cryoprotectants, solutions can be cryocooled into the glassy state if the temperature drop is very fast, on the order of 10^6 K/s. This can be done with very thin (micron) size samples. Once cryocooled, the radiation damage resistance rises by orders of magnitude. Solution scattering from these very thin samples requires an ultra-bright source to produce the very thin beams needed to obtain data at reasonable rates.

Workshop 3: Ultrafast Science with Tickle and Probe

If you don't understand function, study structure. Francis Crick [99]

3.1 Introduction

Over the past 100 years, X-rays have played a critical role in developing a large fraction of our fundamental understanding of the atomic-scale structure of matter. Yet, from a biological or technological perspective, understanding function is the goal. Therefore, the next step is developing an atomic-scale understanding of function. Function is a sequence of events in time characterized by structural modifications. Thus, perhaps Crick should have said, "If you want to understand function, study time-dependent structures."

Deciding exactly how to study time-dependent structures is a subtle question. For non-equilibrium systems, the assumption of ergodicity is not true; time averages and ensemble averages are not equivalent. Even for ergodic systems, time-averaged quantities can behave differently from their ensemble-averaged counterparts, irrespective of how long the measurement time becomes [100]. Single molecule-tracking experiments, which follow the behavior of a single molecule in time, obtain different values than experiments that measure the ensemble average.

The pump/probe technique is a common method for performing time-resolved experiments. An ultra-fast optical pump pulse initiates evolution in the system, and some time later a probe pulse characterizes the sample. Repeating the measurement many times at many different time delays records the time sequence. In a conventional pump-probe experiment, pumping the system as hard as possible drives the largest possible fraction of the sample into the excited state. In this limit, utilizing the most powerful probe pulse possible maximizes the signal. However, this technique is not universally applicable nor always desired. Some systems saturate, bleach, or have some type of feedback mechanism that limits the response to the pump. For example, optical pumping of charge-density wave systems creates amplitude excitations that destroy the charge-density wave state – pumping too hard "bleaches" the system. Photosynthetic systems have a feedback mechanism that limits the absorption of light. In other cases, the

probe pulse alters the system. The “diffract and destroy” technique for crystallography using nanoparticles recently developed at the LCLS is one example.

At the other limit, an experimenter needs to measure lowest lying excited states – elementary excitations. What, for example, is the structure of the lowest lying electronic or vibrational excitation? In this case, the pump needs to be as delicate as possible and the probe needs to be non-perturbative. Hence, we get the notion of first “tickling” and then probing the system.

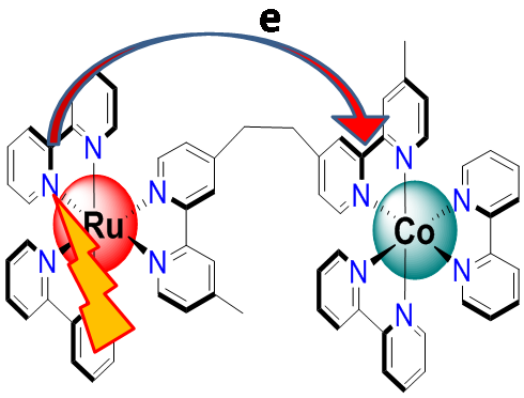

Figure 3.2.1: (left): $[(bpy)_2 Ru^{II}(tpphz)\ Co^{III}(bpy)_2]^{5+}$ (bpy=2,2’–bipyridine, tpphz-tetrapyrido [3,2-a:2’3’-c:3”, 2”-h::2”’,3”’ -j] phenazine), and the photocatalytic process to be studied. This molecule may serve as a template for TR structural dynamics in general: XAS can be used to determine oxidation states (or shifts thereof), XES can reliably determine the spin state and X-ray diffuse scattering (XRD) can deliver information about the environmental dynamics (e.g., internal vibrational relaxation IVR, and cage reorientations). This example demonstrates the need for simultaneous complementary structural tools. (From [104])

The nature of the X-ray pulse train from an ERL is complimentary to that of an X-FEL. An X-FEL produces very intense pulses at low repetition rates (100Hz @ LCLS); the ERL will produce small pulses at very high repetition rates (1.3 GHz); however, the time-averaged flux of these two sources is the same. High repetition-rate pump-probe experiments on atomic length- and time-scales take place in a largely unexplored regime of experimental phase space. Clearly, due to the low signal/X-ray pulse, ERL experiments will require signal averaging over many pulses. On the other hand, ERL pulses will not damage many samples. Since samples must relax between pump pulses, experimenters may be able to utilize several ERL pulses per pump pulse. Weak optical pumps (e.g., Ti:Al_2O_3 laser running at >800MHz), nanofabricated (e.g. stripline) excitation/sample cells, and ultrafast THz pulses are possible ultra-fast pumps.

Spectroscopic studies, especially time-resolved spectroscopic studies, are ideally matched to the ERL. X-ray Absorption (*e.g.,* tr-EXAFS – local structure around specified element, tr-XANES – valence electronic structure) and Emission (tr-XES) spectroscopies require very stable X-ray beams. These spectroscopic techniques can be combined with time-resolved (diffuse) scattering to obtain local structure and are particularly powerful for systems with intrinsically low crystallographic resolution.

3.2 Dynamic Studies in Photochemistry

Understanding ultrafast elementary mechanisms of charge transfer and spin-switching of molecules is a lasting problem, the subject of many efforts in the last decades, both theoretically and experimentally [101-103]. Many details of such processes have been brought to light with ultrafast laser spectroscopies; however, just understanding which intermediates are accessed in the first few tens to hundreds of femtoseconds following photo-excitation remains an elusive component of a complete description. This emphasizes the need to understand fundamental chemical physics phenomena, including the elementary steps of photochemical reactivity. Understanding these phenomena should have direct influence on chemical applications, including improved dye-sensitized solar cells and photo-catalytic activity. Understanding the origin of these different dynamics has the potential to positively impact the future development of functional materials.

Understanding the function of a photocatalytic system is a difficult task, since it involves a complex combination of changes of electronic and geometrical structure. The previously studied entangled dynamic processes in $[Fe(bpy)_3]^{2+}$ is a central theme for various transition metal complexes with photophysical or catalytic functionality, and emphasizes that the overall efficiency is determined on ultrafast time scales. Time-resolved X-ray spectroscopy and scattering have the potential to provide both local and global structural dynamics information down to the molecular time scale of femtoseconds.

Recently, researchers have taken the first steps towards structural dynamics studies of a multichromophoric Ru-Co transition metal complex with its potential for catalytic functions. The transient XAS after 400 ps on the Ru-Co polypyridyl complex (Fig. 3.2.1) reveals the (final) structural changes around the central Co atom [104]. Light absorption by the Ru-moiety results in i) ultrafast electron ejection from the Ru-center followed by ii) intramolecular vibrational relaxation (IVR) processes, which may prove responsible for the observed efficiency for iii) charge transfer to the Co ion, which leads to a iii) spin conversion of the Co moiety (to above 80 %). Combining XES and XRS with fs time resolution has the potential to deliver a quasi-motion-movie of the entire process involving nuclear and electronic rearrangements. With fs-XES, one can monitor the charge arrival to Co and the spin conversion therein. fs-XRS will reveal the overall the molecular structural dynamics between the sandwiched Ru and Co centers, and may prove its capability to observe ligand structural changes as well.

The combination of ultrafast XAS and XRS on transition metal complexes with realistic photochemistry is the first important and necessary step towards the study of fully catalytic complexes. Light absorption in fully functional systems will trigger a complex sequence of electronic structural changes and changes of molecular structure, the latter involving both the catalyst itself, as well as caging solvent molecules (e.g. water), which are believed to take part in the catalytic event. The aforementioned combination of XES (spin state) and XRS (geometric structure) will allow researchers to distinguish the various processes and relate them to the overall catalytic reaction and function of the catalyst.

Pump-probe spectroscopies at pulsed X-ray sources have commenced at 1 kHz repetition rates. This repetition rate was mainly chosen due to the 10^{13}-10^{14} photons per pulse available (ca. 0.1 – 1 mJ pulse energy); typical SR beamlines have on the order of 1-300 micron X-ray spot sizes, which combined with typical sample thicknesses (0.1 mm) and concentrations (0.01 - 0.1 M), have roughly the same number of chromophores in the X-ray (probe) beam as laser photons available for pumping. With the advent of intense fiber-based laser systems with 1-10 µJ pulse energy in the visible domain, and all this at 0.1-10 MHz repetition rate, there is currently a switch going on towards these systems. MHz repetition rates combined with X-ray spot sizes on the order of 10 µm would allow moving every illuminated spot out of the X-ray beam for each shot (with jet speeds on the order of 50 – 100 m/s, which is feasible today). Therefore, such studies can take

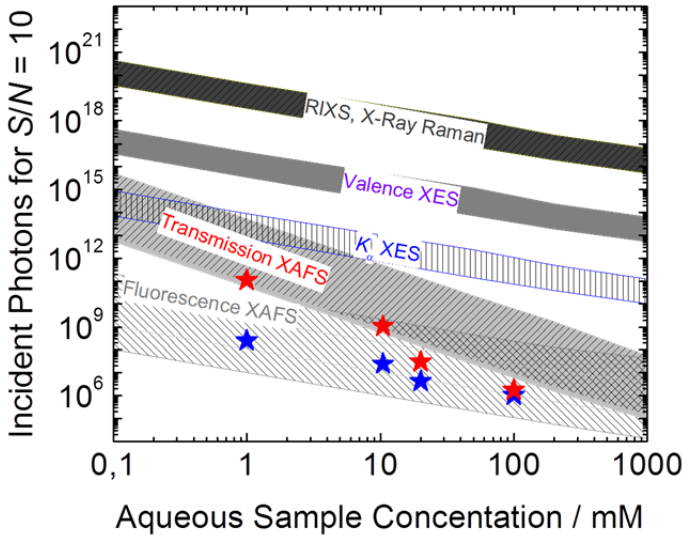

Figure 3.2.2: Feasibility of solution phase experiments. (Courtesy Christian Bressler)

advantage of the much larger X-ray repetition rates at an ERL. Such studies can be quite flux demanding (Fig. 3.2.2).

3.3 Ferroelectric Switching and Superionic Conductivity with All-Optical Control

ERLs offer exciting opportunities for understanding both reversible and metastable dynamical processes in solid state systems, as well as the promise of mapping the boundary between the two. Key to this is developing means of driving repetitive dynamics along well-defined atomic-scale degrees of freedom.

As an example, in order to understand speed limits on ferroelectric/multiferroic switching (important for next generation information storage applications) one would like to be able to resonantly drive the soft modes which underlie ferroelectricity, by applying quasi-half-cycle pulses in all-optical geometries. A recent theoretical paper suggests that efficient ferroelectric switching can be obtained by coherent synchronization of shaped THz pulses with the anharmonic oscillations of the soft modes [105]. This paper also explored bypassing an energy surface barrier between up and down domains by clever manipulation of the polarization of the THz pulse with respect to the polarization of the film, leading to ferroelectric polarization reversal using less total power (Fig. 3.3.1). The high rep-rate of the ERL may enable the generation of this THz sequence directly from the electron beam, which would enable phase-synchronous pump pulses without timing jitter. In this experiment one would like to simultaneously apply X-ray scattering techniques looking at both Bragg peaks as well as diffuse scattering in order to visualize the atomic-scale response.

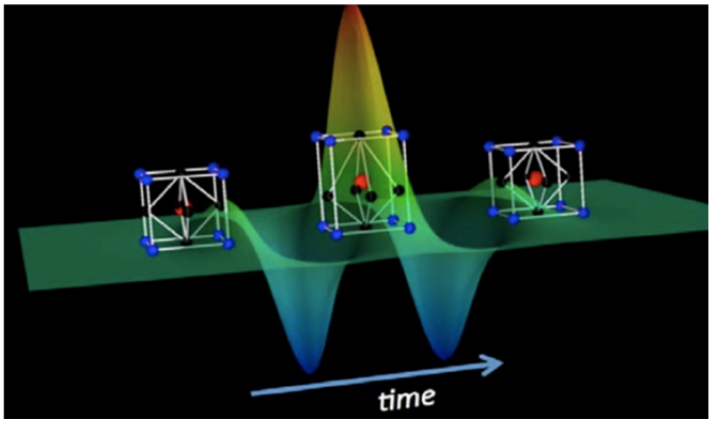

Figure 3.3.1: THz radiation can provide coherent optical control of polarization to bypass the energy surface barrier between up and down states. (From [105])

Another application involves the intrinsic dynamics associated with superionic materials (such as solid-state electrochemical cells), which are important for next generation energy capture and storage applications. These compounds, which exhibit ionic conductivities of order 1 Ω^{-1} cm^{-1}, incorporate one ionic species which moves with liquid-like diffusivity through an otherwise fixed crystalline lattice [81]. One would like to understand the response of the lattice to motion of an ion, but this requires the ability to push an ion in a well-defined direction before coupling to atomic-scale X-ray diffraction probes. Once again, this can be enabled through THz excitation resonant with the ionic plasmon mode of the superionic state. This work could potentially have a large impact on the development of and understanding of the factors limiting the performance of electrochemical devices.

A central goal of the work described above is the demonstrated control of atomic-scale electric functionality - whether by switching and enhancing polarization density or by accurately driving conducting ions - in electrode-less geometries and on “ultrafast” time scales. The combination of high repetition rate mild pumping (tickling), with strictly zero timing jitter makes the ERL an ideal source for these studies. One expects flux increases of 10^4 relative to existing state-of-the-art slicing and low-alpha sources.

3.4 Time and Momentum Domain Inelastic Scattering from Phonons

Time and momentum resolved inelastic scattering from phonons is particularly well suited for studying phonon dynamics: e.g. phonon-phonon and electron-phonon coupling. One motivation is to improve efficiency of photovoltaics. Many of these devices are limited by energy loss from the photo-excited electrons to phonons. High efficiency devices would be optimized so most of the absorbed photon energy, in excess of the band-gap, would not be lost to lattice heating. These measurements can be performed at high-repetition-rate with the femtosecond hard X-ray pulses available from an ERL.

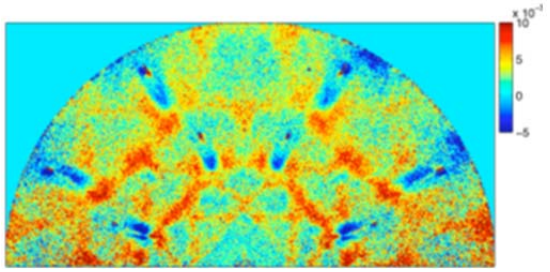

Figure 3.4.1: Time resolved difference in diffuse scattering, 100 and 400 psec after pulsed laser excitation of InP. The method is a momentum and time-resolved spectroscopy of deviations from equilibrium lattice structure, resulting from complex dynamics of phonon populations mediated by electron-phonon and anharmonic coupling between phonon modes. (From [106])

The technique would be uniquely suited for studying electronic and vibrational dynamics with atomic-scale temporal and spatial resolution. In this experiment, an optical laser "pump" pulse is used to excite the sample repetitively, a variable time-delayed hard X-ray "probe" pulse is used to scatter from the excited volume, and the time-resolved diffuse scattering is captured on an area detector. Time resolution comes from a combination of factors: the laser and X-ray pulse length, and time between X-ray pulses. To first order, time-dependent changes in the intensity of a given pixel reflect changes in the population of phonons of a particular momentum transfer (**q**). This would allow one to follow the nonequilibrium phonon population from the initial emission from hot electrons through subsequent anharmonic decay until the lattice thermalizes.

Recent demonstration experiments at a 3rd generation source on photoexcited InP show that the phonon population remains out of equilibrium for hundreds of picoseconds up to nanoseconds (Fig. 3.4.1) [106]. These early experiments have required high optical driving power to massively populate the phonons and the critical early time regime (the first 100 psec. after excitation) was completely inaccessible. The ERL would overcome these limitations by providing both short pulses and the required flux.

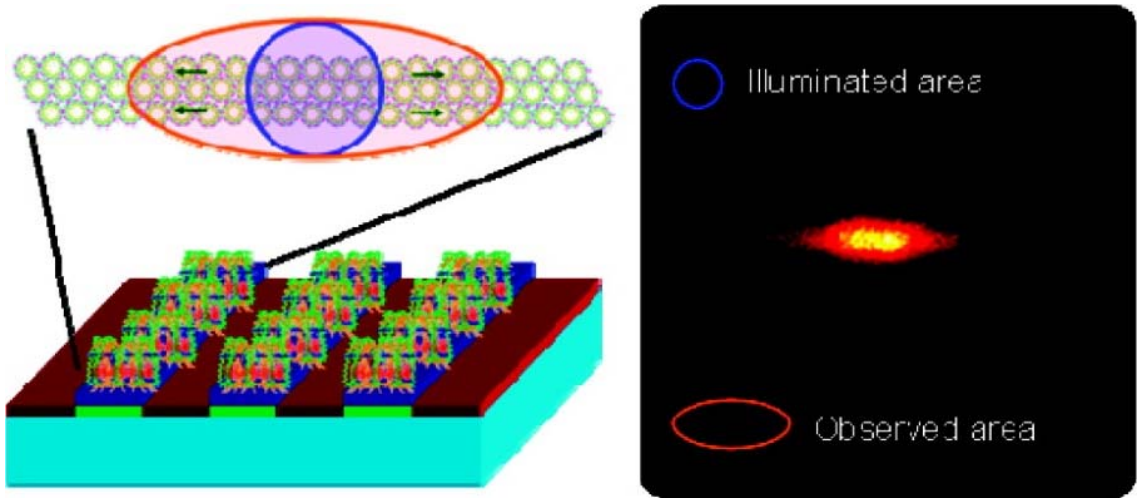

Fig.3.5.1: The first reported observation of long-range transport of excitation energy in a molecular nanoarray constructed from LH2 antenna complexes from Rhodobacter sphaeroides. (From [107])

3.5 Tracking Energy Flow in Light-Harvesting Antenna-Proteins

Biomimetic research attempts to copy or incorporate biological processes or components into engineered materials, processes, and devices. For example, light-harvesting antenna-proteins collect solar energy and efficiently transport the resulting electron-hole pairs to photosynthetic reaction centers where chemistry occurs. The ability of light harvesting molecules to efficiently guide energy makes them intriguing candidates in nanofabricated photonic devices.

In individual proteins, such electronic excitations can travel up to 50 nm and are thought to last hundreds of picoseconds. Figure 3.5.1 illustrates a nanofabricated array of antenna-proteins used in the first direct observations of long-range energy migration in bioengineered, closely packed arrays of LH2 antenna complexes [107]. The experiment showed evidence of excitonic transport of microns, a distance much larger than is required in the parent bacterial system.

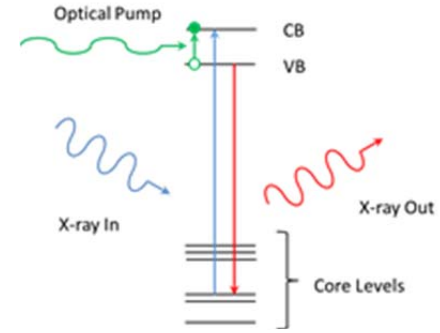

Figure 3.5.2: Resonant coupling of core levels to the valence and conduction band levels can be altered by an optical pulse that controls the relative occupancy.

The spatial extent of transport was determined by an analysis of the fluorescence emission areas in comparison with the excitation area of a laser beam. These results demonstrate the potential of using natural antennas from photosynthetic organisms in hybrid systems for long-range energy propagation. In a wider context, such bioengineering may have a profound impact on strategies to harvest and transport solar energy in devices for sustainable energy production.

The temporal and spatial mapping of charge migration and protein solvation could be resolved on the psec. and 10nm scales using either X-ray Emission Spectroscopy (XES) or Resonant Inelastic X-ray Scattering (RIXS) following an optical excitation. RIXS offers combined sensitivity to unoccupied and occupied electronic structure, so it can distinguish protein response to electron transfer. A mechanism illustrating how RIXS can be sensitive to direct optical excitation is shown schematically in Figure 3.5.2 where laser excitation changes the relative population of valence and conduction bands in a sample. Measurements of this type, requiring X-ray energy tunability, few nm spot size, and high repetition sub-psec. pulses will be enabled by the ultra-high brightness of ERL sources.

3.6 Towards Fourier-limited X-ray Science

X-ray sources did not change much between Roentgen's discovery and the 1st synchrotron sources of the 1970's. These new sources, and the science they enable, have evolved at a phenomenal rate, and now we are on the threshold of a new generation of Linac-based, diffraction-limited light sources, the ERLs and X-FELs. [Diffraction limited implies the product of the X-ray beam physical and angular size is limited (only) by the uncertainty principle.] As amazing as this is, one consequence is that **ERLs offer the opportunity for an ultimate light source; not only diffraction limited, but also Fourier transform limited**. [A Fourier transform (FT-) limited source can perform at the limit set by an uncertainty principle governing the product of the energy bandwidth and pulse width.] These concepts are schematically illustrated in terms of the evolution of synchrotron

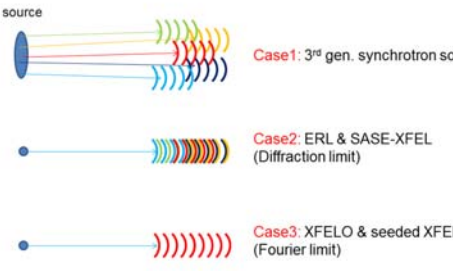

Figure 3.6.1: Linac based sources (SASE-X-FEL and ERL) achieve the diffraction limit but X-FELO or seeded X-FEL sources will be required to achieve the Fourier transform limit. (Courtesy Shin-ichi Adachi)

sources in Figure 3.6.1.

FT-limited sources will generate diffraction-limited beams with 10^9 X-ray photons/pulse within an energy bandwidth of 10^{-6}, at repetition rates up to 1MHz. These beams are ideally suited for studying thermal energy (1meV) excitations that govern most transport properties in solids, as well as technologically important phenomena like superconductivity. For the first time X-ray sources would have all the properties one expects from a laser, and this open up new fields of scientific study. For example: the realm of non-linear X-ray optical processes, the use of multi-photon correlation techniques applied to electronic states and wave packets, and extension of transient grating methods to atomic length-scale. This could allow us to apply the powerful X-ray standing wave method to non-crystalline materials.

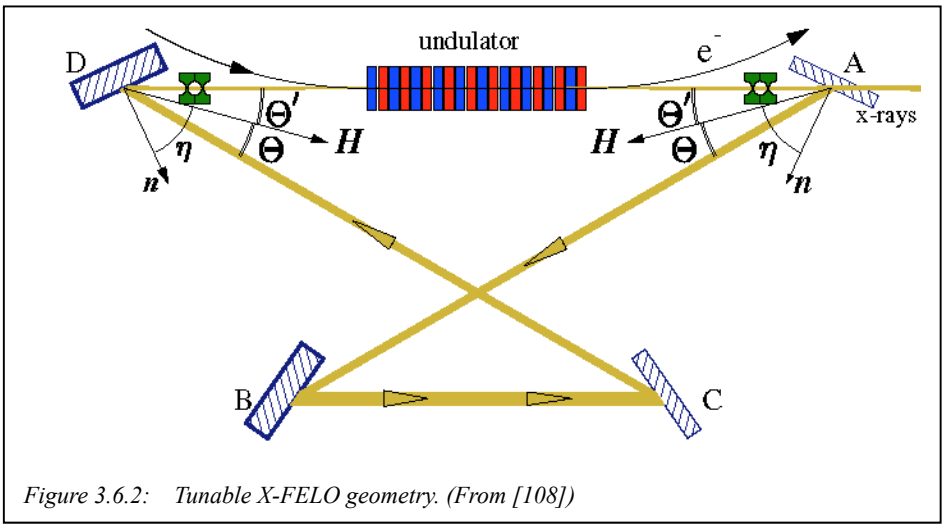

Figure 3.6.2: Tunable X-FELO geometry. (From [108])

This new FT-limited, ERL-driven light source is called an X-ray Free-electron Laser Oscillator (X-FEL-O) [22]. It is based around an energy tunable X-ray optical cavity built of highly perfect diamond crystal plates [108]. The concept is illustrated in Figure 3.6.2.

Workshop 4: High Pressure Science at the Edge of Feasibility

4.1 Introduction

High pressure (HP) studies are a true frontier of condensed matter physics, chemistry, materials, and Earth and planetary science, for exploring physical properties that include phonon, electron and atomic structures, as well as chemical properties such as inter-atomic forces, bonding, reactivity and kinetics. Changes in pressure and temperature cause materials to cross barriers; for example, between insulator-conductor-superconductor, molecular and extended frameworks, and from inert species to vigorously reactive compounds. Along with theory and computation, HP experiments provide insights for understanding the physical and chemical properties of materials as well as their mechanisms of formation.

Third generation light sources have enabled cutting-edge spectroscopy and diffraction studies of materials under compression, but extreme condition studies are almost always photon starved, so many regimes and questions remain unexplored over a wide range of pressures, temperatures, and time scales. For example, static compression studies, even on strong scattering heavy materials, are limited to maximum a pressure of 300 GPa, and for low-Z systems the maximum practical working pressure is below 100 GPa. At the highest pressures, samples are invariably tiny and subject to strain gradients, but ERL X-ray beams can be focused to incredibly small sample volumes. Time-resolved studies require measurement times shorter than the characteristic time-scales for nucleation, growth, change of phase or electronic state, heat transport, atomic diffusion, or chemical reactions. In the extreme pressure region, many time-varying processes are currently inaccessible because they occur on sub-nanosecond time scales.

Recent ambient-pressure studies have shown that full dispersion curves can be obtained from measurement of thermally-scattering X-rays – thermal diffuse scattering (TDS). This enables obtaining dynamical information in seconds and for following dynamics of melting and phase transitions. The upper P-T limits of diamond anvil cells (DACs), currently some 400 GPa and 5000 K, have remained relatively unchanged for a decade. Whole new areas of condensed matter physics, and new physical phenomena, lie tantalizingly out of reach, inaccessible to current techniques.

These important classes of studies require new light sources that produce not only smaller and brighter beams, but generate temporally short pulses with enough photons for time-resolved dynamic experiments under extreme pressure and temperature. The ERL promises to deliver ultra-bright X-ray beams at very high repetition rate with pulse length from a few picoseconds to less than 100 femtoseconds. In contrast to the X-FEL, ERL beams should not damage the DAC and will allow signal averaging by repeated measurement on the same sample. The examples that follow help illustrate potential new avenues of research and discovery that will become possible, or feasible, with an ERL X-ray source.

Dynamic compression creates very much more extreme conditions, but only for very short periods of time, and no structural studies have been performed under such conditions. The short 2ps ERL pulse is ideally suited to diffraction studies of dynamically-compressed matter. Under ramped rather than shock, compression, temperature can be kept low enough for the sample to remain a solid at extreme pressures. While the terapascal behavior of simple matter at 300K will probably always remain unknown, we can expect to obtain detailed knowledge of the structure of solid phases of matter above 1TPa using dynamic compression. *Ab initio* calculations are now predicting a plethora of complex structures at pressures in simple materials such as Li, Al and Mg. We might expect to test these calculations by coupling dynamic compression over ~20 ns, with 2ps pulses from the ERL to study structural phase transitions and melting. Recent experiments at the National Ignition Facility (NIF) have attained pressures of 4.5 TPa in diamond, and future experiments are aiming for 10 TPa in the near future. The installation of a kilo-Joule laser at the ERL will open a new window on matter above 500 GPa, and promises to be transformative.

Next-generation light sources such as ERL offer the possibility to conduct entirely new forms of extreme-conditions science. They provide the means to study structure and dynamics on timescales as short as picoseconds to higher pressures than possible to date, and to make structural studies of dynamically compressed matter of the same quality currently available from DACs. These new machines promise to be transformative and to provide wholly new insight into strongly condensed matter.

4.2 Materials Discovery via High Pressure Processing

High pressure (HP) promotes the synthesis of novel functional materials, not least by suppressing the decomposition of reactants and products that occur under ambient conditions. Large volume high-pressure apparatus produce desirable products unavailable by ambient pressure synthesis, most famously the superhard diamond and c-BN used in industrial composites. The sheer number of phenomena discovered, most without prior recourse to theory as a guide, suggests that there is an ocean of untapped novel materials, potentially with transformative properties. Diamond occurs naturally and was an obvious target for a concerned R&D effort. Theory can provide useful targets for the synthetic chemist, most especially since modern theory can predict those compositions likely to have desirable properties and which structures are stabilized by pressure. Theory continues to generate exciting possibilities for synthesis in areas as diverse as super-hard materials, superconductivity and photo-catalysis. Despite its great promise, HP synthesis is laborious, and compared to high temperature synthesis, is grossly under-utilized - especially in the discovery stage where many experiments may be need to be op-

timized, especially if large volumes of a single phase are needed for bulk property measurements. Further, recovery of non-equilibrium products, which might provide valuable insights into transformational properties, is not always possible. *Is it possible to devise techniques that will allow determination of properties of interest, phase identification and grain boundary mapping to allow imaging of reactions in real time?*

Advances at present generation synchrotron sources notwithstanding, the current infrastructure is not suited to the efficient and exhaustive exploration of *p*T-compositional space that is required to discover transformational materials. Dramatically increasing the amount of information derived from a single HP loading in the LVHPD or DAC would involve combining theory, with the capabilities of ERLs for diffraction and imaging, and with the nation's installed infrastructure and growing expertise in nano-fabrication, to obtain properties, images, and diffraction data *during* the Compression-Heating-Quenching-Decompression (CHQD) cycle from *multiple phases* in the same HP run. If successful, this theory-directed *in-situ*, combinatorial approach will dramatically shorten the discovery cycle, and enhance efforts to identify new materials using more established approaches. The ultimate realization of the goals of this work; to image the materials' properties during the *full* HP synthesis cycle, *in-situ* and in real time, will require the capabilities of ERLs. One example of current topic interest are the oxy-nitrides [109,110] which have potential for water splitting applications. These materials tend to decompose during ambient pressure synthesis, and controls on their composition, especially in the case of solid solutions using commonly used ammonolysis routes, is notoriously difficult.

HP processing offers a novel route toward designer solids and materials discovery, thereby yielding new properties and enhanced performance for energy, biomedical and industrial applications. As a well-known example, HP transforms graphite into diamond that retains the HP structure at ambient conditions. However, most HP structures are unstable, and release of pressure results in loss of the HP structures. For instance, sulfur is a superconductor at HP (as are ~50% of the elements in the periodic table) but this property is usually lost at low pressure [111-113]. Methods to induce metastability of HP structures, so as to preserve HP properties at low pressure, would greatly facilitate useful, real-world applications.

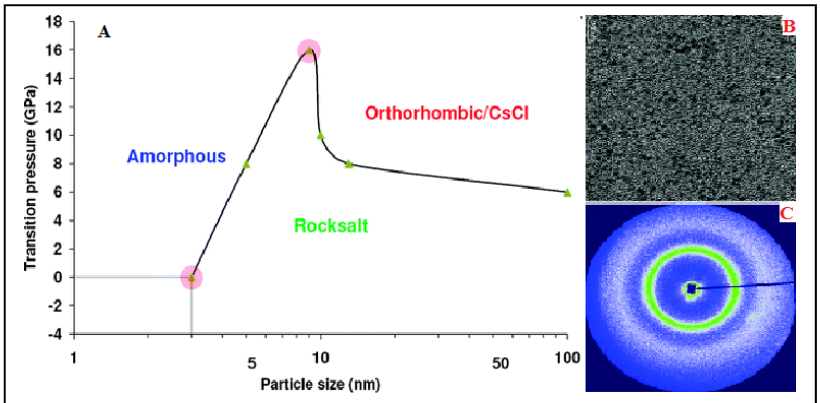

Figure 4.2.1: Schematic of the relationships between the first-order transition pressure and particle size (A); TEM image (B) and corresponding WAXS image (C) of 3 nm PbTe nanoparticles without compression. (From [119])

Nanoparticles (NPs) form a bridge between single atoms and molecules on one side and bulk solids on the other. In addition, they manifest exciting finite-size-related properties in their own right. It was recently shown that NPs undergo structural transformation via single nucleation events under HP [114]. Rather than consisting simply of inorganic cores, many types of NPs require a coating of organic molecules to keep them soluble. Such NPs interact together and assemble into ordered structures of varying complexity [115] and such modification and assembly processes dramatically change the surface energy of NPs. If the surface energy dominates the bulk energy in newly formed designer solids, the structures may be thermodynamically or kinetically trapped as metastable phases at ambient pressure. These strategies require reconstruction of the nucleation and growth routes of metastable structures, from the atomic to the mesoscopic [116]. Pressure and temperature are used to fine-tune the structure of designer solids. High potential energy barriers provided by organic/inorganic and inorganic/inorganic interfaces are introduced

in the material to block the back-transformation to the ambient phase and retain the metastable phase at ambient conditions [117]. To study this, it is necessary to simultaneously observe the structure of the NPs at atomic and super-lattice length scales using simultaneous SAXS/WAXS in a DAC [118]. The resultant X-ray characterization capabilities of materials in well-defined pressure and temperature states are further augmented with several *in-situ* spectroscopic probes.

HP SAXS-WAXS-Spectroscopy in a DAC can be used to study designer solids under HP, tuning the pressure-temperature-composition protocols to yield new metastable materials and examine their properties for potential applications. The scientific impacts can be seen from a series of samples: (1) Materials with metastable structures, discovered under HP, have been retained and further synthesized at ambient conditions only by size-tuning without any pressure at all (Fig. 4.2.1) [119]; (2) Materials consisting of hard composites in organic matrices and displaying enhanced mechanical performance, initially discovered under HP, have now been synthesized so that they are stable at ambient conditions (Fig. 10) [120]; (3) New super-hard materials, created under HP (to obtain higher density), have been trapped in their states by introducing high energy barriers at interfaces; properties were retained at ambient conditions [121]; (4) New catalytic porous nanomaterials have been synthesized by NP fusion via pressure tuning [122]; (5) Single crystal composites for biomineralization have been prepared using the pressure tuning mechanism [123]; and, (6) Strain-tuned and coupling enhanced LED displays, first understood by *in-situ* pressure monitoring of core-shell NPs and inter-NP distance-correlated coupling for NPs in an ordered way [124], have been created by ligand-directed assembly of nanowire arrays without HP [125].

4.3 Understanding Planetary Interiors with an ERL

Seismological and cosmochemical observations indicated that Earth is composed of the crust, mantle and core. However, the compositions and states of the deep lower mantle and the core of Earth, separated by the core-mantle boundary (CMB) at the depth of 2900 km from the surface, largely remain uncertain. The complexities in this region can be seen from a rich range of seismological features observed [126]. To understand the generation of such complexities for better interpretation of seismic data and thus provide new insights about the dynamics, compositions, structure and evolution of Earth and planetary interiors, it requires knowledge of material characteristics such as crystal structure, chemical composition, thermal structure, melt viscosity,

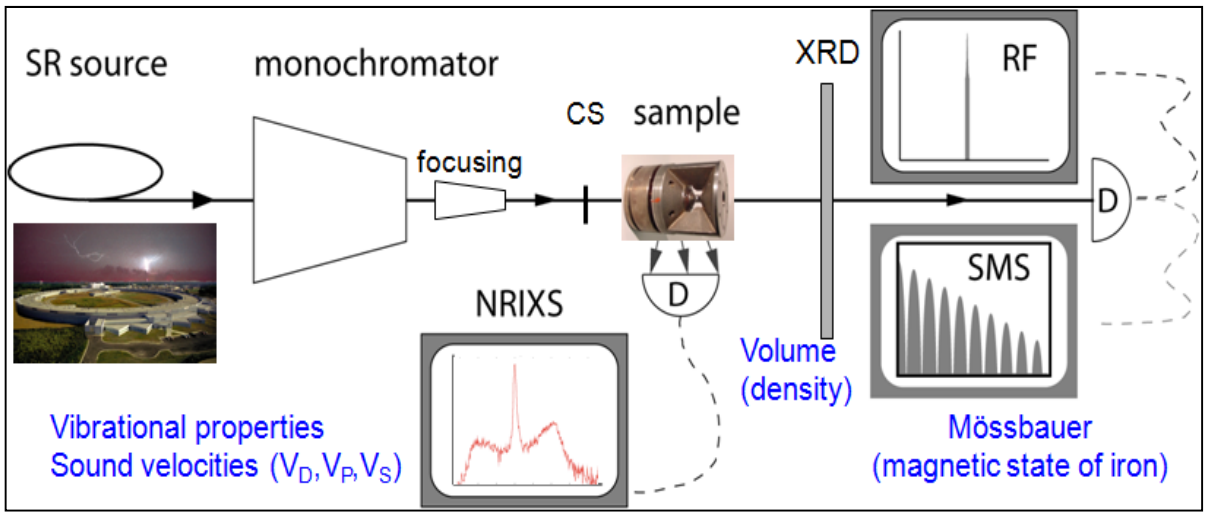

Figure 4.3.1 Measurements of vibrational and other properties using synchrotron X-rays (Courtesy of J. Jackson)

elastic constants, sound velocity and thermodynamic parameters of silicate oxides, iron alloys and other earth materials, in particular for those at pressures in excess of 100 GPa and temperatures greater than 1000K.

These experiments are currently on the edge of feasibility for 3rd generation sources, but many aspects of the structures and properties of materials cannot be performed at extreme pressure and temperature due to complexity of the sample texture or limitation of X-ray flux of small beam. Currently, feasible determination of the vibrational density of states (sound velocities, melt dynamics: other thermodynamics: free energy, vibrational pressure and entropy, mean force constant, atomic displacement, hyperfine parameters) is only enabled at P > 180 GPa at room temperature or P~70 GPa and 2500 K (Fig. 4.3.1). It is pointed out that all these measurements were based only on the single phase loaded into the DAC.

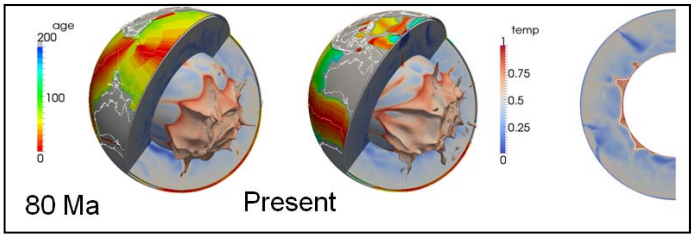

Figure 4.3.2 4D dynamic Earth model that includes surface eruptions, plate motion and thermal plume generation (Courtesy of Gurnis and Bower, Caltech)

However, if we consider the region of the deep lower mantle (70~135 GPa) and the core (135~ 360 GPa) of the Earth, the more realistic assemblages include the multiple phases, sub-micron grain size and multiple orientations. Thus, the ideal experiments are to use sub-micron or nanobeam with enough flux to determine quantitatively the elastic constants for each single phase through focusing X-ray beam on a single grain in the orientation matrix.

The ERL will deliver 100 times more spectral flux/μm^2 than existing storage rings or those under construction in the energy range of interest for high pressure studies. Thus, this ERL delivered beam will enable new classes of experiment like: momentum-resolved inelastic scattering (IXS) and near-edge spectroscopy (Mossbauer) from individual grains within an assemblage inside a diamond anvil cell (DAC), diffraction at unprecedented pressure and nuclear resonant scattering (NRS) at nanometer length scales.

IXS reveals anisotropy of phonon dispersion relations, melting and structural phases are identified by diffraction, and NRS measures acoustic vibrations that yield sound speed. Emission and absorption spectroscopy can simultaneously provide chemical information. Multiple types of information collected from individual grains inside many phased assemblages can be integrated together, providing a systematic understanding of chemistry and physics of the nature sample, and avoiding any uncertainties from integration from separate measurements on each single phase.

The ERL will deliver unprecedented sub-100 nm focused beams to select and image individual grains, measure diffusion constants at microsecond time scales, and reveal liquid dynamics in the pico-to-nanosecond range. Eventually, these measurements will enable us not only to understand seismic anisotropy at the Earth's core-mantle boundary and core and the generation of the melting and magma, but also provide materials property parameters for construction of 4D dynamic earth model (3 Dimensions + Direction of the time) (Figure 4.3.2).

4.4 Synchrotron Techniques: X-ray Tomography and Imaging in Diamond Anvil Cells

The long-term future of the world's energy relies mainly upon transformative materials with extremely useful properties. High-pressure appears as one of the most efficient tools for a broad of studies towards discovering advanced materials and novel phenomena. Achieving such goal requires initial understanding and reconstruction of the nucleation and growth pathway of novel structural materials under pressure, thus allowing for designing alternative routes either to bring

the novel metastable materials formed at pressure to ambient conditions, or to directly make these materials at ambient conditions for real world applications.

The structural stability and newly manifested properties of advanced materials depend on many structural parameters that are related not only to particle size, crystallinity, defect and voids, but also to complex interactions inside bulk materials through various textures, interfaces and boundaries (Figure 4.4.1). These structural components inside bulk display length scale from bulk down to nanometer, and eventually to single molecular and atomic level. Believing is seeing, so one straightforward way is capable of direct observing and unambiguous imaging of crystalline structure, texture and orientation inside materials. This certainly requires development of a series of high resolution tomography and imaging techniques, allowing for *in-situ* visual reconstruction of materials strain distribution, deformation texture and structure change under extreme compression of materials through DAC.

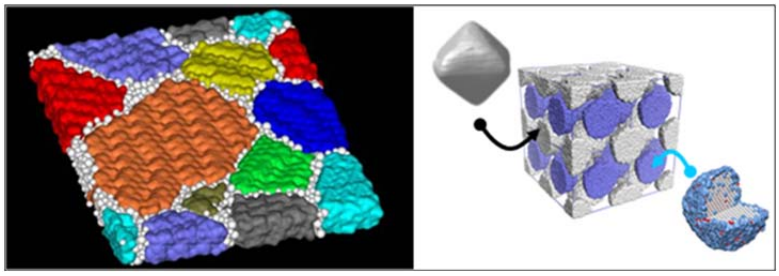

Figure 4.4.1 a) Full atomistic model of a slice cut through a nanopolycrystalline materials generated using amorphisation and recrystallization. The colored domains represent various missoriented grains; grain boundary atoms are shown as white spheres; b) schematic illustrating the positioning of nanocrystals (analogous to atoms) in a face-centered-cubic crystalline structure (Courtesy of Dean Sayle).

Upon rapid development of new generation synchrotron light sources, nanofocused X-ray beams have been developed and used to understand the phase and grain boundary evolution, measure the density *in-situ*, study structure of confined liquids and non-crystalline solids, and monitor strain as a function of pressure. Of particular interest is combining nanobeam X-ray computed tomography (nanoXCT) with diamond anvil cell technology [127]. This capability enables the study of multi-component materials under high pressure and at high temperature. NanoXCT contrast mechanisms not only include absorption, scattering, and element-specific fluorescence, but also inelastic scattering and X-ray Raman scattering [127]. These methods are of high interest to be able to distinguish between different phases and their shape and volume changes under extreme conditions.

Coherent diffraction imaging (CDI) of nanoscale strain has wide application for understanding nanomaterials under extreme pressure and temperature and during deformation or chemical processing. X-ray methods are especially suited for *in-situ* measurements, for example, inside a diamond anvil cell (DAC). Nanoscale materials often exhibit unusual strength so it is important to examine them under stresses that lead to breakdown (Figure 4.4.2). X-ray CDI can also be used to study pattern formation in materials synthesis, for example to understand growth limitations associated with self-assembly in the presence of surfactants.

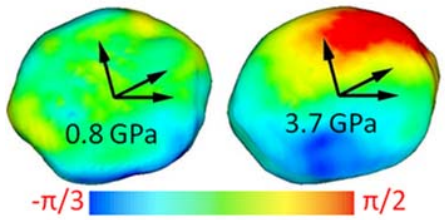

Figure 4.4.2 CDI reconstruction yields lattice strain map of gold under pressure. Left: Phase retrieval methods can produce 3-dimensional strain maps – color represents atomic scale lattice strain along specific directions resulting from pressures and surface truncation. (Courtesy of Wenge Yang at APS)

For these applications [27], the coherent length at current synchrotron sources is very much limited, only allowing one to use very limit source size. ERL will overcome such a limitation, and deliver beam with unprecedented transverse coherence and flux up to 60 keV. The small round X-ray beam source is ideal not only for nanometer focusing but also for matching horizontal and vertical coherence lengths. It turns out that the large co-

herent length will enable probing the sample in size from several hundred nanometers to tens of microns. Thus, using ERL source, coherent diffraction will be able to monitor strain distribution of the samples as a function of pressure, and Bragg CDI and small angle CDI provide ultimate spatial resolution for 3d imaging of the pressurized samples through DAC.

4.5 Static and Dynamic Heating of Materials

An understanding of melting phenomena at high pressure is of fundamental interest, critical for estimating planetary interior temperature and understanding the forming dynamics of planets that create magnetic fields and material transport within planetary cores, mantles and tectonic plates [128].

Melting measurements of materials under pressures have been carried out on a series of metals (e.g. Fe, Mo, W) and silicate oxides (e.g. MgO, FeO, MgSiO3). These materials are either structurally similar to or compositionally related to the dominant minerals of Earth and planetary interiors [128]. The melting data were produced mostly through laser-heated diamond anvil cell (DAC) and shockwave driven experiments [129,130] that represent the state-of-the-art static and dynamic driven techniques, respectively. However, serious disagreement exists between melting phase diagrams of these metals and silicate oxides [131]. As is shown in Figure 4.2.1, the shock-wave studies provided much higher melting temperature at extreme pressures than the static DAC studies.

Many factors could result in such great discrepancies between measured melting temperatures [132]. In shock-wave studies, the determination of reliable melting temperature very much suffers from unknown transport properties of window-used materials through dynamic compression of materials. It was found that use of various window materials dramatically caused the change of melting temperature for the same material over the magnitude of 1000K. In static DAC studies, the laser-induced melting was judged mostly by direct observations of fluid flow, glass formation or some indirect correlations of melting to the sample properties and features. As one additional but very serious concern, previous studies neglected consideration of the sample instabilities and chemical reaction through heating, and lacked direct monitoring of the melting-induced structural change and temperature fluctuation as a function of time as well. For many years, researchers have made attempts to measure melting temperature of materials by synchrotron X-ray diffraction, but systematic melting measurements at extreme conditions of temperature and pressure have not been possible due to the effect of long exposure time on sample environments and unknown structure change of the samples in short time scale.

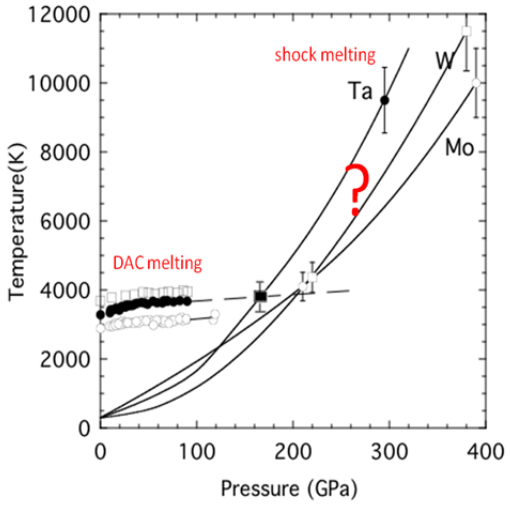

Figure 4.5.1 Melting curves of Ta, W and Mo measured by laser-DAC and shockwave techniques. (From [131])

Recent SEM studies indicate that experimental problems can be circumvented if diffraction measurements can be made at millisecond time scales. This could be accomplished if millisecond pulse-laser heating of samples in the DAC (Figure 4.2.2) were monitored, in time, by sequential, microsecond X-ray diffraction in which the time scale is equilibrant to the order of thermally achieved time scale on the heated samples. Recent discovery indicated that this approach can effectively avoid thermal drifting, chemical reaction and structural transformation that mostly impact on accurate determination of melting temperature. In addition, achieving extreme

pressure in DAC over several megabars reduces the sample size down to several microns or even smaller. Correspondingly, the X-ray scattering signals from such a small volume of samples become dramatically poor or even sink underneath the featureless background. Use of such techniques in characterizing materials melting and associated kinetics requires very small and short pulse X-ray beam that has extremely high flux.

The flux available in ERL pulses and their flexible pulse structure would provide the certainly answer in helping address the possible existence of a plastic-like state before melting of bcc metals like Ta, W and Mo, and the structural evolution of freezing event after melting, and thus precisely understand the melting point of materials aimed at defining the absolute melting temperature unambiguously. Meanwhile, the time-dependent kinetic processes of materials melting, freezing and recrystallization can be also simultaneously mapped out. Through focusing of extremely bright ERL beams, one could selectively sample local stress-strain behavior across the pulse-laser heated sample. This would help provide estimates of sound velocity that will lead to better understanding of the Earth's mantle and core.

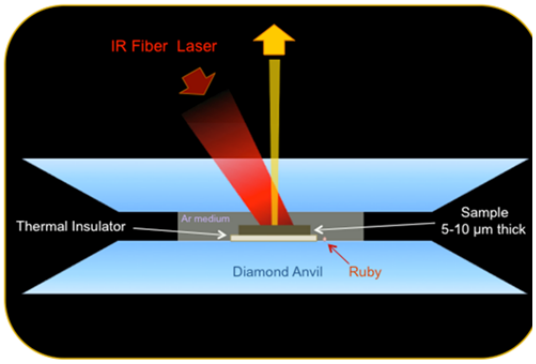

Figure 4.5.2 Diamond cell pulsed laser heating and below melting curves from DAC and shock experiments. (Courtesy of R. Boehler)

Workshop 5: Materials Science with Coherent Nanobeams at the Edge of Feasibility

5.1 Introduction

Advances in materials science lie on the critical path of many technological solutions to society's most pressing problems, such as sustainable energy, environmental remediation and health. Increasingly, scientists and engineers want to build materials that have directed functionalities, mimicking the ability enzymes have in biological systems to build every more complicated structures to accomplish functional goals. As a result, the study of materials will, out of necessity, evolve towards ever increasing complexity such as, for example, larger unit cells, more complicated multi-elemental compositions, heterostructures with sub-micrometer dimensions, and structural modifications at the nanoscale. We will need to control and fabricate structures on many different length scales, from the atomic, through nano, to micron and macroscopic scales. Achieving knowledge and control at these levels requires powerful tools and techniques able to resolve extremely subtle effects. For example, bond-length changes of hundredths of an Angstrom result in large changes in material properties, such as the metal insulator transition in colossal magneto-resistance manganites [133] and the low thermal conductivity above room temperature in PbTe that render promising thermoelectric properties [134].

It will not be sufficient to have tools that can only characterize static structures. We need to probe real materials, *in-situ*, under realistic operating conditions (*in operando)*. We also need to capture information as materials evolve in time, an increasingly important capability because of the growing need to understand and control realistic fabrication and processing conditions. An ideal X-ray probe has to be positioned with sub-micron accuracy, have variable beam size down to a few nanometers, and enough flux and energy tunability to carry out diffraction on nano-sized samples embedded in a macroscopic materials. Most importantly, it must be a non-destructive probe so that materials can be studied as they function.

These goals present two overarching experimental challenges. First, the huge variety in materials systems calls for a large suite of experimental techniques. Second, in many cases the complexity of such systems will require that multiple techniques be brought to bear on the same sampled volumes. 3rd generation synchrotron sources have made tremendous strides in building X-ray nanoprobe instruments to address these needs [135]. For example, the nanoprobe commissioned by the Center for Nanoscale Materials and APS combines a hard X-ray nanobeam of 40 –50 nm with high precision sample positioning [136]. The microscope can run in scanning and full-field modes using a variety of condenser and X-ray imaging lenses. Scanning images based on X-ray fluorescence and scattering contrast can be combined with nanoXRF mapping and is used for strain mapping [137], studies of phase transitions [138], and elemental analysis. In addition Bragg coherent diffraction can be used to obtain images of domains [139]. A second instrument was added to address the needs of the biological, medical, and environmental sciences [140]. This tools will study, for example, fresh water diatom [61] (see Fig. 5.1.1), that play an important role in carbon sequestration in the oceans, or tissue samples for cancer research [141], where trace elements such as copper and zinc have been correlated with tumors or are prevalent in tissues of patients affected by specific diseases [142]. Therapeutic and diagnostic agents often utilize metallic trace elements, and the effect of these drugs and agents on target tissues can be characterized in detail by X-ray probes; proteins or DNA that serve as nanomedicine vectors can be tagged with titania nanoparticles, and their interaction with cell components can be traced [143,144] [13].

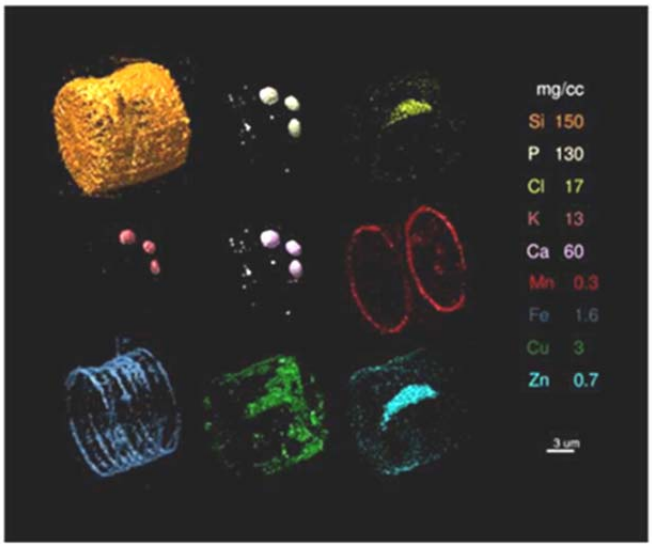

Figure 5.1.1: 3D trace element distributions in a fresh water diatom obtained with nanobeam fluorescence tomography at 50 nm resolution. (From [140])

As tantalizing results arrive, it is clear that applications and needs are pushing tools to work *routinely* – as opposed to heroically - at the nanometer or sub-nanometer length scale. Next generation sources such as ERLs have the potential to expand the spectrum of applications from select examples to a mainstream user technique. High flux, fast scanning, and high-performance detectors will be a great opportunity for ERLs to obtain 3D information in the time-domain on evolving systems. Notably the “round” beams of ERL sources, both with regard to source size and divergence, will help focusing optics achieve optimal efficiency and with superb spatial and angular resolution (with long working distances) with nanometer focal spot sizes.

In terms of impact, below we discuss several experimental techniques and applications showing how nanobeam X-ray technology has the exciting potential to close the resolution gap between real space and scattering length scales, which will be highly beneficial for studying hierarchic structures in materials science as well as biology and medicine. Three-dimensional information will become available via tomography techniques, utilizing absorption and phase contrast as well as fluorescence and scattering [145], including samples under extreme conditions (i.e. diamond-anvil-cells). It has also become apparent that nanobeams have a high degree of coherence – a perfect beam and perfect optics will transform a plane wave into a spherical waves [146]; the coherence of nanobeams can be exploited for coherent diffraction imaging (CDI) [147]. CDI of soft tissue components has been demonstrated, with application to mammography [148] and imaging of collagen fibrils [149]. At an ERL such measurements could be

performed in a time-resolved fashion. An ERL will enable ptychographic Bragg coherent diffraction with curved wavefronts, which has the potential to study structure and strain of both isolated and continuous crystalline nanoscale regions in 3D, in complex matrices and *in-situ* [150]. Nanoprobe beamlines on an ERL source will make it routine to combine imaging, spectroscopy, and scattering into a single instrument, in order to obtain the as complete a suite of information as possible from a single illuminated spot in a specimen.

5.2 Nanoprobes for Incipient Surface Damage: Art Conservation

The study and preservation of objects of significance to cultural heritage often involves extremely challenging science: such objects are typically highly heterogeneous and chemically complex. Moreover, it is preferable – in some cases required – that such objects be examined nondestructively. X-ray microprobe techniques such as diffraction, scanning XRF and spectroscopic techniques such as microprobe XANES are finding increased application in this area [151,152]. Yet, because of sample complexity and because the relevant length scales extend to the nanometer regime, such studies increasingly need faster scan speeds and smaller beams. The increased brilliance of an ERL source would significantly impact these studies.

A particular concern of growing importance is the preservation of 20th century masterpieces of Impressionist and early modern art, which are undergoing degradation phenomena ranging from fading and color shifts to catastrophic failure (Fig. 5.2.1). These phenomena have been documented in the works of van Gogh, Matisse, Monet, Picasso, Seurat and Matisse [153-156]. Photo-induced degradation is a surface phenomenon, often occurring in only the top 1–5 microns of the paint layer, and the photo-degradation products are often minor phases within

Figure 5.2.1: "A Sunday Afternoon on the Island of La Grande Jatte," Georges-Pierre Seurat, (Francesca Casadio, Art Institute of Chicago). A paint chip obtained from the painting (inset) shows color alteration in the surface layer. (Courtesy of Jennifer Mass)

this alteration layer. The preservation of the icons of early modern art hinges on the spatially-resolved atomic and molecular characterization of these minute heterogeneous alteration layers, an analytical challenge requiring non-destructive chemical imaging with at least nanogram sensitivity. New rapid, high-resolution and high-sensitivity chemical imaging tools for inorganic and organic components of disfiguring degradation layers are needed.

The current state-of-the-art techniques include XANES with a 1-2 μm beam to probe surface alteration layers. However, to preserve these icons of early modern art for future generations, it is critical that we identify incipient photodegradation, chemical evidence of photodegradation prior to any change in the painting's appearance. Incipient photodegradation occurs in the top 1-2 microns of the paint layer, and is often characterized by an altered/photodegraded coating, tens of nanometers thick, of degradation products covering individual pigments particles. As a result, increased resolution, on the order of at least tens of nanometers, is required to study the composition of the incipient photodegradation layer (including the compositional "coring" of individual pigment particles) as a function of depth. NanoXANES is anticipated to be of great utility for these systems. Other SR-based methods that have potential for the characterization of these alteration layers are nXRF, nXRF tomography, tomography and confocal nXRF. The chemical imaging methods developed must also be rapid to permit screening of representative paint cross-sections from our most important early modern art collections such as those at MOMA, The Barnes Foundation, The Metropolitan Museum of Art, and the Art Institute of Chicago.

Through analysis of damage mechanisms, efforts in art conservation aim to detect damage in its early stages and prevent further degradation. Analyzing the surface pigment layers requires XRF and XANES microscopy with nanoscale resolution. An ERL will have major impact on these efforts.

5.3 Nanodiffraction in 3D to Advance Polycrystalline Materials

3D micro- and nano-diffraction mapping is an emerging area of electron microscopy and synchrotron science, providing quantitative information on how small sample volumes respond to their local environment and to external forces. Because the behavior of most material systems is dominated by local heterogeneities and defects, X-ray diffraction mapping is proving to be an especially important tool in the quest to test and refine materials theory. Indeed, the ability to study small "local" volumes represents a transformative advance over ensemble average information and is certain to revolutionize our understanding of materials. X-ray methods are particularly important because they interrogate local strain, structure and texture in 3D volumes in a nondestructive way and, if fast enough, can follow real materials responding to applied loads, heating, and other processing conditions. This information has simply not been available previously.

Section 1.2 discusses a variety of techniques currently in use, or continuing to be developed to address these needs. An Energy Recovery Linac will have huge impacts on techniques like differential aperture microscopy or X-ray diffraction contrast tomography (DCT) [157,158] (figure 5.3.1), to name a few: (1) The high focused beam intensity will allow rapid measurements, enabling either novel scanning modes or time resolution for evolving systems, and (2) the much smaller, round beam size will allow for advanced achromatic optics with diffraction-limited beam sizes and longer working distances. For example, with fly-scan methods and new (yet-feasible) X-ray detectors, it will be possible to map volumes with 2×10^6 volume elements/hour. This will enable unprecedented visualization of materials structure and behavior in minutes, instead of days. Beyond existing methods, the instrumentation developed for

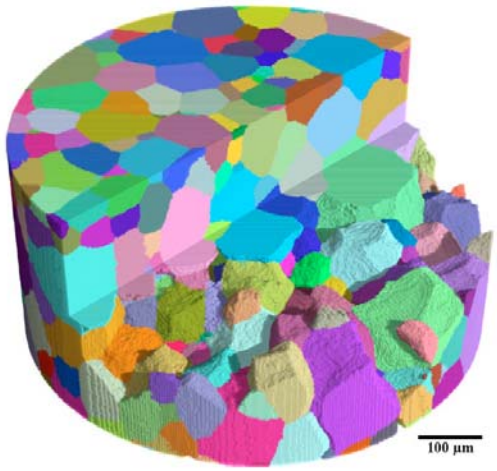

Figure 5.3.1: Color rendition of the 3D grain structure in a cylindrical beta-Ti specimen containing 1008 grains, as obtained by the X-ray diffraction contrast tomography. (See in [157, 158])

differential aperture microscopy has implications for coherent imaging of important materials. Already coherent imaging has achieved spatial resolution of 2 nm. Given the proposed brilliance of ERLs, it will be possible to extend the differential-aperture microscopy into the coherent regime to gain spatial resolution at far smaller length scales than possible today.

5.4 Probing Organic Microstructures with NanoGISAXS

As nanotechnology and organic electronics move more towards everyday device applications and production, new objects to study include small organic deposits on a substrate as microdrops (inkjet printing, offset printing) or microwires (organic circuits). These structures introduce new challenges to characterize and understand the effects of various new types of boundary conditions and external influences such as substrate interactions, curved interfaces, drying and kinetics due to assorted types of processing [159-162]. This requires probing such structures on a submicron scale *in-situ* and in real-time. Of interest are both the surface and the interior of the micro- and nanodeposits [163]. While first nanoGISAXS has been demonstrated on static samples [164], much more development remains to be done to make this a standard application.

From the materials point of view it is highly desirable to combine multiple probes with the X-ray nanobeam, so that small sample volumes can be probed simultaneously for both chemical and physical information. Towards these goals the most efficient tools combine flexible X-ray detectors (area detectors, fluorescence detectors) and ancillary probes such as optical microscopy, ellipsometry, or AFM into the beamline instrumentation and trained on the same spot. Several existing facilities demonstrate this point: an imaging ellipsometer was recently commissioned at MiNaX beamline of the Petra III facility [165], and the D1 end station at CHESS combines scattering and optical reflectometry and spectroscopy [166] as well as X-ray microbeams and optical microscopy [159,167]. NanoGISAXS can be combined with other methods such as microtomography, using either the absorption or the scattering signal [145] to retrieve 3D information. In the spatio-temporal regime first experiments reaching up to 10 micron spatial and 10msec temporal resolution under grazing incidence have been demonstrated [167,168]. These proof-of-principle studies need to be extended into the submicron length-scale as well as into a submillisecond time-scale.

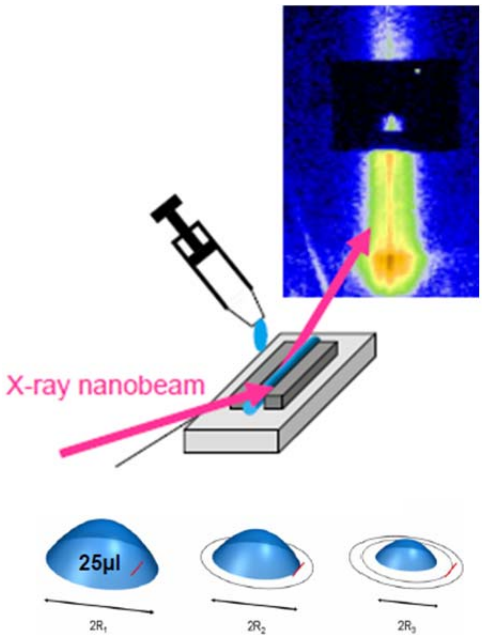

Figure 5.4.1: Microdeposits from inkjet printing or gravure printing are essential to the future production of organic electronics devices; however, this geometry produces very different boundary conditions than better-known thin film. GISAXS and GIWAXS with X-ray nanobeams can elucidate self-organization processes during drying and annealing of such confined deposits. The understanding of these processes will be critical to obtain optimum device performance. (Courtesy of Stephan Roth)

For the study of complex microdeposits such as drying solution patterns, micro- and nanoGISAXS can be combined with microtomography, using either the absorption or the scattering signal [145], to retrieve 3D information of density and structure, respectively. Other options are full-field imaging under grazing incidence [169] and coherent image reconstruction [170,171]. Such techniques circumvent the problem of modeling scattering data from complex structures and morphologies. These ideas have been demonstrated on selected systems at 3rd generation sources; however, more brilliance is needed to transform these exciting possibilities

into routine X-ray methods for a large variety of samples in materials science and biology. Moreover, the goal would be to not only study structure but also kinetics.

The highly coherent nanobeams at an ERL will facilitate a reconstruction of the real space electron density via coherent diffraction imaging, as demonstrated in first test experiments [172]. An ERL will provide the coherent flux for fast real-time studies. With the advent of new brilliant sources, GISAXS with micro-and nanobeams is looking into a bright future.

Fast scanning nanoGISAXS for real-time studies helps to stay one step ahead of the radiation damage. Again, 3-4 orders of brightness are needed to approach the submicron and submillisecond regime, to study, for instance, the dynamics of a single nanoparticle at the solution-substrate interface or at a cell membrane.

The highly coherent nanobeams at an ERL will facilitate a reconstruction of the real space electron density via coherent diffraction imaging, as demonstrated in first test experiments [172]. An ERL will provide the coherent flux for fast real-time studies. With the advent of new brilliant sources, GISAXS with micro- and nanobeams is looking into a bright future.

5.5 CDI: Application to Complex Biomaterials: Plant Cell Walls

Coherent Diffraction Imaging (CDI) will provide an extraordinary tool for the study of complex materials that make up a large fraction of the volume of multi-cellular organisms and constitute a very important but poorly characterized class of biomaterials [173]. CDI is particularly well suited to the study the crystalline components of these structures. Mineral inclusions and biomineral structures form an important component of plant cell walls, connective tissues, bone, and shell. This is of particular note in bone loss and degradation in our aging population. Understanding the organization of these structures, the architectural principles that govern their design, and the means by which they are assembled will contribute significantly to efforts aimed at re-engineering them, repairing them, and modulating their properties in response to human needs. Mineral inclusions in plant cell walls are of great current interest due to their impact on processes for production of biofuels [174,175].

The technical barriers to making progress in understanding these complex materials are formidable. Scanning electron microscopy can be used to visualize surface components, but study of embedded structures requires disruptive sample preparation. Analytical chemistry and mass spectrometry may be useful in identifying individual components and determining their relative abundances. But, the inhomogeneity of these systems limits the impact of these studies, and their struc-

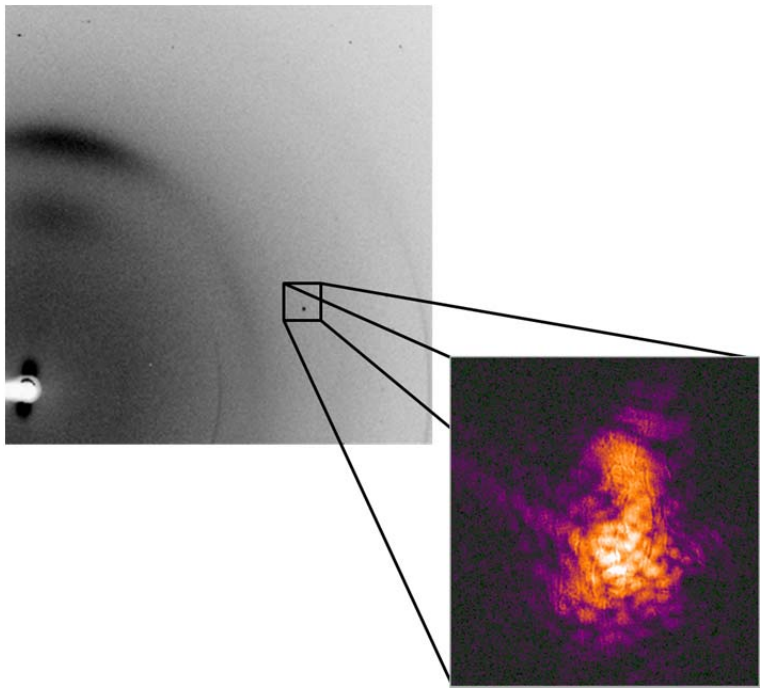

Figure 5.5.1: Fiber diffraction patterns from corn stover exhibit the characteristic intensity distribution expected from cellulose fibrils. Overlaid on that scattering, sharp Bragg reflections from mineral inclusions are frequently observed. Very high point-to-point collection of the three-dimensional intensity distribution of these Bragg peaks provides the information necessary for full three-dimensional reconstruction of the shapes of the mineral inclusions from which they arise. (Courtesy of L. Makowski)

tures are inherently distributed in three dimensions: two-dimensional analysis alone is insufficient to solve their structures. It may be possible to identify the relative orientations of different fibrous materials by conventional X-ray scattering, but the inhomogeneity often renders this information irrelevant.

By contrast, CDI is uniquely capable of providing three-dimensional real-space images of specific crystalline domains at high resolution (< 50 nm) within intact, micron to millimeter-thick tissue samples [149]. By careful choice of X-ray energy, CDI is also sensitive to the chemical composition of individual components by their intrinsic lattice periodicity through the positions of the Bragg reflections. For example, plant cell walls (Fig. 5.5.1) are complex polymeric matrices of cellulose, lignin and other materials [174]. Initial studies have been carried out using dried material [176]. Bragg scattering from crystalline inclusions of minerals identified from their Bragg scattering angles as Whewelite was collected and used to reconstruct images of the associated crystals.

The success of Bragg CDI for the in-situ study of these crystallites indicates that it may be applicable more generally to the mineral components of complex biological tissues that include crystalline domains of some constituents. Tissues of this kind are abundant and diverse. The high brilliance of the ERL source will render 3D reconstructions such as these routine. Developing a robust approach to mapping the distribution of different chemical constituents within these tissues will have broad scientific impact. The ongoing studies of mineral inclusions in plant cell walls will produce information important to our understanding of the structural principles underlying their distribution, thereby contributing substantially to efforts to process biomass for bioenergy applications. By similar rationale, comparable insights may be gained into the age-related degradation of mineralized tissues such as bone that will have a profound impact on our ability to treat the afflictions of aging, with potentially huge financial impact.

5.6 3D XRF at the Nanoscale: Find an Atom

X-ray fluorescence tomography and confocal XRF imaging using synchrotron radiation are among the most sensitive, non-destructive microanalytical methods providing 3D quantitative information on the elemental distributions in the probed sample volume with trace-level detection limits. XRF methods are now widespread and needs are growing to improve spatial resolution (smaller illuminated volumes), reduce scanning times (more intensity) and increase sensitivity (improve signal to noise). An example that epitomizes these needs is the non-destructive 2D/3D elemental analysis of unique extraterrestrial particles, including cometary and interstellar grains which were sampled and brought to Earth in the framework of NASA's Stardust mission [177-179]. The captured interstellar grains, which have sub-micron dimensions, cannot be studied with sufficient detail at the currently available resolution levels at SR nanoprobes. The non-destructive determination of elemental distributions within these unique materials (with average dimensions in the range of 300 - 600 nm) will require beam-sizes down to the 10 nm level or below for exploring their chemical composition in three-dimensions.

The dramatic increase of spectral brightness at the ERL source compared to current 3rd generation SR sources will lead to the reduction of X-ray beam size to the sub-10 nm range using appropriate X-ray focusing optics (e.g. nano-focusing CRL lenses, FZP's, 2D waveguides, new generation of KB mirror-optics). Potential exists at the ERL for obtaining 1 nm hard X-ray beams with 10^{11}–10^{12} photons per second per square-nanometer. This will not only result in a new level of spatial resolution, but will also offer the potential for sub-zg (10^{-21} gram) absolute detection limits for elemental analysis, *i.e.,* the potential for single atom sensitivity. Using ERL-based X-ray nanobeams with advanced detectors (e.g. Maia detector array), the reduction of 2D/3D data collection times for full-3D elemental nano-analysis down to a few minutes are expected, down from the currently impractical 10-20 hours of measuring time. This will open new opportunities not only for the non-destructive, non-invasive studies of unique extraterrestrial par-

ticles, but also for the studies of e.g. (potentially toxic) nanoparticles, nanomaterials, individual biological cells etc.

With the high brilliance of ERL sources, X-ray microscopy and nanoanalysis can be pushed to well beyond the current capabilities. For real space structure determination on the nanoscale as well as for spectroscopic imaging, the main figure of merit (or limitation) is the dose density on the sample [180]. The high dose density is prone to introduce radiation damage in a variety of samples. For biological systems it may be difficult to go beyond the radiation damage threshold [57] and new acquisition schemes and preparation techniques of the samples may be necessary. For materials science samples, however, a nanoprobe opens a large variety of new possibilities. For example, complex materials exhibiting multi-ferroicity, itinerant magnetism, or topological insulators, can be studied at the mesoscopic scale, investigating individual structural domains, defects, etc. The Nanoprobe opens also the way to chemical studies, for example in heterogeneous catalysis, investigating single catalyst particles. All the above can and in most cases must be carried out *in-situ* or *in-operando*, requiring sample environments, such as furnaces and chemical reactors with gaseous or liquid environments. Chemical reactions, e. g., precipitation and redox reactions, can be studied with fast time resolution in microfluidics, pushing the time resolution to the nanosecond level and below [181].

Workshop 6: X-ray Photon Correlation Spectroscopy (XPCS) using Continuous Beams

6.1 Introduction

The need to characterize, understand and manipulate the dynamical structure of matter at the nanoscale constitutes an emerging and critical frontier for science in the 21st century. This frontier is defined by a wide range of materials and technological demands and spans all scientific disciplines. For example, the time evolution of microstructures formed under nonequilibrium conditions – conditions pertinent to the synthesis of most industrialized materials - is notoriously difficult to study, yet strongly influences (and may dominate) the physical and mechanical properties of materials such as tensile strength and failure, chemical reactivity and magnetic coercivity. The behavior of complex fluids such as polymers, colloids, emulsions, and foams are governed by microscopic structural relaxation processes and flows that perturb systems far from equilibrium. However important these phenomena are, obtaining basic information about such systems poses serious challenges because of the need to record structural information in a non-destructive way, over a very wide range of timescales, on systems in various states of equilibrium, and with varying (but usually opaque) macroscopic densities.

3rd generation sources have demonstrated that a wealth of information can be learned by carefully examining X-ray intensity profiles inside the seemingly innocuous “Bragg peak.” By combining coherent X-ray radiation with high-resolution, high-speed X-ray detectors, scientists can record time variations across of diffraction peak profiles – called speckle – that result from spatial and time variations in the atomic and molecular ordering within a sample. Because diffraction peaks are associated with real-space periodicities, measuring the time variations of speckle patterns provides a near-unique probe of the *time* scale of fluctuations at particular, selectable *length* scales. Despite heroic experiments using “X-ray photon correlation spectroscopy,” or XPCS, this relatively new X-ray technique has not reached its fullest potential because present X-ray sources produce photon beams with coherence well below 1%. X-FEL sources have high coherence, but the destructive energy density of the beams makes them unsuitable for the majority of XPCS applications. As a result, most systems of interest are well out of reach of even the most advanced storage ring sources.

Most of the advanced features of ERL source directly and significantly enhance the experimental scope of XPCS and open new avenues of research into the dynamical structure of materials. The impact of increased brilliance on XPCS is particularly strong since the signal-to-noise ratio in XPCS studies scales as the square of source brilliance. The 100-fold increased coherent flux of an ERL at high energies (see figure 1) will allow time scales that are 10^4 times faster, making possible experiments that are starved for photons today [12]. At storage ring sources XPCS is limited by coherent flux to time scales greater than 1 second at scattering vector length $Q \approx 1$ Å^{-1} and 10 microsecond at $Q \approx 10^{-3}$ Å^{-1} (a negative power law relates these quantities at the boundary of what is currently accessible [182]). Inelastic X-ray and neutron scattering and proposed X-FEL pulse delay methods will probe length scales below 1 Å, but cannot sense dynamical processes slower than 100 ns. Thus there is an important gap (6 orders of magnitude in time for $Q \approx 1$ Å^{-1}) that ERL experiments could fill, provided fast area detectors with appropriately-sized pixels and fast image readout time become available.

The round ERL beams are an additional benefit to XPCS measurements because optimizing signal-to-noise (and interference contrast) requires experimenters matching speckle shape with pixel geometry on the X-ray detector. Since virtually all X-ray detectors have square pixels, measurements at an ERL source gain over storage rings by avoiding the need to use slits or apertures to generate a round secondary source. On an ERL, all incident coherent flux will be immediately useful. XPCS will also make full use of the tunability of the delta undulator. Not only will a long Delta undulator produce unprecedented coherent flux in a narrow energy bandwidth, but in helical mode very few photons will need to be rejected by apertures or X-ray optics because the harmonics and excess heat are suppressed on-axis [13]. At 10 keV, for example, inside the coherence solid angle the first harmonic radiation has 15 eV bandwidth, integrated coherent flux of 3.4×10^{14} ph/s and coherent beam power of 0.54 Watts; this beam delivers a coherent power density of nearly 54 Watts/mm^2 at 60 meters from the source [12].

The time and pulse structure of ERL radiation also helps optimize XPCS range. Short pulse lengths (below 2 picoseconds) allow fast exposures, and the high 1.3 GHz repetition rate allows time averaging to minimize pulse shot noise. The quasi-continuous time structure and 1.3 GHz frequency will push the time domain towards nanosecond resolution. The Linac-based injection cycle of the ERL also avoids "gaps," or missing pulses, characteristic of storage ring sources. Reference [12] discusses in detail the relative merits of smaller incident photons per bunch for ERL versus heating issues inherent at X-FEL sources.

Areas ripe for study include systems far from equilibrium such as glasses and materials under shear and flow, complex fluids such as polymers and colloidal suspensions, moving domain walls, defects in crystals, and protein in solution. The results from such experiments will impact the synthesis of next generation materials and provide a more profound understanding of

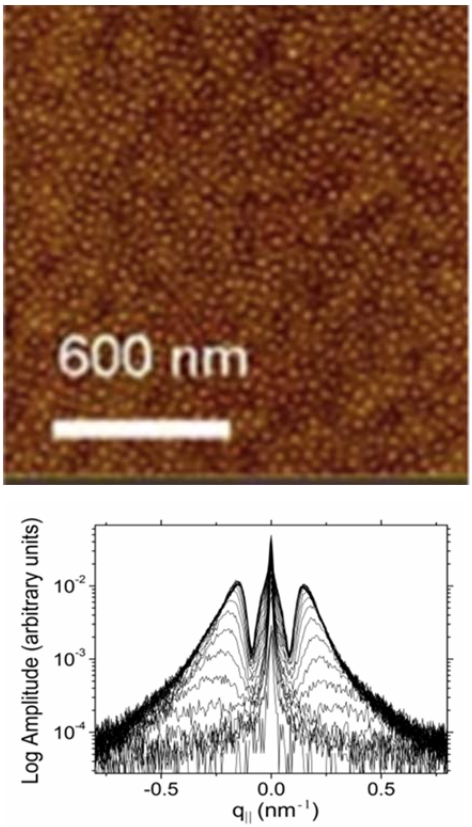

Figure 6.2.1: (top) Silicon nanodots formed via sputter erosion of a Mo-seeded Silicon surface, and (bottom) surface diffuse X-ray scattering obtained by in-situ measurements during that process. The well-defined side-lobes arise from the formation of nanodots. The atomistic processes giving rise to this pattern formation are not understood, and could be measured using XPCS from a high-brilliance ERL source. (From [184])

connections between dynamics and rheological macroscopic properties of highly interacting complex fluids. Increased coherent intensity will be used to measure signals from scarce or highly dilute systems, including *in-situ* XPCS observations of surface fluctuations at well-defined time and length scales, offering a powerful new approach to study catalytic processes at surfaces, for instance. Composed mainly of light elements with low density contrast, high coherent beam intensities are needed to study biological materials and systems that exhibit complicated multiscale structures evolving over a wide range of length and time scales. ERL X-ray beams will make XPCS measurements sensitive to direction-specific atomic diffusion in bulk materials, which requires measurement of fluctuations in weak, diffuse scattering between Bragg Peaks.

6.2 Steady-State, Non-equilibrium Surface Dynamics

Surfaces provide some of the most academically interesting and technologically important systems for study. Often the surface properties of a system are vastly different from a bulk material, while at the same time being greatly influenced by history and preparation. For example, metals and metal-oxides provide a rich environment for the study of catalytically driven reactions. Chemical processes such as CO or NO oxidation, or O_2 reduction in the presence of hydrogen, are important for energy related technologies. Fuel cell applications, batteries, and cleaner burning technologies can all benefit from an increased understanding of the fundamental electrochemistry and corrosion processes that often occur at surfaces. The penetrating nature of X-rays does not limit such studies to vacuum systems, but also extend them to solid-solid, solid-liquid, and liquid-liquid interfaces. However, despite significant gains in our understanding of such systems, there is much we do not yet know. In particular, the equilibrium dynamics of model catalytic surfaces remains largely unknown. This is not due to a lack of experimental effort or ingenuity, but rather reflects difficulties inherent in studying *in-situ* systems with electron-based techniques and atomic scanning microscopies.

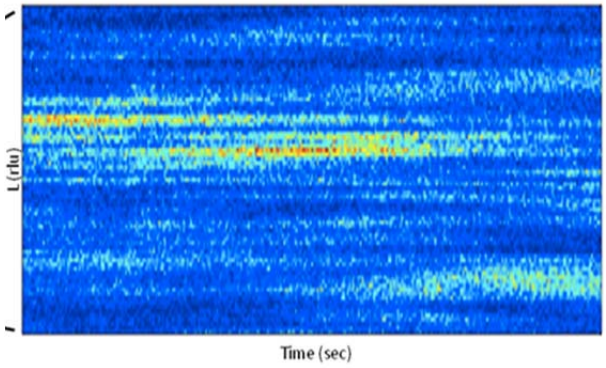

Figure 6.2.2: Time dynamics of speckles from an Au surface obtained at (0 0 0.2) *showing evolution of the surface morphology submerged in* $HClO_4$ *. (From [185])*

Likewise, surface processing is ubiquitous in industry, yet often poorly understood due to inherent challenges of characterizing non-equilibrium processes at atomic length scales, in challenging process environments, and with sufficient high speed. Dynamic light scattering is a very useful tool to characterize open surfaces, but the wavelength range makes it unsuitable for atomic scales studies or penetration into reaction vessels or opaque specimens. Electron and neutron-based probes are often constrained by *in-situ* environmental preparations or too little intensity to record high signal-to-noise. These experimental difficulties and lack of understanding places severe limits on the rate at which new and existing processes can be developed and applied to technological innovation.

The most significant limitation to this approach has been source brilliance: surface scattering is inherently weak, and XPCS requires a coherent beam. An ERL would make such measurements routine. *In-situ* XPCS allows direct observation of surface fluctuations at well-defined time and length scales, and has recently been extended from soft-matter films and interfaces to metal crystal surfaces with height fluctuations on the scale of a single atomic distance [183]. A prototypical system needing *in-situ* XPCS is shown in Fig. 6.2.1, where a pattern of nanodots form during sputter erosion of an initially smooth, Mo-seeded silicon surface. Surface

diffuse scattering profiles recorded during the process [184] reveals snapshots of the average structure during the process, hinting at the underlying dynamics of this process; however, critical questions remain about fluctuation, mobilities, vacancy formation, hopping potentials, etc. A sufficiently brilliant source, such as the ERL, would allow XPCS-based measurement of the dynamics of fluctuations associated with these nanodots, and thus provide direct information of the mechanisms by which they form.

Similarly, electrochemical processes are of critical importance in a broad range of fields, yet remain challenging to study. For instance, XPCS measurements obtained from an Au surface under a perchlorate solution demonstrated the feasibility of this approach (Fig. 6.2.2) [185]. However, 3rd generation source brilliance limits these studies to high Z materials and time scales of 1 second and above. Thanks to the quadratic dependence of XPCS signal-to-noise on brilliance, the 2-3 orders of magnitude increase in brilliance provided by and ERL would allow *in-situ* XPCS on a large variety of technologically-relevant surfaces; *e.g.* studying electrolytic salt systems like KI for NaI. ERL intensities should also push time scales below milliseconds, potentially approaching microseconds or shorter.

6.3 Protein and Biomembrane Dynamics

Protein actions are usually described in terms of their static structure but *biological function requires motion*. There is growing evidence that proteins and other macromolecules have evolved to take functional advantage not only of mean conformational states but also of the inevitable fluctuations about the mean [186,187]. However, despite the fundamental importance of molecular motion in proteins, experimental data, especially measurements on the collective dynamics of ensembles of proteins on relatively slow time scales (*i.e.* microseconds to milliseconds) is almost completely missing.

Biological materials and systems are true "multi-scale materials" exhibiting complicated structures that evolve with dynamics occurring over a wide range of length and time scales (Figure 6.3.1). Dynamics of biological membranes includes, for example, diffusion of lipids and proteins and phonon-like excitations and coherent relaxations, such as undulations, on fast picosecond to nanosecond time scales. Conformational changes of membrane embedded proteins are known to happen on much slower microsecond to millisecond times. These dynamics are assumed to relate to function since they often involve movements of large structural groups, which together form large macromolecular systems. It is of great interest to study these dynamics in membrane embedded proteins *in-situ* under physiological conditions. While the time scale perfectly falls into the XPCS window, the corresponding length scales of single molecules are challenging.

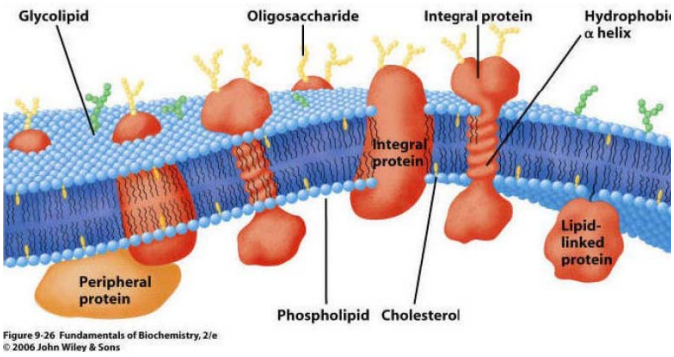

Figure 6.3.1: Cartoon of a biomembrane. Characteristic length scales range from nanometers (the thickness of a biomembrane) to micrometers (the length of polymers that form the cytoskeleton). They are chemically diverse – building blocks include proteins, nucleic acids, lipids and polysaccharides – and formidably complex. (2006 John Wiley & Sons)

Dynamics at longer length scales involve fluctuation dynamics of lipid rafts and nanodomains. Membranes in their physiologically-relevant fluid phase are thought to be heterogeneous structures. Composition of membranes may change on nanometer (3-50 nm) lengths and microsecond times. While more and more evidence is reported that those nanodomains

actually exist, these structures have so far not been observed directly in experiments. Some measurements have been made on membranes using dynamic light scattering (DLS) [188] and XPCS measurements have been made on membrane stacks at low wavevectors [189]. However, the DLS measurements were only at long length scales, and the XPCS measurements were made in (slow) glycerol solutions on systems where dynamics were dominated by collective rather than individual membrane motions. In order to study materials of relevance to the biological community it is important to study dynamics in water. This leads by necessity to the microsecond regime. Flux at 3rd generation SR sources is insufficient for this task

XPCS at an ERL source might be the only technique that can achieve relevant lengths and time scales. It has been known for years that information about dynamics of molecules in crystal is recorded in the diffuse scatter around Bragg peaks; molecular motions in protein microcrystals coupled over large scales generates diffraction signatures in the diffuse scattering around the main Bragg peaks [190]. The experimental method has been propose, "Speckle Visibility Spectroscopy," a variant of XPCS, that hopes to measure dynamics associated with this type of molecular motion from a single diffraction patterns ("speckle snapshot") obtained with coherent X-ray light [191]. This method seeks to minimize the required X-ray dose and radiation damage artifacts and also access dynamics that are faster than the speed of current detectors. Other approaches are being proposed, including taking multiple exposures using slow detectors but varying the delay between photon pulses. (These methods complement Neutron Spin Echo (NSE) studies of fast (sub-nanosecond) molecular dynamics and Nuclear Magnetic Resonance (NMR) measurements of individual bond vector motion in small molecules.)

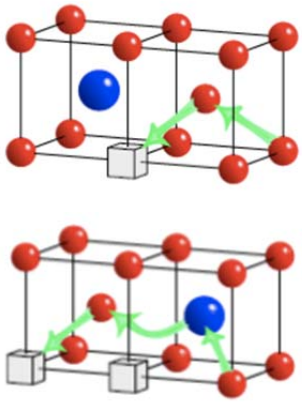

Figure 6.4.1: Different jump mechanisms in a two-component crystal. XPCS provides the means of directly distinguishing which mechanisms are present in a real system. (From [198])

XPCS at an ERL source should be the premier tool to study interactions and collective dynamics between membrane embedded proteins. Typical protein-protein distances in membranes are in the order of 6-10 nanometers. The time evolution of the protein-protein correlations most likely fall into the microseconds XPCS time window. Protein-protein interactions and aggregation could then be studied as a function of membrane composition, such as cholesterol content and protein concentration. Understanding these processes is an extremely important step towards developing a molecular picture of neurodegenerative diseases such as Alzheimer's disease and Apoptosis and learn, for instance, how to quantify risk factors. XPCS, with the 2-3 orders of magnitude increase in brilliance provided by an ERL, may reveal direct signatures of biomembrane domains through their fluctuations, which are beyond the reach of other techniques and storage ring sources, and also not appropriate for destructive beams from X-FELs.

6.4 New Insights into Atomic Diffusion

Atomic diffusion is critical to materials synthesis and stability, and thus dictates the behavior of much of the material world. Yet, it is extraordinarily difficult to measure directly and imperfectly characterized in most systems of interest. Knowledge of atomic diffusion is a fundamental issue and there is broad agreement that studying temperature-driven motion of single atoms in solids is more complex than getting out their structure. Sophisticated methods have been developed to study particular types of diffusion behavior, including neutron scattering (H diffusion in metals [192]), helium atom scattering (fast surface diffusion [193]), and field ion microscopy (slow surface diffusion [194]). Existing 3rd generation synchrotron sources enabled new kinds of diffusion

studies with XPCS, however, a very limited number of model systems have profited and their scope is often limited to either heavy elements or very high temperatures.

New high brightness ERL sources will significantly expand the range of materials systems that can be studied and the types of environmental conditions accessible. With significantly higher brightness and coherent flux, an ERL source will make it possible to use XPCS to study diffusion in compound materials systems with atomic numbers close to each other (instead of studying only systems with contrasting heavy and light atoms). As an example are proposed technologically important Ti-Al heavy-duty alloys or Fe-Co-Ni alloys. An entirely new avenue of potential research could be using X-rays to study the motion of light interstitials like hydrogen, lithium or carbon in host lattices. Although small atoms diffusing through the lattice might give little X-ray signal, fluctuating lattice distortions caused by interstitial diffusion could be recorded by XPCS [195]. XPCS on light elements could have immediate impact on studies of hydrogen-storage systems and batteries utilizing light element (Li, S, etc.).

Higher quality experimental data promises new and deeper insights into the details of dynamics. For example, studies of amorphous systems like metallic and silica glasses will profit from resolving tiny differences between regular, stretched or compressed form of the relaxation function. Completely new insight into surface diffusion will be possible, including dynamics of surface steps growth or fluctuations (section 6.2 above) and even diffusion of single atoms on surfaces might be measurable [196]. Moreover, studies of fundamental phenomena like the impact of photons on atomic dynamics or studies of systems beyond the linear-regime of the scattering theory [197,198] will reveal additional information about lattice jump processes (Fig. 6.4.1). XPCS provides direction-specific sensitivity to atomic diffusion in bulk materials, but requires measurement of fluctuations in weak, diffuse scattering between Bragg Peaks. Heroic demonstration experiments at ESRF [199] employed count rates of 1 count per 10 minutes per pixel! An ERL would increase count rates by upwards of 3 orders of magnitude, rendering such measurements routine, and allow different jump mechanisms to be distinguished.

6.5 Dynamics of Soft Matter and Complex Fluids

Soft matter and complex fluids cover the spectrum of simple to advanced materials, impacting almost all foods, cosmetics, plastics, films, rubbers, and medical and biomedical materials. To the scientists these are complex colloids, polymers, emulsions, surfactants, granular composites, and biomembranes, to name a few. These classes of materials are characterized by complexity, flexibility, structural relaxation and non-equilibrium dynamics. Most of the fabrication and processing of such materials, either self-organized or driven, takes place far from the equilibrium. Understanding how to control far-from-equilibrium phenomena like jamming under flow, aging, and plastic deformations under stress – to name a few - are important steps needed to achieve breakthrough applications in nanotechnology, material science, and biotechnology. The get an idea of how active these fields are, consider that probing visco-elastic properties of complex fluids under shear in non-equilibrium is currently being pursued at nearly 80 universities (40%, estimated) of the MPI's in Germany [200].

As an example of the longstanding challenges in these fields, our present understanding of the properties of high-weight polymer liquids is based on a reptation model of polymer dynamics, which depicts the motion of a polymer as a random walk along a tube delimited by temporary entanglements with neighboring chains [201-203]. Microscopic evidence for the existence of tubes and entanglement lengths has been provided by neutron spin-echo (NSE) measurements [204]. However, the delay times accessible with NSE are shorter than needed to observe reptative relaxation directly. After more than 30 years, NSE measurements have been able to only characterize the early time behavior [202,205,206]. How these systems behave at long times and details of long-time relaxations themselves await XPCS measurements at a much brighter, high repetition-rate source.

Unfortunately, there is a large gap in time and length scale measurements available to researchers investigating these subjects. For example, many types of rubber, especially those used to make road vehicle tires, add nanoparticles to reinforce and dramatically improve mechanical and dynamical viscoelastic properties. Scientists do not know the cause(s) of this reinforcement effect. To develop good performance tires, for example, it is necessary to understand (and engineer) dynamic behaviors of nanoparticles over enormously disparate time scales; rolling resistance and traction performance are properties in widely different frequency regimes (figure 6.5.1). Rolling resistance dominates fuel efficiency of vehicles and results from wheel rotation and flexure at approximately 10 Hz. At the same time, propulsion and braking depend upon traction and frictional forces determined at individual contact points occurring at frequencies of 10^4 to 10^6 Hz. This is just one example where fundamental materials knowledge is needed to make tractable a global engineering challenge.

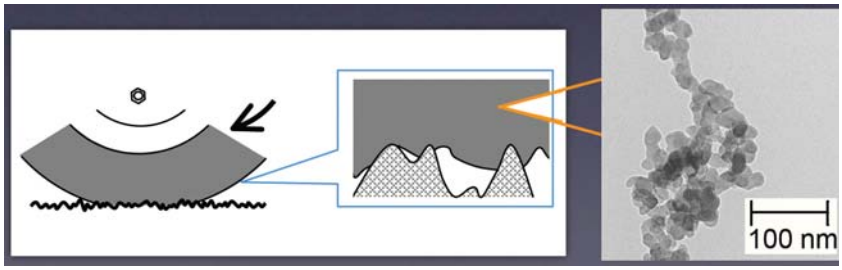

Figure 6.5.1: Examples of dynamics of particles on different time scales: left, tire rotation at 10 Hz stretches and shears automobile tire sidewalls; inset, contact surface irregularities impact braking, adhesion, and materials longevity; right, nanoparticle additives reinforce mechanical and dynamic properties of rubber. (Courtesy of Shinohara)

ERL sources will dramatically improve XPCS capabilities to visualize dynamical heterogeneities, dissipative mesoscale fluctuations, and advective responses to shear in non-equilibrium fluids [207]. The 100-fold increase in coherent flux from the ERL (versus 3rd generation source) will allow measuring time scales that are 10^4 times faster and make possible numerous experiments that today are beyond reach. These experiments will impact the synthesis of next generation soft materials and expand understanding of connections between dynamics and rheological macroscopic properties of highly interacting complex fluids. In terms of the impact on society, it is important to recognize that most materials of interest to industry are complex in both dynamics and structure, which together complicate data analysis and interpretation. The origins of many materials properties and behaviors involve molecular-scale fluctuations on length scales of 10-1000 nm and 10^{-6}-10^{-2} second time scales. XPCS can directly measure these fluctuations, but extracting useful information from most materials on these length and time scales require 2-3 orders more coherence flux to be practical.

Table 1: Parameters used to compare third and fourth generation X-ray sources

		APS	ESRF	Spring8	NSLS II	ERL High Coherence	ERL High Flux	ERL nanofocus
Electron Source	Energy (GeV)	7.0	6.03	8.0	3.0	5.0	5.0	5.0
	$\Delta E/E$ (%)	0.096	0.11	0.11	0.099	0.02	0.02	0.02
	Current (mA)	100	200	100	500	25	100	25
	ε_N[a] (nm·rad)	2.5	4.025	3.4	0.508	0.016[a]	0.06[a]	0.016[a]
	Coupling	0.00969	0.006	0.002	0.016	1	1	1
	$\varepsilon_x / \varepsilon_y$ (nm·rad)	2.49/0.024	4.0 / 0.024	3.39 / 0.007	0.5 / 0.008	0.008 / 0.008	0.03 / 0.03	0.008 / 0.008
	β_x / β_y (m)	14.4 / 4	0.5 / 2.73	21.7 / 14.1	2.02 / 1.06	3.98 / 3.98	3.98 / 3.98	0.16 / 0.16
	α_x / α_y	0 / 0	0 / 0	0 / 0	0 / 0	0 / 0	0 / 0	0 / 0
	η_x / η_y (m)	0.124 / 0	0.037 / 0	0.103 / 0	0 / 0	0 / 0	0 / 0	0 / 0
	η'_x / η'_y	0 / 0	0 / 0	0 / 0	0 / 0	0 / 0	0 / 0	0 / 0
	σ_x / σ_y (μm)	224 / 9.82	60.5 / 8.10	294 / 9.78	31.8 / 2.91	5.64 / 5.64	10.9 / 10.9	0.98 / 0.98
	σ'_x / σ'_y (μrad)	13.2 / 2.46	89.5 / 2.97	12.5 / 0.69	15.7 / 2.75	1.42 / 1.42	2.75 / 2.75	8.17 / 8.17
Undulator / X-ray Source	Type	Undulator A	In vacuum undulator	In vacuum undulator	U20 undulator	Helical Delta	Helical Delta	Helical Delta
	Beamline	8ID	ID27	BL19XU	Projected	Projected	Projected	Projected
	Length (m)	2.4	4	25	3	25	25	0.75
	Period (mm)	33	23	32	20	18	18	18
	Min. Gap (mm)	10.5	6	12	5	5	5	5
	B_{max} (T)	0.891	0.75	0.59	0.97	0.85	0.85	0.85
	K_{max}	2.74	1.61	1.76	1.81	1.43	1.43	1.43
	Σ_x / Σ_y (μm)[b]	224 / 10.1	60.5 / 8.56	294.1 / 12.0	32.1 / 5.11	8.99 / 8.99	13.0 / 13.0	1.55 / 1.55
	Σ'_x / Σ'_y (μrad)[b]	14.3 / 6.21	89.6 / 5.31	12.6 / 1.89	18.0 / 9.21	2.26 / 2.26	3.26 / 3.26	13.1 / 13.1
	Spectral Brightness[bc]	4.2×10^{19}	1.6×10^{20}	6.4×10^{20}	8.9×10^{20}	8.0×10^{22}	8.9×10^{22}	3.5×10^{21}
	Coherent Fraction (%)[b]	0.080	0.054	0.085	0.82	24	6.6	36
	Coherent Flux (ph/s/0.1%)[b]	2.5×10^{11}	9.5×10^{11}	3.9×10^{12}	5.4×10^{12}	4.8×10^{14}	5.4×10^{14}	2.1×10^{13}

[a] SPECTRA-8.0.10 calculates ε_x and ε_y based on a "Natural Emittance" parameter (ε_N) and the coupling constant, so we have included ε_N in this table. Spectra models an isotropic source as having unit coupling, ε_N is therefore double that of ε_x and ε_y. When comparing an ERL with existing sources, ε_x and ε_y are the relevant parameters, not ε_N.

[b] Values at 8 keV. Σ, Σ' refer to width and divergence, resp.

[c] Spectral Brightness reported in standard units of ph/s/mm^2/mrad^2/0.1% bw.

Table 1. Parameters used to calculate spectral brightness and coherent flux in figure 1. Values for other sources are good faith estimates based on information posted by the sources on their websites. Nominal values were used where possible to give a fair comparison between existing and projected sources. In the case of NSLS II, the emittances used are for the 8 damping wiggler configuration. All calculations were performed using SPECTRA-8.0.10 [208].

Parameters based on table shown in Reference [12]

References

[1] D. Dale, S. M. Gruner, J. Brock, D. Bilderback, and E. Fontes, "Science at the Hard X-ray Diffraction Limit (XDL2011), Part 1," Synchrotron Radiation News **24**, 4-11 (2012).

[2] Zhongwu Wang, Ken Finkelstein, Detlef Smilgies, Arthur Woll, and Ernie Fontes, "Science at the Hard X-ray Diffraction Limit (XDL2011), Part 2," Synchrotron Radiation News **25** (1), 9-16 (2012).

[3] Ivan V. Bazarov, "Synchrotron radiation representation in phase space," Physical Review Special Topics - Accelerators and Beams **15** (5), 050703 (2012).

[4] Kwang-Je Kim, "Brightness, coherence and propagation characteristics of synchrotron radiation," Nuclear Instruments and Methods in Physics Research Section A: Accelerators, Spectrometers, Detectors and Associated Equipment **246** (1-3), 71-76 (1986).

[5] Kwang-Je Kim, "Characteristics of synchrotron radiation," AIP Conference Proceedings **184** (1), 565-632 (1989).

[6] Kalyan Das, Sergio E. Martinez, Joseph D. Bauman, and Eddy Arnold, "HIV-1 reverse transcriptase complex with DNA and nevirapine reveals non-nucleoside inhibition mechanism," Nature Structural & Molecular Biology **19** (2), 253-259 (2012).

[7] DESY, "Brilliant future for PETRA III," CERN Courier **43** (6), 7 (2003).

[8] A. Ropert, Filhol, J.M., Elleaume, P., Farvacque, L., Hardy, L, Jacob, J., Weinrich, U., "Towards the ultimate storage ring-based light source," Proc. EPAC 2000, 83.

[9] Martin Magnuson, Mats Fahlman, Roger Uhrberg, Leif Johansson, and - Total of 100 authors in alphabetical orders, "MAX IV Conceptual Design Report (CDR)," 2006, see http://urn.kb.se/resolve?urn=urn:nbn:se:liu:diva-60634.

[10] Cornell ERL Workshops, "X-ray Science Opportunities with an ERL, series of six international workshops at Cornell University, Cornell University, June 5-24, 2006.," 2006, see http://erl.chess.cornell.edu/gatherings/erl%20workshop/index.htm.

[11] SPECTRA, see http://radiant.harima.riken.go.jp/spectra/.

[12] D. H. Bilderback, J. D. Brock, D. S. Dale, K. D. Finkelstein, M. A. Pfeifer, and S. M. Gruner, "Energy recovery linac (ERL) coherent hard x-ray sources," New Journal of Physics **12** (2010).

[13] Alexander Temnykh, "*Helical PPM Undulator for ERL*," 2006, see http://www.lns.cornell.edu/public/CBN/2006/CBN06-3/CBN06-3.pdf.

[14] A.B. Temnykh, "Delta Undulator for Cornell Energy Recovery Linac," Phys. Rev. St Accel Beams **11**, 120702 (2008).

[15] A. Temnykh, M. Babzien, D. Davis, M. Fedurin, K. Kusche, J. Park, and V. Yakimenko, "Delta undulator model: Magnetic field and beam test results," Nuclear Instruments & Methods in Physics Research Section a-Accelerators Spectrometers Detectors and Associated Equipment **649** (1), 42-45 (2011).

[16] Q. Shen, D. H. Bilderback, K. D. Finkelstein, I. V. Bazarov, and S. M. Gruner, "Coherent X-ray imaging and microscopy opportunities with a diffraction-limited Energy Recovery Linac (ERL) synchrotron source," Journal De Physique Iv **104**, 21-26 (2003).

[17] K. D. Finkelstein, I. V. Bazarov, A. Liepe, Q. Shen, D. Bilderback, S. Gruner, and A. Kazimirov, "Energy recovery LINAC: A next generation source for inelastic X-ray scattering," Journal of Physics and Chemistry of Solids **66** (12), 2310-2312 (2005).

[18] M. Tigner, "A Possible Apparatus for Electron Clashing-Beam Experiments," Nuovo Cimento **37** (3), 1228-1231 (1965).

[19] ERL_milestones, "See ERL R&D milestones at http://news.chess.cornell.edu/articles/2012/ERLgoals02152012.html," (2012).
[20] E. Fontes, "Cornell Surpasses Milestones Towards New ERL Coherent X-ray Source," 2011, see http://news.chess.cornell.edu/articles/2011/CoherentOct2011.html.
[21] Bazarov_et_al., "Cornell Energy Recovery Linac Project Definition Design Report (PDDR)," 2012, see http://erl.chess.cornell.edu/PDDR/PDDR.pdf.
[22] K. J. Kim, Y. Shvyd'ko, and S. Reiche, "A proposal for an x-ray free-electron laser oscillator with an energy-recovery linac," Physical Review Letters **100** (24) (2008).
[23] S. Eisebitt, J. Luning, W. F. Schlotter, M. Lorgen, O. Hellwig, W. Eberhardt, and J. Stohr, "Lensless imaging of magnetic nanostructures by X-ray spectro-holography," **432** (7019), 885-888 (2004).
[24] I. Mcnulty, J. Kirz, C. Jacobsen, E. H. Anderson, M. R. Howells, and D. P. Kern, "High-Resolution Imaging by Fourier-Transform X-Ray Holography," Science **256** (5059), 1009-1012 (1992).
[25] S. Marchesini, S. Boutet, A. E. Sakdinawat, M. J. Bogan, S. Bajt, A. Barty, H. N. Chapman, M. Frank, S. P. Hau-Riege, A. Szoke, C. W. Cui, D. A. Shapiro, M. R. Howells, J. C. H. Spence, J. W. Shaevitz, J. Y. Lee, J. Hajdu, and M. M. Seibert, "Massively parallel X-ray holography," Nature Photonics **2** (9), 560-563 (2008).
[26] Jianwei Miao, Pambos Charalambous, Janos Kirz, and David Sayre, "Extending the methodology of X-ray crystallography to allow imaging of micrometre-sized non-crystalline specimens," Nature **400** (6742), 342-344 (1999).
[27] I. Robinson and R. Harder, "Coherent X-ray diffraction imaging of strain at the nanoscale," Nature Materials **8** (4), 291-298 (2009).
[28] D. Shapiro, P. Thibault, T. Beetz, V. Elser, M. Howells, C. Jacobsen, J. Kirz, E. Lima, H. Miao, A. M. Neiman, and D. Sayre, "Biological imaging by soft X-ray diffraction microscopy," Proceedings of The National Academy of Sciences of the United States of America **102** (43), 15343-15346 (2005).
[29] J. M. Rodenburg, A. C. Hurst, A. G. Cullis, B. R. Dobson, F. Pfeiffer, O. Bunk, C. David, K. Jefimovs, and I. Johnson, "Hard-x-ray lensless imaging of extended objects," Phys Rev Lett **98** (3), 034801 (2007).
[30] D. Sayre, "Some Implications of a Theorem Due to Shannon," Acta Crystallographica **5** (6), 843-843 (1952).
[31] Gerchber. R. and W. O. Saxton, "Practical Algorithm for Determination of Phase from Image and Diffraction Plane Pictures," Optik **35** (2), 237-242 (1972).
[32] J. R. Fienup, "Phase Retrieval Algorithms - a Comparison," Applied Optics **21** (15), 2758-2769 (1982).
[33] V. Elser, "Random projections and the optimization of an algorithm for phase retrieval," Journal of Physics a-Mathematical and General **36** (12), 2995-3007 (2003).
[34] P. Thibault, V. Elser, C. Jacobsen, D. Shapiro, and D. Sayre, "Reconstruction of a yeast cell from X-ray diffraction data," Acta Crystallographica Section A **62**, 248-261 (2006).
[35] Ian Robinson and Ross Harder, "Coherent X-ray diffraction imaging of strain at the nanoscale," Nat Mater **8** (4), 291-298 (2009).
[36] M.P. Miller, R. M. Suter, U. Lienert, A.J. Beaudoin, E. Fontes, J. Almer, and J.C. Schuren, "High-energy Needs and Capabilities to Study Multiscale Phenomena in Crystalline Materials," Synchrotron Radiation News **25** (6), 18 (2012).
[37] H. F. Poulsen, S. F. Nielsen, E. M. Lauridsen, S. Schmidt, R. M. Suter, U. Lienert, L. Margulies, T. Lorentzen, and D. J. Jensen, "Three-dimensional maps of grain boundaries and the stress state of individual grains in polycrystals and powders," Journal of Applied Crystallography **34**, 751-756 (2001).

[38] B. C. Larson, W. Yang, G. E. Ice, J. D. Budai, and J. Z. Tischler, "Three-dimensional X-ray structural microscopy with submicrometre resolution," Nature **415** (6874), 887-890 (2002).
[39] M. A. Meyers and L. E. Murr, "Model for Formation of Annealing Twins in Fcc Metals and Alloys," Acta Metallurgica **26** (6), 951-962 (1978).
[40] G. S. Rohrer, E. A. Holm, A. D. Rollett, S. M. Foiles, J. Li, and D. L. Olmsted, "Comparing calculated and measured grain boundary energies in nickel," Acta Materialia **58** (15), 5063-5069 (2010).
[41] S. Mahajan, C. S. Pande, M. A. Imam, and B. B. Rath, "Formation of annealing twins in f.c.c. crystals," Acta Materialia **45** (6), 2633-2638 (1997).
[42] BB Rath, MA Imam, and CS Pande, "Nucleation and growth of twin interfaces in Fcc metals and alloys," Mater. Phys. Mech. **1**, 61-66 (2000).
[43] M. C. Newton, S. J. Leake, R. Harder, and I. K. Robinson, "Three-dimensional imaging of strain in a single ZnO nanorod," Nature Materials **9** (2), 120-124 (2010).
[44] G. J. Williams, M. A. Pfeifer, I. A. Vartanyants, and I. K. Robinson, "Three-dimensional imaging of microstructure in Au nanocrystals," Phys Rev Lett **90** (17), 175501 (2003).
[45] Mark A. Pfeifer, Garth J. Williams, Ivan A. Vartanyants, Ross Harder, and Ian K. Robinson, "Three-dimensional mapping of a deformation field inside a nanocrystal," Nature **442** (7098), 63-66 (2006).
[46] E. Dagotto, "Complexity in strongly correlated electronic systems," Science **309** (5732), 257-262 (2005).
[47] M. Uehara, S. Mori, C. H. Chen, and S. W. Cheong, "Percolative phase separation underlies colossal magnetoresistance in mixed-valent manganites," Nature **399** (6736), 560-563 (1999).
[48] E. Dagotto, J. Burgy, and A. Moreo, "Nanoscale phase separation in colossal magnetoresistance materials: lessons for the cuprates?," Solid State Communications **126** (1-2), 9-22 (2003).
[49] J. Lee, K. Fujita, K. McElroy, J. A. Slezak, M. Wang, Y. Aiura, H. Bando, M. Ishikado, T. Masui, J. X. Zhu, A. V. Balatsky, H. Eisaki, S. Uchida, and J. C. Davis, "Interplay of electron-lattice interactions and superconductivity in Bi2Sr2CaCu2O8+delta," Nature **442** (7102), 546-550 (2006).
[50] K. K. Gomes, A. N. Pasupathy, A. Pushp, S. Ono, Y. Ando, and A. Yazdani, "Visualizing pair formation on the atomic scale in the high-T-c superconductor Bi2Sr2CaCu2O8+delta," Nature **447** (7144), 569-572 (2007).
[51] M. Vershinin, S. Misra, S. Ono, Y. Abe, Y. Ando, and A. Yazdani, "Local ordering in the pseudogap state of the high-T-c superconductor Bi2Sr2CaCu2O8+delta," Science **303** (5666), 1995-1998 (2004).
[52] O. G. Shpyrko, E. D. Isaacs, J. M. Logan, Y. J. Feng, G. Aeppli, R. Jaramillo, H. C. Kim, T. F. Rosenbaum, P. Zschack, M. Sprung, S. Narayanan, and A. R. Sandy, "Direct measurement of antiferromagnetic domain fluctuations," Nature **447** (7140), 68-71 (2007).
[53] F. Ye, J. A. Fernandez-Baca, P. C. Dai, J. W. Lynn, H. Kawano-Furukawa, H. Yoshizawa, Y. Tomioka, and Y. Tokura, "Electronically smecticlike liquid-crystal phase in a nearly half-doped manganite," Physical Review B **72** (21), 212404-212408 (2005).
[54] J. W. Miao, R. L. Sandberg, and C. Y. Song, "Coherent X-Ray Diffraction Imaging," Ieee Journal of Selected Topics in Quantum Electronics **18** (1), 399-410 (2012).
[55] H. D. Jiang, C. Y. Song, C. C. Chen, R. Xu, K. S. Raines, B. P. Fahimian, C. H. Lu, T. K. Lee, A. Nakashima, J. Urano, T. Ishikawa, F. Tamanoi, and J. W. Miao, "Quantitative 3D imaging of whole, unstained cells by using X-ray diffraction microscopy," Proceedings of The National Academy of Sciences of the United States of America **107** (25), 11234-11239 (2010).
[56] J. Nelson, X. J. Huang, J. Steinbrener, D. Shapiro, J. Kirz, S. Marchesini, A. M. Neiman, J. J. Turner, and C. Jacobsen, "High-resolution x-ray diffraction microscopy of specifically labeled yeast cells," Proceedings of The National Academy of Sciences of the United States of America **107** (16), 7235-7239 (2010).

[57] M. R. Howells, T. Beetz, H. N. Chapman, C. Cui, J. M. Holton, C. J. Jacobsen, J. Kirz, E. Lima, S. Marchesini, H. Miao, D. Sayre, D. A. Shapiro, J. C. H. Spence, and D. Starodub, "An assessment of the resolution limitation due to radiation-damage in X-ray diffraction microscopy," Journal of Electron Spectroscopy and Related Phenomena **170** (1-3), 4-12 (2009).

[58] X. J. Huang, J. Nelson, J. Kirz, E. Lima, S. Marchesini, H. J. Miao, A. M. Neiman, D. Shapiro, J. Steinbrener, A. Stewart, J. J. Turner, and C. Jacobsen, "Soft X-Ray Diffraction Microscopy of a Frozen Hydrated Yeast Cell," Physical Review Letters **103** (19) (2009).

[59] E. Lima, L. Wiegart, P. Pernot, M. Howells, J. Timmins, F. Zontone, and A. Madsen, "Cryogenic X-Ray Diffraction Microscopy for Biological Samples," Physical Review Letters **103** (19) (2009).

[60] C. U. Kim, J. L. Wierman, R. Gillilan, E. Lima, and S. M. Gruner, "A high-pressure cryocooling method for protein crystals and biological samples with reduced background X-ray scatter," Journal of Applied Crystallography **46** (1), 234-241 (2013).

[61] M. D. de Jonge, C. Holzner, S. B. Baines, B. S. Twining, K. Ignatyev, J. Diaz, D. L. Howard, D. Legnini, A. Miceli, I. McNulty, C. J. Jacobsen, and S. Vogt, "Quantitative 3D elemental microtomography of Cyclotella meneghiniana at 400-nm resolution," Proc Natl Acad Sci U S A **107** (36), 15676-15680 (2010).

[62] S. Gunes, H. Neugebauer, and N. S. Sariciftci, "Conjugated polymer-based organic solar cells," Chemical Reviews **107** (4), 1324-1338 (2007).

[63] J. J. M. Halls, C. A. Walsh, N. C. Greenham, E. A. Marseglia, R. H. Friend, S. C. Moratti, and A. B. Holmes, "Efficient Photodiodes from Interpenetrating Polymer Networks," Nature **376** (6540), 498-500 (1995).

[64] G. Yu, J. Gao, J. C. Hummelen, F. Wudl, and A. J. Heeger, "Polymer Photovoltaic Cells - Enhanced Efficiencies Via a Network of Internal Donor-Acceptor Heterojunctions," Science **270** (5243), 1789-1791 (1995).

[65] Brian A. Collins, Eliot Gann, Lewis Guignard, Xiaoxi He, Christopher R. McNeill, and Harald Ade, "Molecular Miscibility of Polymer−Fullerene Blends," The Journal of Physical Chemistry Letters **1** (21), 3160-3166 (2010).

[66] B. Watts, W. J. Belcher, L. Thomsen, H. Ade, and P. C. Dastoor, "A Quantitative Study of PCBM Diffusion during Annealing of P3HT:PCBM Blend Films," Macromolecules **42**, 8392 (2009).

[67] Neil D. Treat, Michael A. Brady, Gordon Smith, Michael F. Toney, Edward J. Kramer, Craig J. Hawker, and Michael L. Chabinyc, "Interdiffusion of PCBM and P3HT Reveals Miscibility in a Photovoltaically Active Blend," Advanced Energy Materials **1** (1), 82-89 (2011).

[68] R. Radbeh, E. Parbaile, J. Boucle, C. Di Bin, A. Moliton, V. Coudert, F. Rossignol, and B. Ratier, "Nanoscale control of the network morphology of high efficiency polymer fullerene solar cells by the use of high material concentration in the liquid phase," Nanotechnology **21** (3) (2010).

[69] W. Ma, C. Yang, X. Gong, K. Lee, and A. J Heeger, "Thermally Stable, Efficient Polymer Solar Cells with Nanoscale Control of the Interpenetrating Network Morphology," Advanced Functional Materials **15** (10), 1617-1622 (2005).

[70] Henry J. Snaith, Ana C. Arias, Arne C. Morteani, Carlos Silva, and Richard H. Friend, "Charge Generation Kinetics and Transport Mechanisms in Blended Polyfluorene Photovoltaic Devices," Nano Letters **2** (12), 1353-1357 (2002).

[71] J. K J van Duren, X. Yang, J. Loos, C. W T Bulle-Lieuwma, A. B Sieval, J. C Hummelen, and R. A J Janssen, "Relating the Morphology of Poly(p-phenylene vinylene)/Methanofullerene Blends to Solar-Cell Performance," Advanced Functional Materials **14** (5), 425-434 (2004).

[72] Henry J. Snaith and Richard H. Friend, "Morphological dependence of charge generation and transport in blended polyfluorene photovoltaic devices," Thin Solid Films **451** (0), 567-571 (2004).

[73] S. E. Shaheen, C. J. Brabec, N. S. Sariciftci, F. Padinger, T. Fromherz, and J. C. Hummelen, "2.5%

efficient organic plastic solar cells," Applied Physics Letters **78** (6), 841-843 (2001).
[74] H. Hoppe, M. Niggemann, C. Winder, J. Kraut, R. Hiesgen, A. Hinsch, D. Meissner, and N. S Sariciftci, "Nanoscale Morphology of Conjugated Polymer/Fullerene-Based Bulk- Heterojunction Solar Cells," Advanced Functional Materials **14** (10), 1005-1011 (2004).
[75] G. Li, V. Shrotriya, J. S. Huang, Y. Yao, T. Moriarty, K. Emery, and Y. Yang, "High-efficiency solution processable polymer photovoltaic cells by self-organization of polymer blends," Nature Materials **4** (11), 864-868 (2005).
[76] J. Peet, J. Y. Kim, N. E. Coates, W. L. Ma, D. Moses, A. J. Heeger, and G. C. Bazan, "Efficiency enhancement in low-bandgap polymer solar cells by processing with alkane dithiols," Nature Materials **6** (7), 497-500 (2007).
[77] A. R. Campbell, J. M. Hodgkiss, S. Westenhoff, I. A. Howard, R. A. Marsh, C. R. McNeill, R. H. Friend, and N. C. Greenham, "Low-Temperature Control of Nanoscale Morphology for High Performance Polymer Photovoltaics," Nano Letters **8** (11), 3942-3947 (2008).
[78] F. Padinger, R. S. Rittberger, and N. S. Sariciftci, "Effects of postproduction treatment on plastic solar cells," Advanced Functional Materials **13** (1), 85-88 (2003).
[79] M. Y. Chiu, U. S. Jeng, C. H. Su, K. S. Liang, and K. H. Wei, "Simultaneous use of small- and wide-angle X-ray techniques to analyze nanometerscale phase separation in polymer heterojunction solar cells," Advanced Materials **20** (13), 2573-2579 (2008).
[80] X. N. Yang, J. Loos, S. C. Veenstra, W. J. H. Verhees, M. M. Wienk, J. M. Kroon, M. A. J. Michels, and R. A. J. Janssen, "Nanoscale morphology of high-performance polymer solar cells," Nano Letters **5** (4), 579-583 (2005).
[81] Svetlana S. van Bavel, Erwan Sourty, Gijsbertus de With, and Joachim Loos, "Three-Dimensional Nanoscale Organization of Bulk Heterojunction Polymer Solar Cells," Nano Letters **9** (2), 507-513 (2008).
[82] S. O. Hruszkewycz, M. V. Holt, A. Tripathi, J. Maser, and P. H. Fuoss, "Framework for three-dimensional coherent diffraction imaging by focused beam x-ray Bragg ptychography," Optics Letters **36** (12), 2227-2229 (2011).
[83] M. Dierolf, P. Thibault, A. Menzel, C. M. Kewish, K. Jefimovs, I. Schlichting, K. Von Konig, O. Bunk, and F. Pfeiffer, "Ptychographic coherent diffractive imaging of weakly scattering specimens," New Journal of Physics **12**, 035017-035024 (2010).
[84] B. A. Collins, Z. Li, J. R. Tumbleston, E. Gann, C. R. McNeill, and H. Ade, "Absolute Measurement of Domain Composition and Nanoscale Size Distribution Explains Performance in PTB7:PC71BM Solar Cells," Advanced Energy Materials **3** (1), 65-74 (2013).
[85] M. S. Hunter and P. Fromme, "Toward structure determination using membrane-protein nanocrystals and microcrystals," Methods **55** (4), 387-404 (2011).
[86] P. Fromme and J. C. H. Spence, "Femtosecond nanocrystallography using X-ray lasers for membrane protein structure determination," Current Opinion in Structural Biology **21** (4), 509-516 (2011).
[87] R. Koopmann, K. Cupelli, L. Redecke, K. Nass, D. P. DePonte, T. A. White, F. Stellato, D. Rehders, M. N. Liang, J. Andreasson, A. Aquila, S. Bajt, M. Barthelmess, A. Barty, M. J. Bogan, C. Bostedt, S. Boutet, J. D. Bozek, C. Caleman, N. Coppola, J. Davidsson, R. B. Doak, T. Ekeberg, S. W. Epp, B. Erk, H. Fleckenstein, L. Foucar, H. Graafsma, L. Gumprecht, J. Hajdu, C. Y. Hampton, A. Hartmann, R. Hartmann, G. Hauser, H. Hirsemann, P. Holl, M. S. Hunter, S. Kassemeyer, R. A. Kirian, L. Lomb, F. R. N. C. Maia, N. Kimmel, A. V. Martin, M. Messerschmidt, C. Reich, D. Rolles, B. Rudek, A. Rudenko, I. Schlichting, J. Schulz, M. M. Seibert, R. L. Shoeman, R. G. Sierra, H. Soltau, S. Stern, L. Struder, N. Timneanu, J. Ullrich, X. Y. Wang, G. Weidenspointner, U. Weierstall, G. J. Williams, C. B. Wunderer, P. Fromme, J. C. H. Spence, T. Stehle, H. N. Chapman, C. Betzel, and M. Duszenko, "In vivo protein crystallization opens new routes in structural

biology," Nature Methods **9** (3), 259-U254 (2012).
[88] R. B. von Dreele, "Characterization of proteins by powder diffraction," Zeitschrift Fur Kristallographie, 27-32 (2009).
[89] S. Boutet, L. Lomb, G. J. Williams, T. R. M. Barends, A. Aquila, R. B. Doak, U. Weierstall, D. P. DePonte, J. Steinbrener, R. L. Shoeman, M. Messerschmidt, A. Barty, T. A. White, S. Kassemeyer, R. A. Kirian, M. M. Seibert, P. A. Montanez, C. Kenney, R. Herbst, P. Hart, J. Pines, G. Haller, S. M. Gruner, H. T. Philipp, M. W. Tate, M. Hromalik, L. J. Koerner, N. van Bakel, J. Morse, W. Ghonsalves, D. Arnlund, M. J. Bogan, C. Caleman, R. Fromme, C. Y. Hampton, M. S. Hunter, L. C. Johansson, G. Katona, C. Kupitz, M. N. Liang, A. V. Martin, K. Nass, L. Redecke, F. Stellato, N. Timneanu, D. J. Wang, N. A. Zatsepin, D. Schafer, J. Defever, R. Neutze, P. Fromme, J. C. H. Spence, H. N. Chapman, and I. Schlichting, "High-Resolution Protein Structure Determination by Serial Femtosecond Crystallography," Science **337** (6092), 362-364 (2012).
[90] B. Nagar and J. Kuriyan, "SAXS and the working protein," Structure **13** (2), 169-170 (2005).
[91] David A. Jacques and Jill Trewhella, "Small-angle scattering for structural biology—Expanding the frontier while avoiding the pitfalls," Protein Science **19** (4), 642-657 (2010).
[92] I. Grillo, "Applications of stopped-flow in SAXS and SANS," Current Opinion in Colloid & Interface Science **14** (6), 402-408 (2009).
[93] H. Y. Park, X. Y. Qiu, E. Rhoades, J. Korlach, L. W. Kwok, W. R. Zipfel, W. W. Webb, and L. Pollack, "Achieving uniform mixing in a microfluidic device: Hydrodynamic focusing prior to mixing," Analytical Chem **78** (13), 4465-4473 (2006).
[94] L. Pollack, Tate, M.W., Darnton, N.C., Knight, J.B., Gruner, S.M., Eaton, W.A., Austin, R.H., "Compactness of the denatured state of a fast-folding protein measured by submillisecond small-angle x-ray scattering," Proc. Natl. Acad. Sci. USA **96**, 10115-10117 (1999).
[95] L. Pollack, Tate, M.W., Finnefrock, A.C., Kalidas, C., Trotter, S., Darnton, N.C., Lurio, L., Austin, R.H., Batt, C.A., Gruner, S.M., Mochrie, S.G.J., "Observation of Time-Resolved Collapse of a Folding Protein," APS Forefront, published by Argonne National Laboratory, 128-130 (2001).
[96] L. W. Kwok, I. Shcherbakova, J. S. Lamb, H. Y. Park, K. Andresen, H. Smith, M. Brenowitz, and L. Pollack, "Concordant exploration of the kinetics of RNA folding from global and local perspectives," Journal of Molecular Biology **355** (2), 282-293 (2006).
[97] R. Russell, Millett, I.S., Tate, M.W., Kwok, L.W., Nakatani, B., Gruner, S.M., Mochrie, S.G.J., Pande, V., Doniach, S., Herschlag, D., Pollack, L., "Rapid compaction during RNA folding," Proc Natl Acad Sci USA **99** (7), 4266-4271 (2002).
[98] H. S. Cho, N. Dashdorj, F. Schotte, T. Graber, R. Henning, and P. Anfinrud, "Protein structural dynamics in solution unveiled via 100-ps time-resolved x-ray scattering," Proceedings of The National Academy of Sciences of the United States of America **107** (16), 7281-7286 (2010).
[99] Francis Crick, *What Mad Pursuit: A Personal View of Scientific Discovery*. (Basic Books, New York, 1988), p.150.
[100] Jae-Hyung Jeon and Ralf Metzler, "Inequivalence of time and ensemble averages in ergodic systems: Exponential versus power-law relaxation in confinement," Physical Review E **85** (2), 021147 (2012).
[101] C. Bressler, M. Saes, M. Chergui, R. Abela, and P. Pattison, "Optimizing a time-resolved X-ray absorption experiment," Nuclear Instruments & Methods in Physics Research Section a-Accelerators Spectrometers Detectors and Associated Equipment **467**, 1444-1446 (2001).
[102] C. Bressler, M. Saes, M. Chergui, D. Grolimund, R. Abela, and P. Pattison, "Towards structural dynamics in condensed chemical systems exploiting ultrafast time-resolved x-ray absorption spectroscopy," Journal of Chemical Physics **116** (7), 2955-2966 (2002).
[103] C. Bressler and M. Chergui, "Ultrafast X-ray absorption spectroscopy," Chemical Reviews **104** (4), 1781-1812 (2004).

[104] G. Vanko, P. Glatzel, V. T. Pham, R. Abela, D. Grolimund, C. N. Borca, S. L. Johnson, C. J. Milne, and C. Bressler, "Picosecond Time-Resolved X-Ray Emission Spectroscopy: Ultrafast Spin-State Determination in an Iron Complex," Angewandte Chemie-International Edition **49** (34), 5910-5912 (2010).

[105] Tingting Qi, Young-Han Shin, Ka-Lo Yeh, Keith A. Nelson, and Andrew M. Rappe, "Collective Coherent Control: Synchronization of Polarization in Ferroelectric $PbTiO_3$ by Shaped THz Fields," Physical Review Letters **102** (24), 247603 (2009).

[106] M. Trigo, J. Chen, V. H. Vishwanath, Y. M. Sheu, T. Graber, R. Henning, and D. A. Reis, "Imaging nonequilibrium atomic vibrations with x-ray diffuse scattering," Physical Review B **82** (23), 235205 (2010).

[107] Maryana Escalante, Aufried Lenferink, Yiping Zhao, Niels Tas, Jurriaan Huskens, C. Neil Hunter, Vinod Subramaniam, and Cees Otto, "Long-Range Energy Propagation in Nanometer Arrays of Light Harvesting Antenna Complexes," Nano Letters **10** (4), 1450-1457 (2010).

[108] Kwang-Je Kim and Yuri V. Shvyd'ko, "Tunable optical cavity for an x-ray free-electron-laser oscillator," Physical Review Special Topics - Accelerators and Beams **12** (3), 030703 (2009).

[109] K. Maeda and K. Domen, "New non-oxide photocatalysts designed for overall water splitting under visible light," Journal of Physical Chemistry C **111** (22), 7851-7861 (2007).

[110] T. Hirai, K. Maeda, M. Yoshida, J. Kubota, S. Ikeda, M. Matsumura, and K. Domen, "Origin of visible light absorption in GaN-Rich (Ga1-xZnx)(N1-xOx) photocatalysts," Journal of Physical Chemistry C **111** (51), 18853-18855 (2007).

[111] Ji Feng, Wojciech Grochala, Tomasz Jaroń, Roald Hoffmann, Aitor Bergara, and N. W. Ashcroft, "Structures and Potential Superconductivity in SiH_{4} at High Pressure: En Route to "Metallic Hydrogen"," Physical Review Letters **96** (1), 017006 (2006).

[112] Russell J. Hemley, "Superconductivity in a Grain of Salt," Science **281** (5381), 1296-1297 (1998).

[113] Viktor V. Struzhkin, Russell J. Hemley, Ho-kwang Mao, and Yuri A. Timofeev, "Superconductivity at 10-17[thinsp]K in compressed sulphur," Nature **390** (6658), 382-384 (1997).

[114] Chia-Chun Chen, A. B. Herhold, C. S. Johnson, and A. P. Alivisatos, "Size Dependence of Structural Metastability in Semiconductor Nanocrystals," Science **276** (5311), 398-401 (1997).

[115] C. B. Murray, C. R. Kagan, and M. G. Bawendi, "Synthesis and Characterization Of Monodisperse Nanocrystals and Close-Packed Nanocrystal Assemblies," Annual Review of Materials Science **30** (1), 545-610 (2000).

[116] Z. W. Wang, X. D. Wen, R. Hoffmann, J. S. Son, R. P. Li, C. C. Fang, D. M. Smilgies, and T. Hyeon, "Reconstructing a solid-solid phase transformation pathway in CdSe nanosheets with associated soft ligands," Proceedings of The National Academy of Sciences of the United States of America **107** (40), 17119-17124 (2010).

[117] Z. W. Wang, C. Schliehe, T. Wang, Y. Nagaoka, Y. C. Cao, W. A. Bassett, H. M. Wu, H. Y. Fan, and H. Weller, "Deviatoric Stress Driven Formation of Large Single-Crystal PbS Nanosheet from Nanoparticles and in Situ Monitoring of Oriented Attachment," Journal of the American Chemical Society **133** (37), 14484-14487 (2011).

[118] Z. W. Wang, O. Chen, C. Y. Cao, K. Finkelstein, D. M. Smilgies, X. M. Lu, and W. A. Bassett, "Integrating in situ high pressure small and wide angle synchrotron x-ray scattering for exploiting new physics of nanoparticle supercrystals," Review of Scientific Instruments **81** (9), 093902 (2010).

[119] Zewei Quan, Yuxuan Wang, In-Tae Bae, Welley Siu Loc, Chenyu Wang, Zhongwu Wang, and Jiye Fang, "Reversal of Hall–Petch Effect in Structural Stability of PbTe Nanocrystals and Associated Variation of Phase Transformation," Nano Letters **11** (12), 5531-5536 (2011).

[120] Kaifu Bian, Zhongwu Wang, and Tobias Hanrath, "Comparing the Structural Stability of PbS Nanocrystals Assembled in fcc and bcc Superlattice Allotropes," Journal of the American

Chemical Society **134** (26), 10787-10790 (2012).
[121] J. Cheng, V.I. Levitas, H. Zhu, J. Chaudhuri, A. Marathe, and Y. Ma, "Shear-induced phase transition of nanocrystalline hexagonal boron nitride to wurtzitic structure at room temperature and lower pressure," Proceedings of The National Academy of Sciences of the United States of America **109** (47), 19108-19112 (2012).
[122] H. Wu, F. Bai, Z. C. Sun, R. E. Haddad, D. M. Boye, Z. W. Wang, J. Y. Huang, and H. Y. Fan, "Nanostructured Gold Architectures Formed through High Pressure-Driven Sintering of Spherical Nanoparticle Arrays," Journal of the American Chemical Society **132** (37), 12826-12828 (2010).
[123] Zhongwu Wang, Constanze Schliehe, Tie Wang, Yasutaka Nagaoka, Y. Charles Cao, William A. Bassett, Huimeng Wu, Hongyou Fan, and Horst Weller, "Deviatoric Stress Driven Formation of Large Single-Crystal PbS Nanosheet from Nanoparticles and in Situ Monitoring of Oriented Attachment," Journal of the American Chemical Society **133** (37), 14484-14487 (2011).
[124] H. M. Wu, F. Bai, Z. C. Sun, R. E. Haddad, D. M. Boye, Z. W. Wang, and H. Y. Fan, "Pressure-Driven Assembly of Spherical Nanoparticles and Formation of 1D-Nanostructure Arrays," Angewandte Chemie-International Edition **49** (45), 8431-8434 (2010).
[125] T. Wang, J. Q. Zhuang, J. Lynch, O. Chen, Z. L. Wang, X. R. Wang, D. LaMontagne, H. M. Wu, Z. W. Wang, and Y. C. Cao, "Self-Assembled Colloidal Superparticles from Nanorods," Science **338** (6105), 358-363 (2012).
[126] D. V. Helmberger, L. Wen, and X. Ding, "Seismic evidence that the source of the Iceland hotspot lies at the core-mantle boundary," Nature **396** (6708), 251-255 (1998).
[127] S. Huotari, T. Pylkkanen, R. Verbeni, G. Monaco, and K. Hamalainen, "Direct tomography with chemical-bond contrast," Nature Materials **10** (7), 489-493 (2011).
[128] R. Boehler, "Melting temperature of the earth's mantle and core: Earth's thermal structure," Annual Review of Earth and Planetary Sciences **24**, 15-40 (1996).
[129] A. Zerr, A. Diegeler, and R. Boehler, "Solidus of Earth's deep mantle," Science **281** (5374), 243-246 (1998).
[130] J. H. Nguyen and N. C. Holmes, "Melting of iron at the physical conditions of the Earth's core," Nature **427** (6972), 339-342 (2004).
[131] D. Errandonea, B. Schwager, R. Ditz, C. Gessmann, R. Boehler, and M. Ross, "Systematics of transition-metal melting," Physical Review B **63** (13) (2001).
[132] R. Jeanloz and A. Kavner, "Melting criteria and imaging spectroradiometry in laser-heated diamond-cell experiments," Philosophical Transactions of the Royal Society a-Mathematical Physical and Engineering Sciences **354** (1711), 1279-1305 (1996).
[133] S. J. Billinge, R. G. DiFrancesco, G. H. Kwei, J. J. Neumeier, and J. D. Thompson, "Direct Observation of Lattice Polaron Formation in the Local Structure of La1-xCaxMnO3," Phys Rev Lett **77** (4), 715-718 (1996).
[134] E. S. Bozin, C. D. Malliakas, P. Souvatzis, T. Proffen, N. A. Spaldin, M. G. Kanatzidis, and S. J. Billinge, "Entropically stabilized local dipole formation in lead chalcogenides," Science **330** (6011), 1660-1663 (2010).
[135] G. E. Ice, J. D. Budai, and J. W. L. Pang, "The Race to X-ray Microbeam and Nanobeam Science," Science **334** (6060), 1234-1239 (2011).
[136] R. P. Winarski, M. V. Holt, V. Rose, P. Fuesz, D. Carbaugh, C. Benson, D. M. Shu, D. Kline, G. B. Stephenson, I. McNulty, and J. Maser, "A hard X-ray nanoprobe beamline for nanoscale microscopy," Journal of Synchrotron Radiation **19**, 1056-1060 (2012).
[137] C. E. Murray, A. Ying, S. M. Polvino, I. C. Noyan, M. Holt, and J. Maser, "Nanoscale silicon-on-insulator deformation induced by stressed liner structures," Journal of Applied Physics **109** (8) (2011).
[138] M. M. Qazilbash, A. Tripathi, A. A. Schafgans, B. J. Kim, H. T. Kim, Z. H. Cai, M. V. Holt, J. M.

Maser, F. Keilmann, O. G. Shpyrko, and D. N. Basov, "Nanoscale imaging of the electronic and structural transitions in vanadium dioxide," Physical Review B **83** (16), 165108-165125 (2011).
[139] S. Hudelson, B. K. Newman, S. Bernardis, D. P. Fenning, M. I. Bertoni, M. A. Marcus, S. C. Fakra, B. Lai, and T. Buonassisi, "Retrograde Melting and Internal Liquid Gettering in Silicon," Advanced Materials **22** (35), 3948-3968 (2010).
[140] M. D. de Jonge and S. Vogt, "Hard X-ray fluorescence tomography--an emerging tool for structural visualization," Curr Opin Struct Biol **20** (5), 606-614 (2010).
[141] T. Paunesku, S. Vogt, J. Maser, B. Lai, and G. Woloschak, "X-ray fluorescence microprobe imaging in biology and medicine," Journal of Cellular Biochemistry **99** (6), 1489-1502 (2006).
[142] L. Finney, S. Mandava, L. Ursos, W. Zhang, D. Rodi, S. Vogt, D. Legnini, J. Maser, F. Ikpatt, O. I. Olopade, and D. Glesne, "X-ray fluorescence microscopy reveals large-scale relocalization and extracellular translocation of cellular copper during angiogenesis," Proc Natl Acad Sci U S A **104** (7), 2247-2252 (2007).
[143] T. Paunesku, T. Rajh, G. Wiederrecht, J. Maser, S. Vogt, N. Stojicevic, M. Protic, B. Lai, J. Oryhon, M. Thurnauer, and G. Woloschak, "Biology of TiO2-oligonucleotide nanocomposites," Nat Mater **2** (5), 343-346 (2003).
[144] T. Paunesku, S. Vogt, B. Lai, J. Maser, N. Stojicevic, K. T. Thurn, C. Osipo, H. Liu, D. Legnini, Z. Wang, C. Lee, and G. E. Woloschak, "Intracellular distribution of TiO2-DNA oligonucleotide nanoconjugates directed to nucleolus and mitochondria indicates sequence specificity," Nano Letters **7** (3), 596-601 (2007).
[145] M. Kuhlmann, J. M. Feldkamp, J. Patommel, S. V. Roth, A. Timmann, R. Gehrke, P. Muller-Buschbaum, and C. G. Schroer, "Grazing Incidence Small-Angle X-ray Scattering Microtomography Demonstrated on a Self-Ordered Dried Drop of Nanoparticles," Langmuir **25** (13), 7241-7243 (2009).
[146] X. H. Xiao and Q. Shen, "Wave propagation and phase retrieval in Fresnel diffraction by a distorted-object approach," Physical Review B **72** (3), 033103-033107 (2005).
[147] C. G. Schroer, R. Boye, J. M. Feldkamp, J. Patommel, A. Schropp, A. Schwab, S. Stephan, M. Burghammer, S. Schoder, and C. Riekel, "Coherent x-ray diffraction imaging with nanofocused illumination," Physical Review Letters **101** (9), 090801-090805 (2008).
[148] X. Wu, H. Liu, and A. Yan, "X-ray phase-attenuation duality and phase retrieval," Optics Letters **30** (4), 379-381 (2005).
[149] F. Berenguer de la Cuesta, M. P. Wenger, R. J. Bean, L. Bozec, M. A. Horton, and I. K. Robinson, "Coherent X-ray diffraction from collagenous soft tissues," Proc Natl Acad Sci U S A **106** (36), 15297-15301 (2009).
[150] Stephan O. Hruszkewycz, Martin V. Holt, Ash Tripathi, Jörg Maser, and Paul H. Fuoss, "Framework for three-dimensional coherent diffraction imaging by focused beam x-ray Bragg ptychography," Opt. Lett. **36** (12), 2227-2229 (2011).
[151] A.R Woll, J. Mass, C. Bisulca, M. Cushman, C. Griggs, T. Wazny, and N. Ocon, "The Unique History of The Armorer's Shop: an application of confocal x-ray fluorescence microscopy," Studies in Conservation **53** (2), 93-109 (2008).
[152] A. R. Woll, J. Mass, C. Bisulca, R. Huang, D. H. Bilderback, S. Gruner, and N. Gao, "Development of confocal X-ray fluorescence (XRF) microscopy at the Cornell high energy synchrotron source," Applied Physics a-Materials Science & Processing **83** (2), 235-238 (2006).
[153] F. Casadio, S. Xie, S. C. Rukes, B. Myers, K. A. Gray, R. Warta, and I. Fiedler, "Electron energy loss spectroscopy elucidates the elusive darkening of zinc potassium chromate in Georges Seurat's A Sunday on La Grande Jatte-1884," Analytical and Bioanalytical Chemistry **399** (9), 2909-2920 (2011).
[154] L. Monico, G. Van der Snickt, K. Janssens, W. De Nolf, C. Miliani, J. Dik, M. Radepont, E. Hendriks,

M. Geldof, and M. Cotte, "Degradation Process of Lead Chromate in Paintings by Vincent van Gogh Studied by Means of Synchrotron X-ray Spectromicroscopy and Related Methods. 2. Original Paint Layer Samples," Analytical Chemistry **83** (4), 1224-1231 (2011).

[155] L. Monico, G. Van der Snickt, K. Janssens, W. De Nolf, C. Miliani, J. Verbeeck, H. Tian, H. Y. Tan, J. Dik, M. Radepont, and M. Cotte, "Degradation Process of Lead Chromate in Paintings by Vincent van Gogh Studied by Means of Synchrotron X-ray Spectromicroscopy and Related Methods. 1. Artificially Aged Model Samples," Analytical Chemistry **83** (4), 1214-1223 (2011).

[156] G. Van der Snickt, J. Dik, M. Cotte, K. Janssens, J. Jaroszewicz, W. De Nolf, J. Groenewegen, and L. Van der Loeff, "Characterization of a Degraded Cadmium Yellow (CdS) Pigment in an Oil Painting by Means of Synchrotron Radiation Based X-ray Techniques," Analytical Chemistry **81** (7), 2600-2610 (2009).

[157] S. F. Li and R. M. Suter, "Adaptive Reconstruction Method for Three-Dimensional Orientation Imaging," Journal of Applied Crystallography **46**, 512-524 (2013).

[158] W. Ludwig, P. Reischig, A. King, M. Herbig, E. M. Lauridsen, G. Johnson, T. J. Marrow, and J. Y. Buffiere, "Three-dimensional grain mapping by x-ray diffraction contrast tomography and the use of Friedel pairs in diffraction data analysis," Review of Scientific Instruments **80** (3), 033905-033914 (2009).

[159] R. P. Li, J. W. Ward, D. M. Smilgies, M. M. Payne, J. E. Anthony, O. D. Jurchescu, and A. Amassian, "Direct Structural Mapping of Organic Field-Effect Transistors Reveals Bottlenecks to Carrier Transport," Advanced Materials **24** (41), 5553-5558 (2012).

[160] S. M. Park, M. P. Stoykovich, R. Ruiz, Y. Zhang, C. T. Black, and P. E. Nealey, "Directed assembly of lamellae-forming block copolymers by using chemically and topographically patterned substrates," Advanced Materials **19** (4), 607-620 (2007).

[161] J. K. Bosworth, M. Y. Paik, R. Ruiz, E. L. Schwartz, J. Q. Huang, A. W. Ko, D. M. Smilgies, C. T. Black, and C. K. Ober, "Control of self-assembly of lithographically patternable block copolymer films," ACS Nano **2** (7), 1396-1402 (2008).

[162] H. Hlaing, X. H. Lu, T. Hofmann, K. G. Yager, C. T. Black, and B. M. Ocko, "Nanoimprint-Induced Molecular Orientation in Semiconducting Polymer Nanostructures," ACS Nano **5** (9), 7532-7538 (2011).

[163] M. J. Campolongo, S. J. Tan, D. M. Smilgies, M. Zhao, Y. Chen, I. Xhangolli, W. L. Cheng, and D. Luo, "Crystalline Gibbs Monolayers of DNA-Capped Nanoparticles at the Air-Liquid Interface," ACS Nano **5** (10), 7978-7985 (2011).

[164] S. V. Roth, T. Autenrieth, G. Grubel, C. Riekel, M. Burghammer, R. Hengstler, L. Schulz, and P. Muller-Buschbaum, "In situ observation of nanoparticle ordering at the air-water-substrate boundary in colloidal solutions using x-ray nanobeams," Applied Physics Letters **91** (9), 091915-091918 (2007).

[165] S. V. Roth, G. Herzog, V. Korstgens, A. Buffet, M. Schwartzkopf, J. Perlich, M. M. A. Kashem, R. Dohrmann, R. Gehrke, A. Rothkirch, K. Stassig, W. Wurth, G. Benecke, C. Li, P. Fratzl, M. Rawolle, and P. Muller-Buschbaum, "In situ observation of cluster formation during nanoparticle solution casting on a colloidal film," Journal of Physics-Condensed Matter **23** (25), 254208-254221 (2011).

[166] A. Amassian, V. A. Pozdin, R. P. Li, D. M. Smilgies, and G. G. Malliaras, "Solvent vapor annealing of an insoluble molecular semiconductor," Journal of Materials Chemistry **20** (13), 2623-2629 (2010).

[167] Detlef- M. Smilgies, Ruipeng Li, Gaurav Giri, Kang Wei Chou, Ying Diao, Zhenan Bao, and Aram Amassian, "Look fast: Crystallization of conjugated molecules during solution shearing probed in-situ and in real time by X-ray scattering," physica status solidi (RRL) – Rapid Research Letters, 177–179 (2012).

[168] J. Perlich, M. Schwartzkopf, V. Korstgens, D. Erb, J. F. H. Risch, P. Muller-Buschbaum, R. Rohlsberger, S. V. Roth, and R. Gehrke, "Pattern formation of colloidal suspensions by dip-coating: An in situ grazing incidence X-ray scattering study," Physica Status Solidi-Rapid Research Letters **6** (6), 253-255 (2012).

[169] P. Fenter, C. Park, Z. Zhang, and S. Wang, "Observation of subnanometre-high surface topography with X-ray reflection phase-contrast microscopy," Nature Phys **2** (10), 700-704 (2006).

[170] J. Gulden, O. M. Yefanov, A. P. Mancuso, R. Dronyak, A. Singer, V. Bernatova, A. Burkhardt, O. Polozhentsev, A. Soldatov, M. Sprung, and I. A. Vartanyants, "Three-dimensional structure of a single colloidal crystal grain studied by coherent x-ray diffraction," Optics Express **20** (4), 4039-4049 (2012).

[171] T. Sun, Z. Jiang, J. Strzalka, L. Ocola, and J. Wang, "Three-dimensional coherent X-ray surface scattering imaging near total external reflection," Nature Photonics **6** (9), 586-590 (2012).

[172] O. M. Yefanov, A. V. Zozulya, I. A. Vartanyants, J. Stangl, C. Mocuta, T. H. Metzger, G. Bauer, T. Boeck, and M. Schmidbauer, "Coherent diffraction tomography of nanoislands from grazing-incidence small-angle x-ray scattering," Applied Physics Letters **94** (12), 123104-123107 (2009).

[173] M. Pauly and K. Keegstra, "Plant cell wall polymers as precursors for biofuels," Current Opinion in Plant Biology **13** (3), 305-312 (2010).

[174] C. Somerville, S. Bauer, G. Brininstool, M. Facette, T. Hamann, J. Milne, E. Osborne, A. Paredez, S. Persson, T. Raab, S. Vorwerk, and H. Youngs, "Toward a systems approach to understanding plant-cell walls," Science **306** (5705), 2206-2211 (2004).

[175] M. Pauly and K. Keegstra, "Cell-wall carbohydrates and their modification as a resource for biofuels," Plant Journal **54** (4), 559-568 (2008).

[176] J. Lal, R. Harder, and L. Makowski, "X-ray coherent diffraction imaging of cellulose fibrils in situ," Conf Proc IEEE Eng Med Biol Soc **2011**, 528-530 (2011).

[177] D. Brownlee, P. Tsou, J. Aleon, C. M. Alexander, T. Araki, S. Bajt, G. A. Baratta, R. Bastien, P. Bland, P. Bleuet, J. Borg, J. P. Bradley, A. Brearley, F. Brenker, S. Brennan, J. C. Bridges, N. D. Browning, J. R. Brucato, E. Bullock, M. J. Burchell, H. Busemann, A. Butterworth, M. Chaussidon, A. Cheuvront, M. Chi, M. J. Cintala, B. C. Clark, S. J. Clemett, G. Cody, L. Colangeli, G. Cooper, P. Cordier, C. Daghlian, Z. Dai, L. D'Hendecourt, Z. Djouadi, G. Dominguez, T. Duxbury, J. P. Dworkin, D. S. Ebel, T. E. Economou, S. Fakra, S. A. Fairey, S. Fallon, G. Ferrini, T. Ferroir, H. Fleckenstein, C. Floss, G. Flynn, I. A. Franchi, M. Fries, Z. Gainsforth, J. P. Gallien, M. Genge, M. K. Gilles, P. Gillet, J. Gilmour, D. P. Glavin, M. Gounelle, M. M. Grady, G. A. Graham, P. G. Grant, S. F. Green, F. Grossemy, L. Grossman, J. N. Grossman, Y. Guan, K. Hagiya, R. Harvey, P. Heck, G. F. Herzog, P. Hoppe, F. Horz, J. Huth, I. D. Hutcheon, K. Ignatyev, H. Ishii, M. Ito, D. Jacob, C. Jacobsen, S. Jacobsen, S. Jones, D. Joswiak, A. Jurewicz, A. T. Kearsley, L. P. Keller, H. Khodja, A. L. Kilcoyne, J. Kissel, A. Krot, F. Langenhorst, A. Lanzirotti, L. Le, L. A. Leshin, J. Leitner, L. Lemelle, H. Leroux, M. C. Liu, K. Luening, I. Lyon, G. Macpherson, M. A. Marcus, K. Marhas, B. Marty, G. Matrajt, K. McKeegan, A. Meibom, V. Mennella, K. Messenger, S. Messenger, T. Mikouchi, S. Mostefaoui, T. Nakamura, T. Nakano, M. Newville, L. R. Nittler, I. Ohnishi, K. Ohsumi, K. Okudaira, D. A. Papanastassiou, R. Palma, M. E. Palumbo, R. O. Pepin, D. Perkins, M. Perronnet, P. Pianetta, W. Rao, F. J. Rietmeijer, F. Robert, D. Rost, A. Rotundi, R. Ryan, S. A. Sandford, C. S. Schwandt, T. H. See, D. Schlutter, J. Sheffield-Parker, A. Simionovici, S. Simon, I. Sitnitsky, C. J. Snead, M. K. Spencer, F. J. Stadermann, A. Steele, T. Stephan, R. Stroud, J. Susini, S. R. Sutton, Y. Suzuki, M. Taheri, S. Taylor, N. Teslich, K. Tomeoka, N. Tomioka, A. Toppani, J. M. Trigo-Rodriguez, D. Troadec, A. Tsuchiyama, A. J. Tuzzolino, T. Tyliszczak, K. Uesugi, M. Velbel, J. Vellenga, E. Vicenzi, L. Vincze, J. Warren, I. Weber, M. Weisberg, A. J. Westphal, S. Wirick, D.

Wooden, B. Wopenka, P. Wozniakiewicz, I. Wright, H. Yabuta, H. Yano, E. D. Young, R. N. Zare, T. Zega, K. Ziegler, L. Zimmerman, E. Zinner and M. Zolensky, "Comet 81P/Wild 2 under a microscope," Science **314** (5806), 1711-1716 (2006).

[178] G. J. Flynn, P. Bleuet, J. Borg, J. P. Bradley, F. E. Brenker, S. Brennan, J. Bridges, D. E. Brownlee, E. S. Bullock, M. Burghammer, B. C. Clark, Z. R. Dai, C. P. Daghlian, Z. Djouadi, S. Fakra, T. Ferroir, C. Floss, I. A. Franchi, Z. Gainsforth, J. P. Gallien, P. Gillet, P. G. Grant, G. A. Graham, S. F. Green, F. Grossemy, P. R. Heck, G. F. Herzog, P. Hoppe, F. Horz, J. Huth, K. Ignatyev, H. A. Ishii, K. Janssens, D. Joswiak, A. T. Kearsley, H. Khodja, A. Lanzirotti, J. Leitner, L. Lemelle, H. Leroux, K. Luening, G. J. Macpherson, K. K. Marhas, M. A. Marcus, G. Matrajt, T. Nakamura, K. Nakamura-Messenger, T. Nakano, M. Newville, D. A. Papanastassiou, P. Pianetta, W. Rao, C. Riekel, F. J. Rietmeijer, D. Rost, C. S. Schwandt, T. H. See, J. Sheffield-Parker, A. Simionovici, I. Sitnitsky, C. J. Snead, F. J. Stadermann, T. Stephan, R. M. Stroud, J. Susini, Y. Suzuki, S. R. Sutton, S. Taylor, N. Teslich, D. Troadec, P. Tsou, A. Tsuchiyama, K. Uesugi, B. Vekemans, E. P. Vicenzi, L. Vincze, A. J. Westphal, P. Wozniakiewicz, E. Zinner, and M. E. Zolensky, "Elemental compositions of comet 81P/Wild 2 samples collected by Stardust," Science **314** (5806), 1731-1735 (2006).

[179] G. Silversmit, B. Vekemans, S. Nikitenko, W. Bras, V. Czhech, G. Zaray, I. Szaloki, and L. Vincze, "Polycapillary-optics-based micro-XANES and micro-EXAFS at a third-generation bending-magnet beamline," J Synchrotron Radiat **16** (Pt 2), 237-246 (2009).

[180] Andreas Schropp and Christian G Schroer, "Dose requirements for resolving a given feature in an object by coherent x-ray diffraction imaging," New Journal of Physics **12** (3), 035016 (2010).

[181] L. Pollack, M.W. Tate, A.C. Finnefrock, C. Kalidas, Trotter S., N.C. Darnton, L. Lurio, R.H. Austin, C.A. Batt, S.M. Gruner, and S.G.J. Mochrie, "Time Resolved Collapse of a Folding Protein Observed with Small Angle x-Ray Scattering," Phys. Rev. Lett. **86** (21), 4962-4965 (2001).

[182] G. Grubel, G. B. Stephenson, C. Gutt, H. Sinn, and T. Tschentscher, "XPCS at the European X-ray free electron laser facility," Nucl Instr Meth Phys Res B **262** (2), 357-367 (2007).

[183] M. S. Pierce, K. C. Chang, D. Hennessy, V. Komanicky, M. Sprung, A. Sandy, and H. You, "Surface X-Ray Speckles: Coherent Surface Diffraction from Au(001)," Physical Review Letters **103** (16), 165501 (2009).

[184] G. Ozaydin, A. S. Ozcan, Y. Y. Wang, K. F. Ludwig, H. Zhou, R. L. Headrick, and D. P. Siddons, "Real-time x-ray studies of Mo-seeded Si nanodot formation during ion bombardment," Applied Physics Letters **87** (16), 163104-163107 (2005).

[185] M. S. Pierce, V. Komanicky, A. Barbour, D. C. Hennessy, C. H. Zhu, A. Sandy, and H. You, "Dynamics of the Au (001) surface in electrolytes: In situ coherent x-ray scattering," Physical Review B **86** (8), 085410 (2012).

[186] A. Mittermaier and L. E. Kay, "New tools provide new insights in NMR studies of protein dynamics," Science **312** (5771), 224-228 (2006).

[187] A. Cooper and D. T. Dryden, "Allostery without conformational change. A plausible model," Eur Biophys J **11** (2), 103-109 (1984).

[188] M. F. Hildenbrand and T. M. Bayerl, "Differences in the modulation of collective membrane motions by ergosterol, lanosterol, and cholesterol: a dynamic light scattering study," Biophys J **88** (5), 3360-3367 (2005).

[189] D. Constantin, G. Brotons, T. Salditt, E. Freyssingeas, and A. Madsen, "Dynamics of bulk fluctuations in a lamellar phase studied by coherent x-ray scattering," Phys Rev E Stat Nonlin Soft Matter Phys **74** (3 Pt 1), 031706 (2006).

[190] G. U. Nienhaus, J. Heinzl, E. Huenges, and F. Parak, "Protein Crystal Dynamics Studied by Time-Resolved Analysis of X-Ray Diffuse-Scattering," Nature **338** (6217), 665-666 (1989).

[191] R. Bandyopadhyay, A. S. Gittings, S. S. Suh, P. K. Dixon, and D. J. Durian, "Speckle-visibility

spectroscopy: A tool to study time-varying dynamics," Review of Scientific Instruments **76** (9), 093110-093121 (2005).
[192] J. L. Flament, F. Zielinski, S. Saude, and R. I. Grynszpan, "Helium diffusion in metals investigated by nuclear reaction analysis," Nuclear Instruments & Methods in Physics Research Section B-Beam Interactions with Materials and Atoms **216**, 161-166 (2004).
[193] J. W. M. Frenken, B. J. Hinch, and J. P. Toennies, "He Scattering Study of Diffusion at a Melting Surface," Surface Science **211** (1-3), 21-30 (1989).
[194] R. Lewis and R. Gomer, "Adsorption Studies with Field Ion Microscope - Phys," Abstracts of Papers of the American Chemical Society (Sep), 6-14 (1970).
[195] F. E. Wagner, R. Wordel, and M. Zelger, "Influence of Interstitial Diffusion on the Mossbauer-Spectra of Iron Solutes in Vd0.78 and Nbh0.84," Journal of Physics F-Metal Physics **14** (2), 535-547 (1984).
[196] B. W. Chang, J. P. Chou, and M. F. Luo, "Adsorption and diffusion of an Au atom and dimer on a theta-Al2O3 (001) surface," Surface Science **605** (11-12), 1122-1128 (2011).
[197] Michael Leitner and Gero Vogl, "Quasi-elastic scattering under short-range order: the linear regime and beyond," Journal of Physics: Condensed Matter **23** (25), 254206 (2011).
[198] M. Leitner, "Studying Atomic Dynamics with Coherent X-rays," Ph. D. Thesis, Springer-Verlag (Berlin Heidelberg), 2012.
[199] M. Leitner, B. Sepiol, L. M. Stadler, B. Pfau, and G. Vogl, "Atomic diffusion studied with coherent X-rays," Nat Mater **8** (9), 717-720 (2009).
[200] Bernd Struth, Kyu Hyun, Efim Kats, Thomas Meins, Michael Walther, Manfred Wilhelm, and Gerhard Grübel, "Observation of New States of Liquid Crystal 8CB under Nonlinear Shear Conditions as Observed via a Novel and Unique Rheology/Small-Angle X-ray Scattering Combination," Langmuir **27** (6), 2880-2887 (2011).
[201] M. F. Marmonier and L. Leger, "Reptation and tube renewal in entangled polymer solutions," Phys Rev Lett **55** (10), 1078-1081 (1985).
[202] S. T. Milner and T. C. B. McLeish, "Reptation and contour-length fluctuations in melts of linear polymers," Physical Review Letters **81** (3), 725-728 (1998).
[203] F. Saulnier, E. Raphael, and P. G. De Gennes, "Dewetting of thin polymer films near the glass transition," Phys Rev Lett **88** (19), 196101 (2002).
[204] P. Schleger, B. Farago, C. Lartigue, A. Kollmar, and D. Richter, "Clear evidence of reptation in polyethylene from neutron spin-echo spectroscopy," Physical Review Letters **81** (1), 124-127 (1998).
[205] A. N. Semenov, "Dynamics of entangled polymer layers: The effect of fluctuations," Physical Review Letters **80** (9), 1908-1911 (1998).
[206] T. P. Lodge, "Reconciliation of the molecular weight dependence of diffusion and viscosity in entangled polymers," Physical Review Letters **83** (16), 3218-3221 (1999).
[207] A. Fluerasu, P. Kwasniewski, C. Caronna, F. Destremaut, J. B. Salmon, and A. Madsen, "Dynamics and rheology under continuous shear flow studied by x-ray photon correlation spectroscopy," New Journal of Physics **12**, 035023-035033 (2010).
[208] R. Das, T. T. Mills, L. W. Kwok, G. S. Maskel, I. S. Millett, S. Doniach, K. D. Finkelstein, D. Herschlag, and L. Pollack, "Counterion distribution around DNA probed by solution X-ray scattering," Physical Review Letters **90** (18), 188103 (2003).